Technical Report

TR-06-30

Mineralogy and sealing properties of various bentonites and smectite-rich clay materials

Ola Karnland, Siv Olsson, Ulf Nilsson
Clay Technology AB

December 2006

Svensk Kärnbränslehantering AB
Swedish Nuclear Fuel
and Waste Management Co
Box 5864
SE-102 40 Stockholm Sweden
Tel 08-459 84 00
+46 8 459 84 00
Fax 08-661 57 19
+46 8 661 57 19

Mineralogy and sealing properties of various bentonites and smectite-rich clay materials

Ola Karnland, Siv Olsson, Ulf Nilsson
Clay Technology AB

December 2006

Contents

1 Background

1.1 General

Around 30 years ago the first studies were made on bentonite with respect to use as buffer material in a repository for spent nuclear fuel. A few commercial high quality bentonites from, inter alia, Bavaria in Germany and Wyoming in the US were studied. Especially the Wyoming bentonite was used for studies in several countries, and much by chance, a material from Am. Colloid Co with the brand name MX-80 was chosen. The material turned out to be very suitable and much important early laboratory work on MX-80 was made, especially by NAGRA in Switzerland, and by SKB in Sweden. There are numerous technical reports dealing with MX-80. Several other countries have more recently studied domestic bentonite/swelling clay qualities, frequently using MX-80 as reference. Large-scale field tests in the Stripa mine and presently at the Äspö hard rock laboratory in Sweden have used MX-80 as buffer material and as admixture in tunnel backfill material.

The present work includes a coherent study of Wyoming bentonite with respect to the most relevant properties for use in a repository, and a parallel study of other potential buffer and tunnel backfilling materials. The reason for this is twofold; to quantify the effect of mineralogical variations on the various important sealing properties of bentonite, and to verify that there are alternative potential sources of bentonite. The latter is motivated by the fact that Sweden alone plans to deposit at least 6,000 copper canisters which include approximately 130,000 metric tones bentonite buffer material and several times more as tunnel backfill material. Different types of sealing clay materials may also be relevant to use, since the demands on the clay will be different at the various locations in a repository. Alternative sources of bentonite would consequently be valuable in order to secure quality, supply, and price.

Important aspects on buffer and tunnel backfilling materials may be summarized as:

- Original sealing properties.
- Hazardous substances in any respect.
- Short-term effects of ground-water chemistry.
- Long-term stability, i.e. effects of temperature and ground-water chemistry.
- Availability.
- Costs.

The focus in this study is on the first three items. The long-term stability is indirectly considered in that mineralogical composition is determined. The availability is only considered in such a way that most of the analyzed materials represent huge clay formations, which contain much more material than needed for a repository. The cost aspects have not been included, mainly because the present day price is not relevant due to the time frame of the construction of a repository.

2 Analyzed materials

2.1 General

Fifteen materials from the Czech Republic (4 materials), Denmark (3), Germany (1), Greece (1), India (5) and the US (1 quality, 5 batches) were chosen for the study. Photos of the materials are shown in Appendix 1. The materials from India, Greece and the US are high-quality bentonites from active mines, representing a significant part of the present global production. The present Czech, Danish and German materials are generally of lower quality and represent smaller producers/production, although some of these deposits also are huge in physical size. Common for all the materials are that they contain significant amounts of swelling minerals, which lead to swelling pressure and a low hydraulic conductivity in a confined volume. However, the materials represent quite different conditions in several aspects. For example, the Czech and Greek materials are in their natural form dominated by calcium as counter-ions, often referred to as Ca-bentonite, while especially some Indian and the US materials are dominated by sodium. The Czech and Indian samples have a relatively high content of iron compared to the others, the German material has a high content of quartz, while the Greek material has a significant amount of calcite etc. Major differences between the materials may be summarized as:

- Age of formation.
- Formation morphology.
- Overall mineralogy.
- Molecular structure of the swelling mineral.
- Type and amount of counter ions.
- Technical quality.
- Sealing properties.

The analyses and tests were made both on the industrial, or natural, delivered materials in order to determine the bulk properties, and on the purified clay fraction from all materials in order to determine the properties of the active swelling mineral alone.

A technique to blend bentonite horizons or locations in optimized proportions is used by most commercial producers in order to keep a defined quality regardless of the natural variation within an individual horizon or location. Several of the industrially produced bentonites in this study represent such blended material.

The following sections describe briefly the origin of the materials, the nomenclature for the analyzed samples, and the preparation of the bulk and purified clay fraction materials.

2.2 Czech republic

The four Czech materials were delivered in natural state by the Institute of Geochemistry, at the Charles University in Prague. Two of the clays originate from deposits within the north Bohemian volcanic areas NW of Prague and two sedimentary clays originate from basins in the south-western/western part of the Czech Republic. Due to different genesis these deposits are traditionally classified as bentonites and smectite-rich clays, respectively /Prikryl and Woller 2002/.

The Dnesice deposit in the Plzen basin, c. 100 km SW Prague represents the sedimentary type, and the clay is therefore often classified as bentonitic rather than as a true bentonite.

The *Rokle* deposit in the Kadan basin, c. 100 km WNW of Prague, is one of the economically most important deposits in the Czech Republic. The deposit is part of a series of argillised volcanoclastic accumulations of Tertiary age, formed in shallow lacustrine basins within the stratovolcano complex of Doupovské Mountains /Konta 1986/. The bentonite is capped by basaltic lava-flows. The lens-shaped bentonite body has a maximum thickness of c. 40 m, and contains more than 40 million tons of bentonite. The volcanic glass is completely altered to smectite, but mm-sized flakes of biotite, which is a primary constituent of the basaltic magma, are relatively frequent. The bentonite is highly variable in colour, ranging from olive-gray to yellow/red due to the admixture of secondary iron and manganese oxides.

The Zelena-*Skalna* deposit in the Cheb basin, near the western Czech border, is a sedimentary smectite-bearing, so called "Green clay" of Tertiary age. The deposit at Skalna is rather small and exploitation is restricted by regulations for the protection of the groundwater (mineral water). The exploitable reserve is estimated at approximately 130 kilo tons.

The deposit at *Strance* in the Ceske Stredohori area, 4 km SE of Most, is genetically of the same type as the Rokle deposit, i.e. it formed by argillization of tuffites and pyroclastic rocks during the Tertiary. The thickness of the deposit ranges from 9 to 16 m and the exploitable reserve is estimated at approximately 7 million tons.

The four clays are characterized by relatively high natural water content and some coarse grains and obvious impurities. In the following the materials are simply denominated Dnesice, Rokle, Skalna and Strance. In diagrams and tables the abridgement DnR1 denominates the reference batch of the Dnesice clay and the DnNa denominates the clay fraction of the Dnesice clay, which has been ion exchanged to sodium form. The same logic is used for all other clays in the study.

2.3 Denmark, Tåsinge island

The three Danish clays originate from a recently opened quarry at Bjerreby on the island of Tåsinge, south of Fyn. The sediment sequence at Bjerreby has been glacially tectonised, and more or less vertically erected layers of Tertiary sediments of various age are exposed in the walls of the quarry. The layers are easily distinguished through their characteristic colors and each clay sample represents a different level of the Upper Palaeocene-Eocene (> 50 million years) stratigraphy of marine clays, the *Ølst*, the *Holmehus* and the *Røsnaes* Formations. The producer (NCC Danmark A/S) classifies the clays at Bjerreby as low to medium grade bentonites and estimates the exploitable reserve at approximately 1 million tons.

The three samples of swelling "plastic clays" were delivered in natural state characterized by a relatively high water content. The clay samples are denominated Holmehus, Rösnäs and Ölst, or simply HoR1 for the reference batch of Holmehus, and HoNa for the sodium ion exchanged clay fraction.

2.4 Germany, Neubrandenburg area

The Friedland clay material is quarried near the town of Neubrandenburg, NE Germany, and is a sedimentary clay formed in a shallow marine basin during the Eocene (57–35 million years ago). The mineralogy of the clay is complex, reflecting the mixture of detrital material derived through erosion of the pre-existing weathering mantle, tephra fall-outs and mineral neoformation during early diagenesis /Henning and Kasbohm 1998/. The quarried deposit is massive and homogeneous with a thickness up to 140 m and the producer estimates the exploitable reserve at approximately 100 million tons.

The Friedland material was industrially milled and dried, and delivered in sacks. It is denominated FrR1 for the reference batch, and FrNa for the sodium ion exchanged clay fraction. Triplicate samples have been used in several of the tests and analyses and are termed FrR1a, b and c, respectively. The suffix m is used for the mean value of the three samples.

2.5 Greece, Milos

The Greek bentonite is quarried in the north-eastern part of the island of Milos, where some of the economically most important bentonite deposits in Europe are concentrated (Figure 2-1). The island of Milos in the Aegean Sea is part of the Hellenic Arc volcanic province. Pyroclastic tuffs and lavas of andesitic to dacitic compositon are the main parent rocks of the bentonite, which forms irregular bodies with a thickness of 10–40 m within the pyroclastics. The volcanic rocks have yielded K-Ar ages in the range 3.5–0.09 million years. Based on isotope data, /Decher et al. 1996/ conclude that the bentonite formation is a result of hydrothermal reactions between the permeable volcanic rocks and percolating groundwater heated to below 90°C during volcanic activity, although there is some disagreement about the genesis e.g. /Christidis et al. 1995/.

The present Milos bentonite is mined by Silver & Baryte Mining Company S.A. The charge compensating cations are dominated by calcium, which is referred to in the commercial name IBECO Deponit CA-N. The analysed materials are denominated MiR1 for the reference batch of Deponit CA-N material, and MiNa for the sodium ion exchanged clay fraction and MiCa for the calcium variant. Triplicate samples have been used in several tests and analyses and are termed MiR1a, b and c respectively. The suffix m is used for the mean value of the three samples.

Figure 2-1. *Bentonite drying and blending area on the Milos island, Greece.*

2.6 India, Gujarat region

Extensive deposits of natural Na-bentonite exist in the Kutch area, 60–80 km from the ports of Kandla and Mandvi on the northwest-coast of India. The bentonite is associated with the basaltic Deccan Trap rocks of Tertiary age and formed through hydrothermal alteration of volcanic ash in saline water /Shah 1997/. The bentonite occurs in scattered and disconnected pockets or as interlayers within the basaltic rocks, with thicknesses ranging from a few meters up to 30 metres (Figure 2-2). Due to the high content of secondary iron oxides the color is normally dark reddish brown but there are also light colored variants low in iron. The total exploitable reserve of Na- and other bentonites in Kutch has been estimated at c. 25 million tons.

Five different materials qualities have been analyzed and tested. The materials were dried and crushed industrially to centimeter-sized grains by Ashapura Minechem Co. and delivered in small bags. The five materials were originally denominated BEN/GN/NW/BN/8936, to 8940, and are here denominated Ku36R1, Ku37R1, Ku38R1, Ku39R1 and Ku40R1. The sodium-exchanged clay fractions are named Ku36Na etc. The Ku39R1and Ku40R1 materials correspond to the commercial names ASHA 505 and ASHA 229, respectively.

2.7 USA, Wyoming

The Wyoming type of bentonite occurs as layers in marine shales, and is widespread and extensively mined, not only in Wyoming but also in parts of Montana and South Dakota. The bentonite formed through alteration of rhyolitic tephra deposited in ancient Mowry Sea basin during the Createceous, more than 65 million years ago /Slaughter and Earley 1965/. There are strong evidence that the tephra altered in contact with the Mowry seawater /Elzea and Murray 1989/, but palaeosalinity and palaeoredox conditions within the semi-restricted basin varied spatially and through time, which explains that the smectite composition varies both stratigraphically and laterally. In addition, differences in wheathering conditions overprints the chemical signatures related to palaeoenvironment and inhomogeneities in parent ash composition /Elzea and Murray 1990/.

Figure 2-2. *Typical bentonite quarry in the Kutch area in India.*

The MX-80 material, produced by Am. Coll. Co., is a blend of several natural sodium dominated bentonite horizons, dried and milled to millimeter-sized grains. The same material, from a mineralogical perspective, is also sold under the name SPV 200, the difference being that the SPV 200 material is milled to a fine powder. The material represents one of quite a number of different mineralogical and technical qualities of Wyoming bentonite used for various purposes.

Bulk material from five different consignments has been analyzed in order to check how well defined the material has been. The first delivery was made in conjunction with the SKB Stripa project around 1980 and the five materials thus represent more than 20 years of production. The analyzed Stripa material was taken from remaining compacted blocks. The other consignments represent material from 1996 and 1999 used in the first and second series of the LOT project at the Äspö HRL /Karnland et al. 2000/, and two batches from 2001 for laboratory use at Clay Technology AB. The denominations used are WySt, WyL1, WyL2, WyR1 and WyR2, respectively. The WyR1 batch has been extensively analyzed and the ion exchanged clay fractions from this batch are denoted WyNa, WyCa etc. for sodium and calcium, respectively.

2.8 Material preparation

2.8.1 Bulk materials

The natural bulk materials were dried and milled to a character similar to that of the industrially prepared MX-80. Large hard rock grains were removed and the material was air dried and mechanically ground to a maximum particle size of 1 mm. The materials are referred to as reference materials and by the suffix R in abridgements.

2.8.2 Homo-ionic clay fractions

Ten grams of the material was dispersed in 1 L de-ionized water. Analytical grade NaCl was added to a concentration of 1 M and the material was left to settle and the supernatant was removed. The addition of de-ionized water and NaCl was repeated three times and the material was thereafter washed by repeated centrifugation, removal of the supernatant and addition of de-ionized water until dispersion started. The remaining slurry except the sedimented coarsest material was transferred to dialysis membranes (Spectrapore 3, 3500 MWCO) placed in plastic tanks with de-ionized water. The water outside the membrane was changed daily until the electrical conductivity was stabilized below 10 µS/cm. The material was dispersed in 1 L de-ionized water and the d > 2µm fraction was removed by sedimentation. Again analytical grade chloride salt of the desired cation was added to a concentration of 1 M. The material was again left to settle and the procedure was repeated three times, followed by the same washing as in the first round including dialyses. The result of the ion exchange was finally checked by analysis of the exchangeable cations (paragraph 3.4)

This rather tedious method was motivated by the fact that significant amount of calcium in exchange positions was found after one round of dialysis was (Table 3-3).

After drying at 60°C, the bentonite was ground to an aggregate grain size similar to that of MX-80. The purified and ion exchanged materials are referred to by the suffixes Na and Ca etc to material names in the following text.

3 Mineralogical analyses, techniques and results

3.1 General

Bentonite is a geological term for soil materials with a high content of a swelling mineral, which usually is montmorillonite. The montmorillonite belongs to the smectite group, in which all members have an articulated layer structure. The thickness of an individual mineral layer is around 1 nm (Figure 3-1) and the extension in the two other directions is often several hundred nanometers. Each layer is composed of a central sheet of octahedrally coordinated cations, which on both sides is linked through shared oxygens to sheets of tetrahedrally coordinated cations. Clay minerals of this type are often referred to as 2:1 layer structures.

By definition, the following applies for the mineral montmorillonite. The octahedral sheet has aluminum as central ion, which is partly substituted principally by Mg. The tetrahedral sheet has silicon as central ion, which partly may be substituted by principally aluminum. The substitutions result in a net negative charge of the montmorillonite layer in the range of 0.4 to 1.2 unit charges per $O_{20}(OH)_4$ -unit, and the octahedral charge is larger than the tetrahedral. The mineral is termed beidellite if the tetrahedral charge dominates. The induced negative layer charge is balanced by cations (c) located between the individual layers (interlayer space). A variable number (n) of water molecules may be intercalated between the individual mineral layers /Newman 1987/.

The montmorillonite ideal formula may consequently be written:

$Si_{8-x}Al_x$	$Al_{4-y}Mg_y(Fe)$	$O_{20}(OH)_4$	$c_{x+y}n(H_2O)$	$(x < y)$ and
tetrahedral	octahedral	anions	interlayer	$0.4 < x+y > 1.2$

and the structure may schematically be illustrated as in Figure 3-1.

In natural bentonite, the charge compensating cations are rarely of one element alone, but a mixture of both mono and divalent ions. The swelling properties are to a large extent dependant on the magnitude and the position of the layer charge, but also on the type of charge compensating cation. The dominating cation is therefore often used to describe the type of bentonite, e.g. sodium bentonite, although the content of other ions may be quite large.

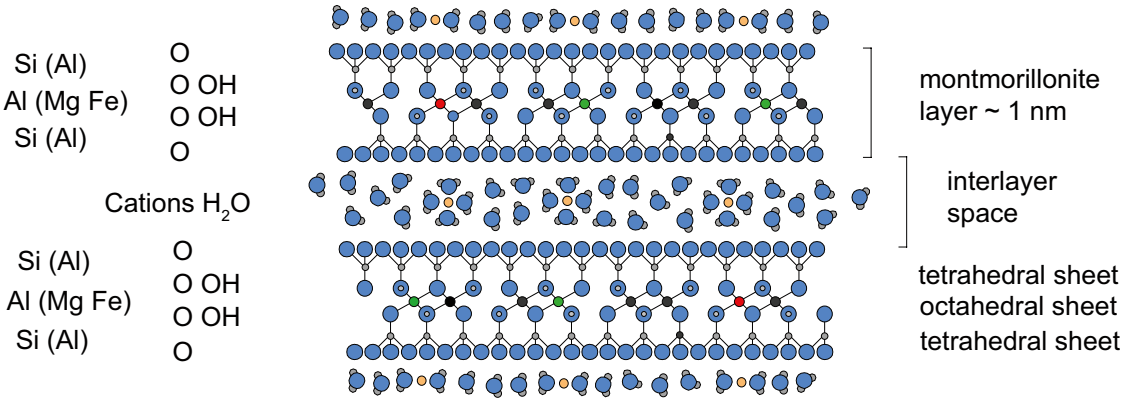

Figure 3-1. *Edge view cartoon of two montmorillonite layers with interlayer cations and water molecules.*

High-quality commercial bentonites normally contain over 80% of montmorillonite, which is expected to give various bentonite products similar sealing properties. However, the other minerals in bentonite may vary substantially within, and especially between, different quarries. Typical accessory minerals are feldspars, quartz, cristobalite, gypsum, calcite and pyrite. Some of these accessory minerals may promote cementation of the buffer, and they may jeopardize the longevity of the swelling mineral or the canister by chemical interaction. Further, the accessory minerals and other substances such as organic matter may affect the transport properties of radionuclides in case of a canister failure.

Based on the above, the following mineralogical analyses have the purpose to describe the fifteen included materials with respect to:

- the type and distribution of accessory minerals,
- the mineral structure of the swelling mineral, including the type and amount of the charge compensating cations.

3.2 X-ray diffraction (XRD)

All bentonite samples were analysed both as random powders of the bulk material and as oriented mounts of the fraction < 2 μm by use of a Seifert 3000 TT diffractometer, equipped with automatic slits and a Cu-tube operated at 50kV/30mA.

3.2.1 Random powders

The bulk samples were dried at room temperature (or, occasionally, at 60°C) and ground in an agate mortar until the size of the maximum particles was less than c. 10 μm. In order to avoid interstratifications between two hydration states, cf. /Brindley and Brown 1980/, p. 203–204, the powders were equilibrated over a saturated solution of $MgCl_2$ (relative humidity c. 33%; ref.) in a desiccator for 4–5 days. The sample was brushed through a small sieve into the cavity of the sample holder to minimize preferred orientation of the particles. A glass slide was used to pack the sample into the cavity, just firmly enough to create a smooth surface that would not deform during the rotation of the sample during scanning. Random powders were X-ray scanned with a step size of 0.02° from 2 to 66° 2θ. Figures (3-2 to 3-8) show the recorded diffractograms arranged in groups representing the country of origin.

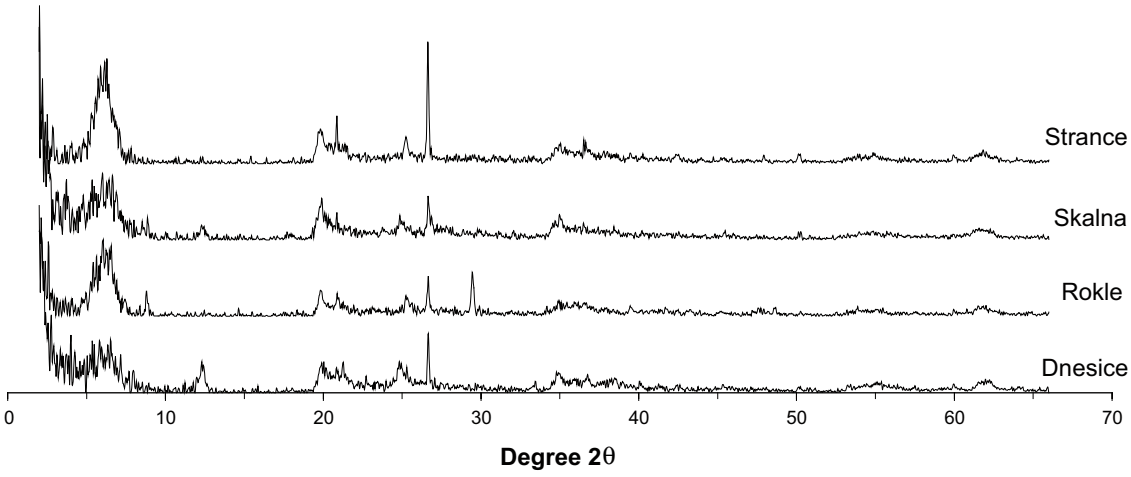

Figure 3-2. *Powder X-ray diffractograms of the Czech bulk materials used for the Siroquant determination of mineral content.*

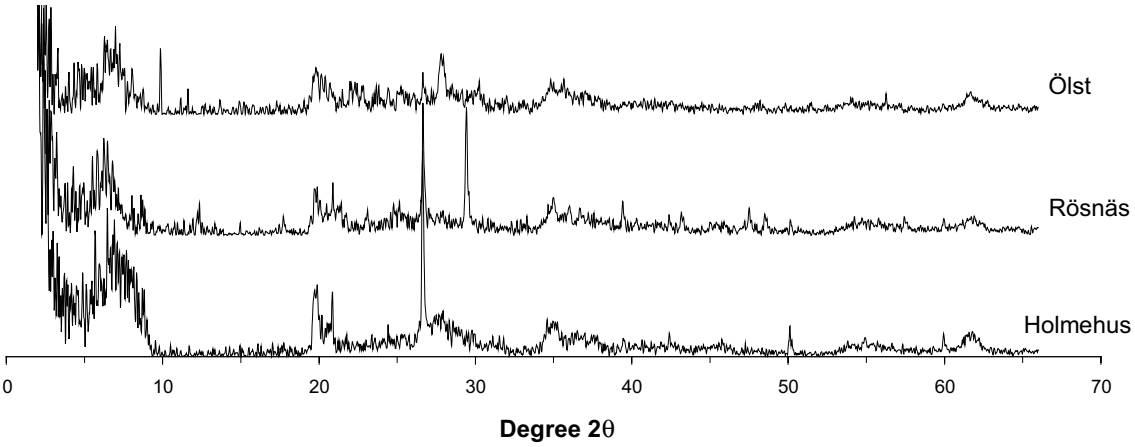

Figure 3-3. *Powder X-ray diffractograms of the Danish bulk materials used for the Siroquant determination of mineral content.*

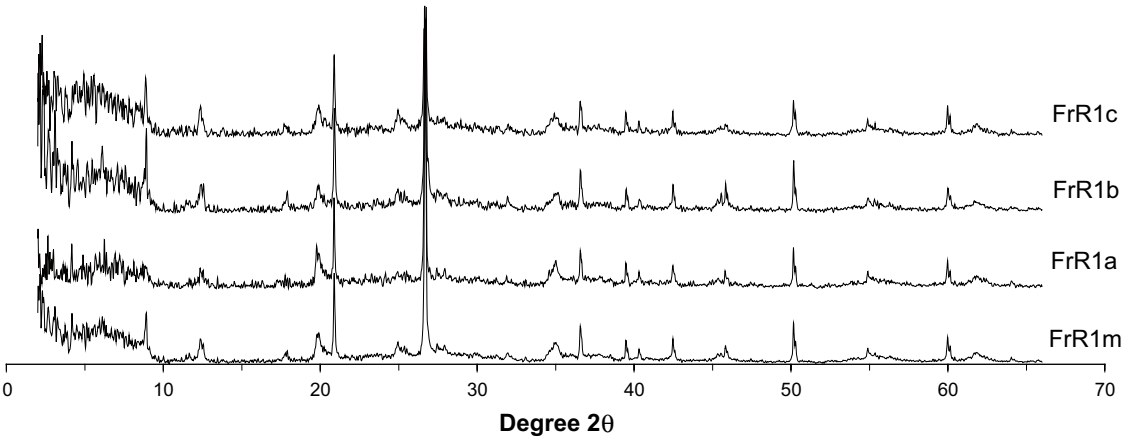

Figure 3-4. *Powder X-ray diffractograms of three separate runs of the Friedland bulk material used for the Siroquant determination of mineral content. FrR1m indicates the calculated mean diffractogram of the three measurements.*

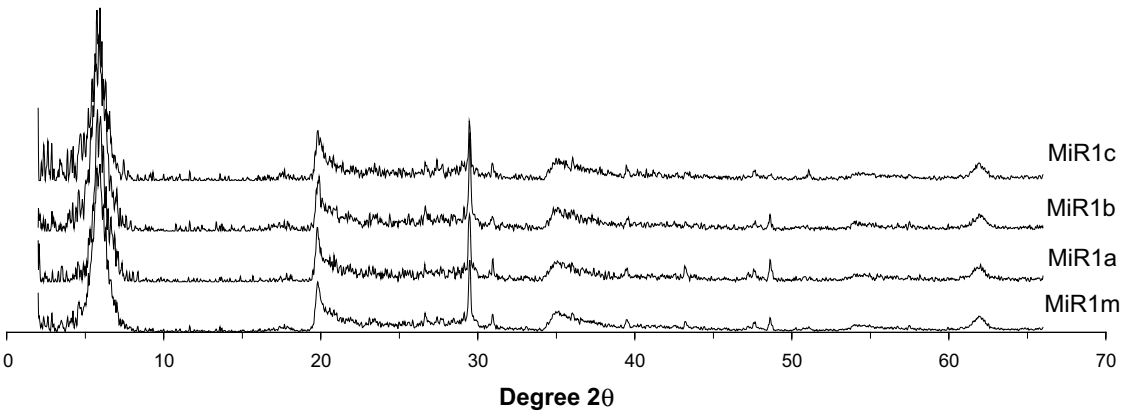

Figure 3-5. *Powder X-ray diffractograms of three different runs of the Deponit CA-N bulk material used for the Siroquant determination of mineral content. MiR1m indicates the calculated mean diffractogram of the three measurements.*

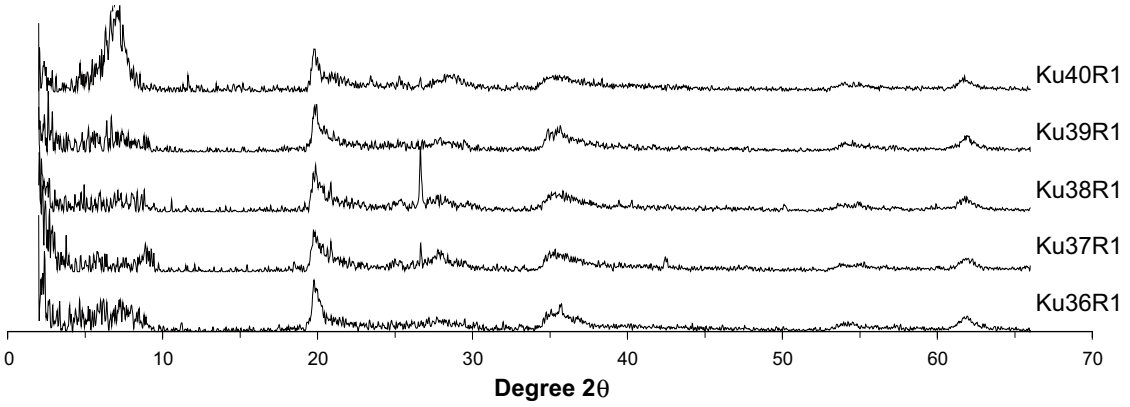

Figure 3-6. *Powder X-ray diffractograms of the five Indian materials used for the Siroquant determination of mineral content.*

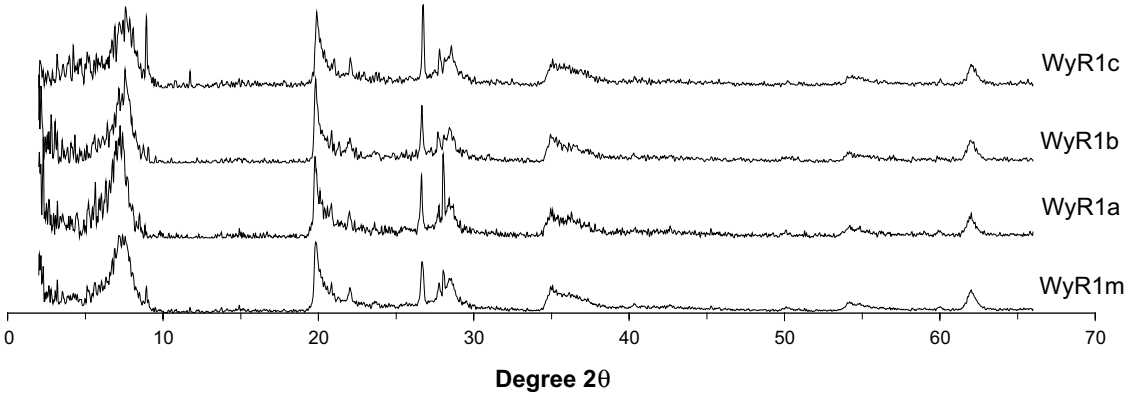

Figure 3-7. *Powder X-ray diffractograms of three different runs of the Wyoming MX-80 bulk material from the consignment WyR1. WyR1m indicates the calculated mean diffractogram of the three measurements.*

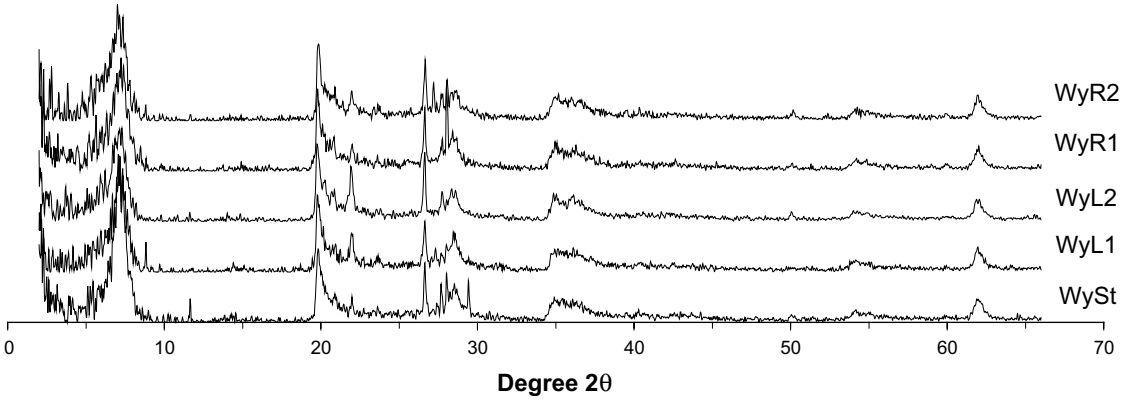

Figure 3-8. *Powder X-ray diffractograms from five different consignments of the Wyoming MX-80 material used for the Siroquant determination of mineral content. The five consignments represent materials delivered around 1980 (WySt), 1995 (WyL1), 1999 (WyL2), and 2001 (WyR1 and WyR2).*

3.2.2 Oriented mounts

Oriented mounts were prepared of the d < 2 μm fractions, which were converted to Mg-form by treatment with 0.5 M $MgCl_2$. The clay suspensions were then vacuum-filtered onto a 0.45 μm membrane filter and rinsed free of excess salts. Mounts were prepared according to the filter-membrane peel-off technique /Drever 1973/ and dried at room temperature prior to X-ray scanning.

Mounts prepared by the filter-peel technique normally fulfill high requirements on surface smoothness and evenness. The preparation technique is, however, unsuitable for Na-smectites, which tend to form gel-like suspensions when mixed with water, and instead a thick suspension of the clay was smeared on a glass slide and dried at room temperature. The technique is simple and frequently used, but the aggregate surface has seldom optimal smoothness.

Mounts of oriented clays were X-ray scanned with a step size of 0.02° from 2 to 33° 2θ (Figure 3-9 to Figure 3-23). Clay mineral identifications rest on criteria given by /Brindley and Brown 1980/ and are based on the reactions to the following pre-treatments:

- The expansion behavior was tested by solvation of the clay with ethylene glycol (eg) at 60°C for 48 hours. Selected samples were tested also with glycerol (gly).
- Illite/smectite mixed-layers were identified according to the method of /Moore and Reynolds1989/ by measurements of the peak angle difference (Δ2θ) distance between the composite peaks (001)illite/(002)smectite and (002)illite/(003)smectite in the diffractograms of the glycolated samples (Table 5-11).
- Kaolin minerals were identified and distinguished from chlorite in relevant materials by the behavior of the 7 and 3.54 Å peaks upon heating at 550°C for 2 hours. Disappearance of the peaks is indicative for kaolin typically shown in the Dnesice material (Figure 3-9).

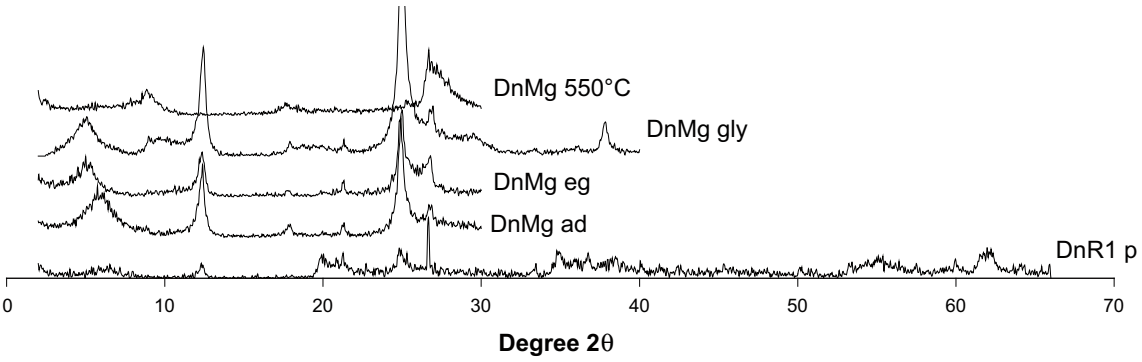

Figure 3-9. *XRD patterns of the Czech Dnesice sample; p indicates the powder sample, ad the air-dry oriented sample, eg the ethylene glycol treated oriented samples, gly the glycerol treated oriented sample, and finally 550°C indicate the oriented sample heated to 550°C.*

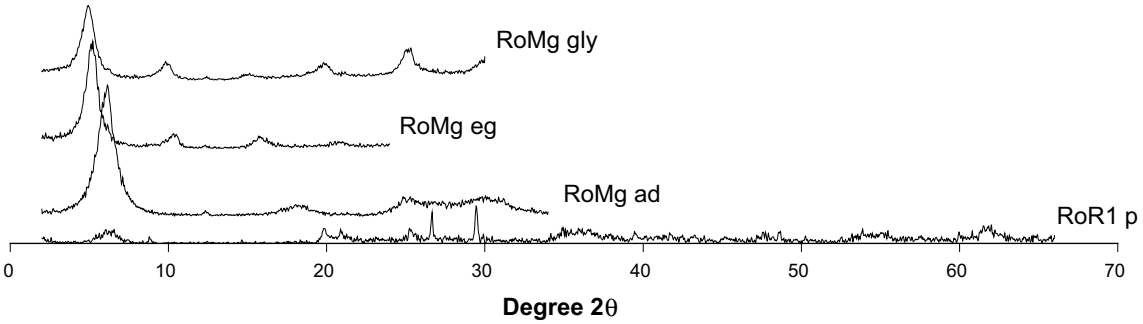

Figure 3-10. *XRD patterns of the Czech Rokle sample; p indicates the powder sample, ad the air-dry oriented sample, eg the ethylene glycol treated oriented samples, and gly the glycerol treated oriented sample.*

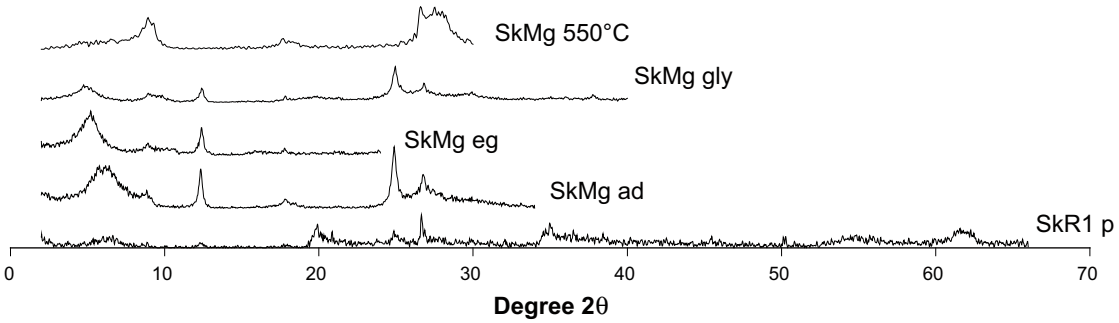

Figure 3-11. *XRD patterns of the Czech Skalna sample; p indicates the powder sample, ad the air-dry oriented sample, eg the ethylene glycol treated oriented samples, gly the glycerol treated oriented sample, and 550°C indicate the oriented sample heated to 550°C.*

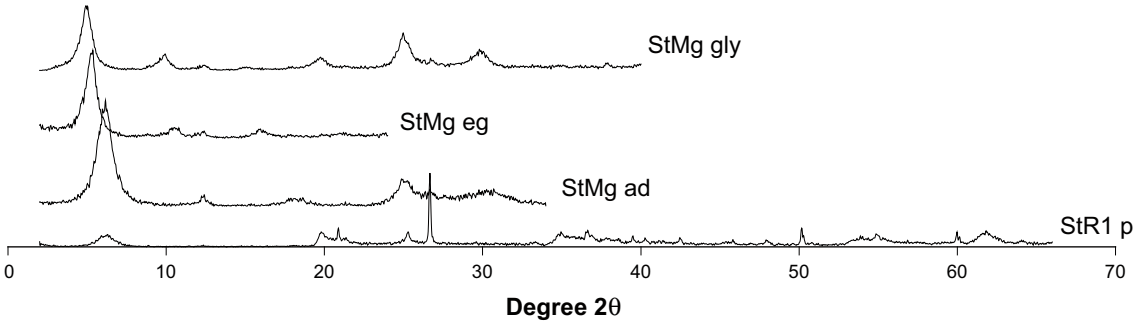

Figure 3-12. *XRD patterns of the Czech Strance sample; p indicates the powder sample, ad the air-dry oriented sample, eg ethylene glycol treated oriented sample, and gly the glycerol treated oriented sample.*

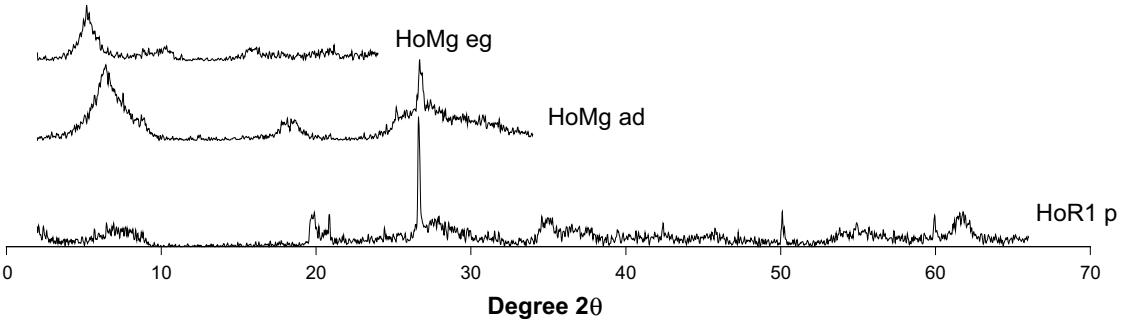

Figure 3-13. *XRD patterns of the Danish Holmehus sample; p indicates the powder sample, ad the air-dry oriented sample, and eg ethylene glycol treated oriented sample.*

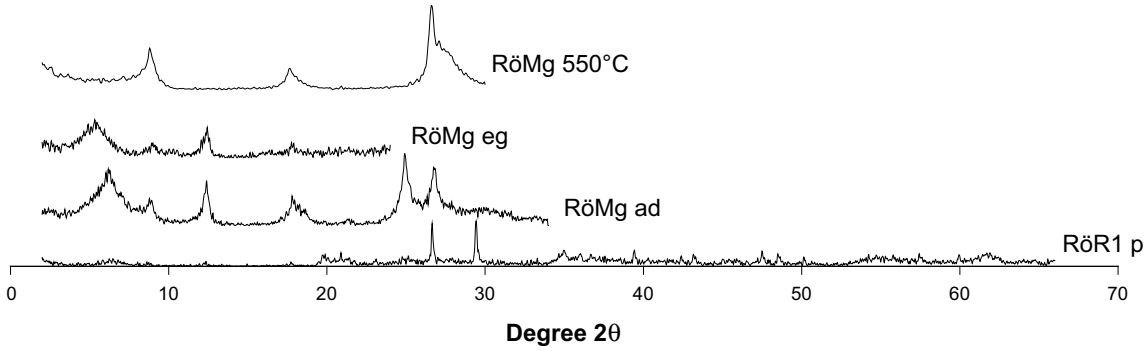

Figure 3-14. *XRD patterns of the Danish Rösnäs sample; p indicates the powder sample, ad the air-dry oriented sample, eg ethylene glycol treated oriented sample, and 550°C indicate the oriented sample heated to 550°C.*

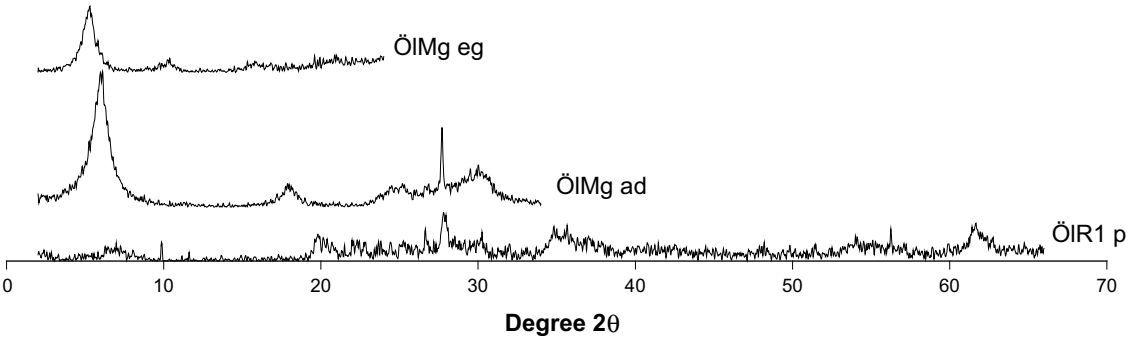

Figure 3-15. *XRD patterns of the Danish Ölst sample; p indicates the powder sample, ad the air-dry oriented sample, and eg ethylene glycol treated oriented sample.*

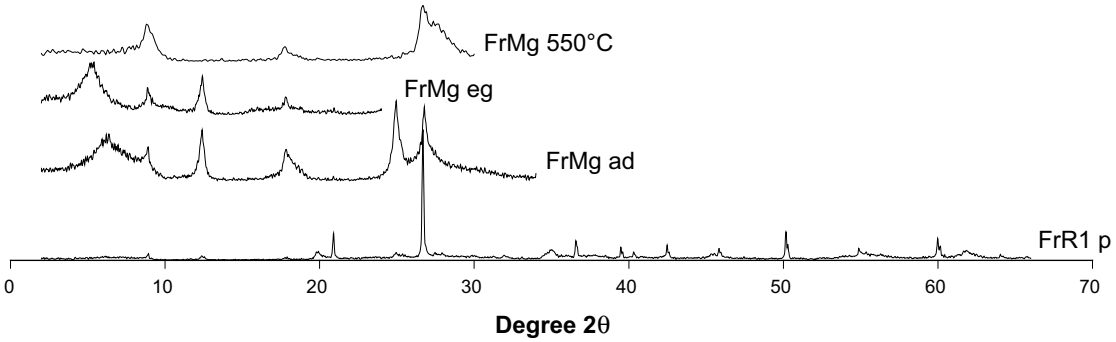

Figure 3-16. *XRD patterns of the German Friedland material; p indicates the powder sample, ad the air-dry oriented sample, eg ethylene glycol treated oriented sample, and 550°C indicate the oriented sample heated to 550°C.*

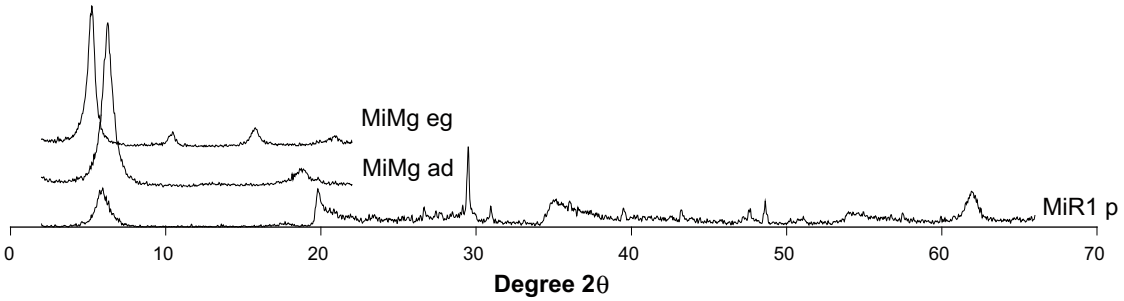

Figure 3-17. *XRD patterns of the Milos Deponit CA-N material; p indicates the powder sample, ad the air-dry oriented sample, and eg ethylene glycol treated oriented sample.*

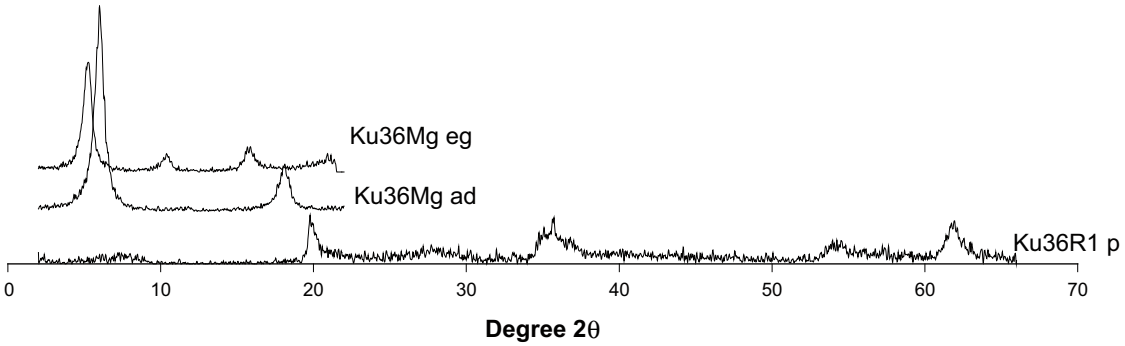

Figure 3-18. *XRD patterns of the Indian Kutch 8936 material; p indicates the powder sample, ad the air-dry oriented sample, and eg ethylene glycol treated oriented sample.*

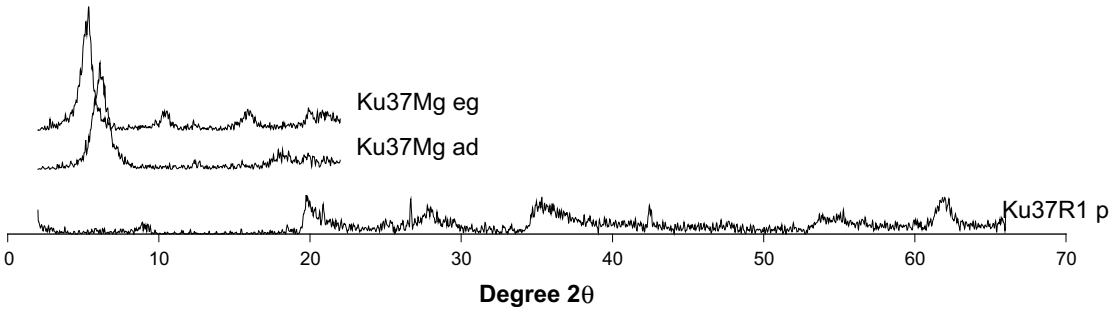

Figure 3-19. *XRD patterns of the Indian Kutch 8937 material; p indicates the powder sample, ad the air-dry oriented sample, and eg ethylene glycol treated oriented sample.*

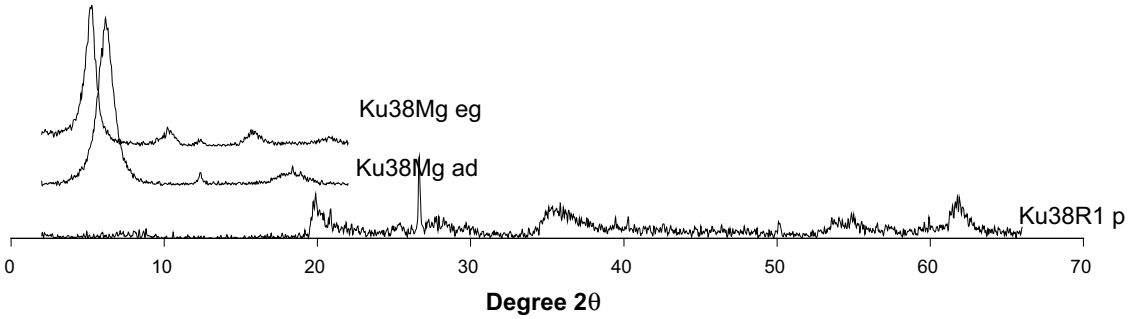

Figure 3-20. *XRD patterns of the Kutch 8938 material; p indicates the powder sample, ad the air-dry oriented sample, and eg ethylene glycol treated oriented sample.*

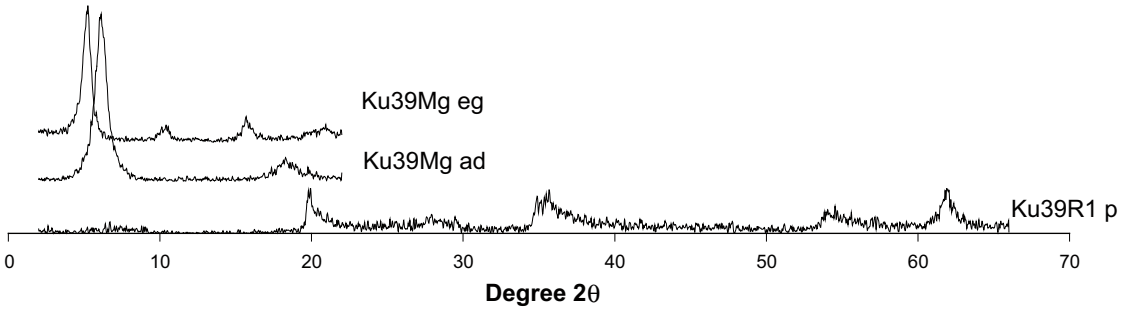

Figure 3-21. *XRD patterns of the Indian Kutch 8939 material; p indicates the powder sample, ad the air-dry oriented sample, and eg ethylene glycol treated oriented sample.*

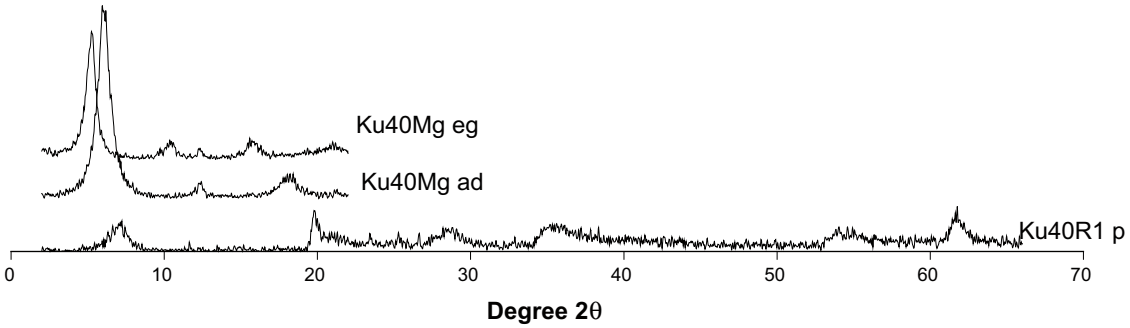

Figure 3-22. *XRD patterns of the Indian Kutch 8940 material; p indicates the powder sample, ad the air-dry oriented sample, and eg ethylene glycol treated oriented sample.*

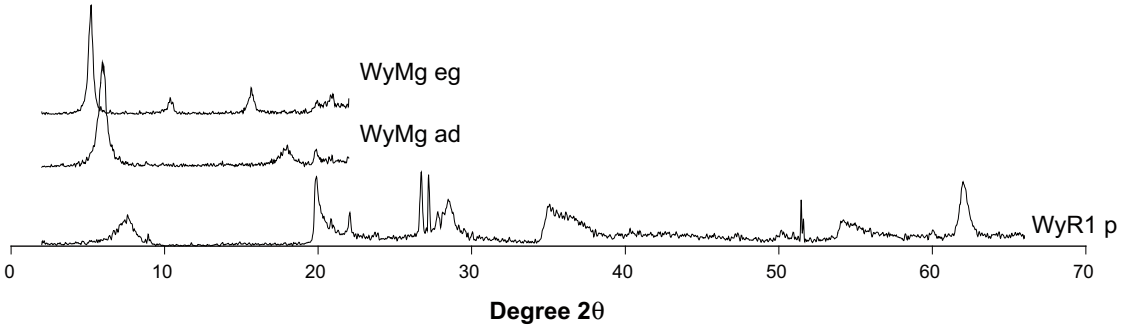

Figure 3-23. *XRD patterns of the Wyoming MX-80 material; p indicates the powder sample, ad the air-dry oriented sample, and eg ethylene glycol treated oriented sample.*

3.3 Cation exchange capacity (CEC)

The cation exchange capacity of both bulk bentonite samples and homo-ionic, dialysed clay fractions (d < 2 μm), was determined as Cu(II)-CEC according to /Meier and Kahr 1999/. The method was slightly modified because CEC-determinations using the concentration suggested by Meier and Kahr resulted in lower and less reproducible CEC for homo-ionic Ca-clays than for the corresponding Na-clays when CEC exceeded c. 0.75 eq/kg, suggesting incomplete exchange of Ca against Cu. An increase of the Cu-concentration by at least a factor of 2 was necessary to get acceptable reproducibility also for the Ca-clays, as shown by tests with homo-ionic Na- and Ca-clays prepared of MX-80 and Deponit CA-N bentonites.

0.4 g (mg resolution) of the air-dry and ground sample was dispersed in 50 ml deionised water by ultrasonic treatment. 20 ml of 15 mM Cu(II)-triethylentetramine was added to the suspension, which was left to react for 15 minutes on a vibrating table. After centrifugation the supernatant was collected and the absorbance at 620 nm was measured using a double-beam spectrophotometer (Perking Elmer Lambda 3) with 1 cm quartz cuvettes. CEC was calculated by the difference in the Cu-concentration before and after ion exchange. The water content of the clay was determined for a separate sample dried at 105°C to constant weight. All results are reported as the mean CEC (eq/kg dry weight) of two separate determinations for the bulk material in Table 3-1 and for the homoionic clay fractions in Table 3-2.

Table 3-1. Cation exchange capacity (CEC) of all bulk materials measured by exchenge against Cu(II)-trien. All result in eq/kg (mole charges/kg).

	Total material Analysis no.	Eq/kg 1	2	3	4	5	Mean
Cz	DnR1	0.27	0.26	0.36	0.36		0.31
	RoR1	0.47	0.50				0.48
	SkR1a	0.37					0.37
	StR1	0.55					0.55
Da	HoR1	0.49					0.49
	RöR1	0.32					0.32
	ÖlR1	0.49	0.48				0.48
Ge	FrR1	0.23	0.20				0.21
							0.00
Gr	MiR1	0.73	0.68	0.70			0.70
In	Ku36R1	0.84	0.88				0.86
	Ku37R1	0.65	0.62				0.63
	Ku38R1	0.73	0.79				0.76
	Ku39R1	0.86	0.85				0.85
	Ku40R1	0.87	0.84				0.86
US	WySt	0.76					0.76
	WyL1	0.75	0.76	0.78	0.78	0.74	0.77
	WyL2	0.72	0.76	0.74	0.77		0.75
	WyR1	0.74	0.75	0.76	0.76	0.76	0.75
	WyR2	0.71					0.71

Table 3-2. Cation exchange capacity (CEC) of all clay fractions measured with the Cu(II)-trien exchange method. All result in eq/kg (mole charges/kg).

	Clay fractions Analysis no	Eq/kg 1	2	3	4	5	Mean
Cz	DnNa	0.40	0.40	0.41	0.40		0.40
	RoNa	0.76	0.73				0.74
	SkNa	0.47					0.47
	StNa	0.76					0.76
	HoNa	0.57	0.59				0.58
	RöNa	0.40					0.40
Da	ÖlNa	0.67					0.67
Ge	FrNa	0.35	0.33				0.34
							0.00
Gr	MiCa	0.78	0.86	0.81			0.82
	MiNa	0.87	0.88	0.88			0.88
In	Ku36Na	1.00					1.00
	Ku37Na	0.88					0.88
	Ku38Na	0.90					0.90
	Ku39Na	0.99					0.99
	Ku40Na	0.88					0.88
US	WyStNa	0.88					0.88
	WyL1Na	0.87	0.88				0.88
	WyL2Na	0.85	0.86	0.87	0.87		0.86
	WyR1Na	0.88	0.88	0.83	0.85	0.87	0.86
	WyR2Na	0.80					0.80

3.4 Original exchangeable cations

Since the raw bentonite materials may contain both carbonates and gypsum, the composition of the extractable exchangeable ions was determined by exchange against ammonium ions (NH_4^+) in an alcoholic solution in order to reduce dissolution errors e.g. /Belyayeva 1967/; /Jackson 1975/and /Polemio and Rhoades 1977/. However, easily soluble salts, such as chlorides and carbonates of alkali metals, will still dissolve in this extractant, and the sum of the exchangeable cations often exceeds the measured Cu-CEC-values of the sample.

Exchangeable cations were extracted by shaking 1 g of the air-dry and ground bentonite for 30 minutes in approximately one third of a total volume of 50 ml 0.5 M NH4Cl in 80% ethanol. After centrifugation the supernatant was decanted in a volumetric flask. The extraction was repeated three times. After evaporation of the alcohol, the concentrations of Ca, Mg, K and Na were determined by use of ICP-AES. The water content of the clay was determined for a separate sample dried at 105° C to constant weight and results are reported as eq/kg dry weight in Table 3-3. The columns “% saturation” show the distribution of exchangeable ions in percent.

Table 3-3. Exchangeable ions in all bulk materials and in the ion-exchanged clay fractions of the MX-80 and Deponit CA-N materials. * Indicate one round of dialysis (Section 2.8.2).

		eq/kg					% saturation			
	Material	Ca	K	Mg	Na	Sum	Ca	K	Mg	Na
Cz	DnR1	0.22	0.01	0.11	0.01	0.34	64	2	32	2
	RoR1	0.57	0.02	0.16	0.01	0.76	76	3	21	1
	SkR1	0.34	0.03	0.07	0.00	0.45	77	7	15	0
	StR1	0.30	0.01	0.35	0.01	0.67	45	2	52	2
Da	HoR1	0.15	0.05	0.09	0.31	0.60	25	8	15	53
	RöR1	0.31	0.02	0.08	0.04	0.45	69	4	18	9
	ÖlR1	0.14	0.05	0.19	0.34	0.72	19	8	26	48
Ge	FrR1	0.01	0.02	0.04	0.23	0.31	4	7	14	76
Gr	MiR1	0.38	0.02	0.24	0.20	0.85	45	2	29	24
	MiCa	1.02	0.01	0.01	0.00	1.04	97	1	1	0
	MiNa*	0.51	0.01	0.03	0.38	0.94	54	1	4	41
	MiNa	0.03	0.01	0.02	1.17	1.23	2	1	2	95
	MiNa	0.02	0.01	0.02	1.15	1.20	2	1	1	96
In	Ku36R1	0.40	0.01	0.31	0.34	1.05	38	1	29	32
	Ku37R1	0.05	0.01	0.22	0.61	0.88	5	1	24	69
	Ku38R1	0.09	0.00	0.15	0.58	0.82	11	0	18	70
	Ku39R1	0.32	0.01	0.28	0.41	1.02	31	1	28	40
	KuR140	0.21	0.01	0.19	0.52	0.93	22	1	20	56
US	WySt	0.08	0.01	0.05	0.67	0.80	9	2	6	83
	WyL2	0.14	0.01	0.04	0.49	0.68	21	2	6	71
	WyR1	0.15	0.02	0.06	0.57	0.80	18	2	8	72
	WyR1	0.11	0.01	0.04	0.54	0.71	15	2	6	77
	WyR1	0.11	0.01	0.05	0.53	0.71	16	2	7	75
	WyR2	0.15	0.01	0.05	0.49	0.70	21	2	7	71
	WyNa	0.02	0.00	0.05	1.14	1.21	2	0	4	94
	WyNa	0.01	0.00	0.02	1.21	1.24	1	0	2	97
	WyNa	0.03	0.00	0.06	0.89	0.98	3	0	6	91
	WyMg	0.01	0.01	0.79	0.00	0.81	1	1	98	1
	WyK	0.03	0.58	0.08	0.02	0.72	5	81	11	3
	WyCa	0.87	0.00	0.04	0.01	0.92	95	0	4	1

3.5 Element analyses

3.5.1 Inductively Coupled Plasma – Atomic Emission Spectrometry (ICP/AES)

The bulk material and the corresponding homo-ionic dialysed clay fractions (< 2 μm) were analyzed for major element composition, using standard ICP-AES technique at an ISO 9002 accredited laboratory (Acme Analytical Labs). Sample pulps were fused using LiBO2 and dissolved in dilute nitric acid prior to analysis. Loss of ignition (LOI) was determined gravimetrically by ignition to 1,000°C. The results are shown for the bulk material in Table 3-4 and for the clay fraction in Table 3-5.

Table 3-4. The chemical composition, expressed as weight percent of major oxides, of the bulk materials. ICP/AES and Leco analyses.

Material	SiO_2	Al_2O_3	Fe_2O_3	MgO	CaO	Na_2O	K_2O	TiO_2	P_2O_5	LOI	C	S	Sum
StR1	52.4	15.1	12.6	2.1	1.6	0.1	0.7	2.9	0.5	11.6	0.1	< .01	99.8
StR1	52.7	15.0	12.5	2.1	1.6	0.1	0.7	2.9	0.5	11.7	0.1	< .01	99.9
SkR1	53.3	18.4	11.3	2.2	1.1	0.2	2.5	1.0	0.1	10.0	0.1	0.0	100.2
RoR1	46.6	12.9	13.0	2.6	5.8	0.2	1.0	4.1	0.8	12.7	1.0	0.0	100.1
DnR1	44.1	25.2	9.9	1.1	0.7	0.1	1.4	1.3	0.1	15.5	0.1	0.0	99.7
ÖlR1	53.6	14.0	11.1	3.6	2.3	1.8	1.6	3.1	0.1	8.5	0.6	0.9	99.8
HoR1	58.1	15.8	9.1	3.2	0.7	1.3	2.9	0.8	0.1	7.4	0.3	0.1	99.5
RöR1	45.4	18.5	9.6	2.4	5.6	0.4	2.8	0.9	0.1	13.5	1.3	0.0	99.8
FrR1	60.9	17.3	6.4	1.9	0.4	1.1	3.1	0.9	0.1	7.6	0.6	0.5	99.7
MiR1	48.3	15.7	4.6	2.9	5.4	0.7	0.8	0.7	0.1	20.0	1.0	0.7	99.3
Ku36R1	53.1	16.0	11.1	3.8	2.3	1.5	0.2	0.8	0.5	10.8	0.2	0.0	100.1
Ku37R1	53.0	18.5	10.2	2.7	1.0	2.9	0.1	0.9	0.1	10.3	0.3	0.1	99.8
Ku38R1	53.9	17.5	10.1	2.4	1.3	2.3	0.1	1.7	0.1	10.1	0.3	0.1	99.6
Ku39R1	52.1	18.0	11.2	3.6	1.3	1.7	0.2	0.9	0.1	10.5	0.1	0.0	99.6
Ku39R1	52.6	18.2	11.1	3.6	1.3	1.6	0.2	0.9	0.1	10.6	0.1	0.0	100.2
Ku40R1	47.1	18.3	12.5	1.8	0.7	2.0	0.1	1.9	0.1	15.4	0.2	0.1	99.8
WySt	58.7	19.2	4.0	2.5	1.5	2.4	0.5	0.2	0.1	10.4	0.5	0.3	99.5
WyL1	61.4	19.2	3.6	2.3	1.2	2.0	0.5	0.1	0.1	9.2	0.3	0.3	99.4
WyL2	62.2	18.4	3.7	2.2	1.2	1.8	0.5	0.1	0.0	9.2	0.3	0.3	99.4
WyR1	57.3	18.5	3.6	2.3	1.3	2.0	0.5	0.2	0.0	13.7	0.3	0.3	99.7
WyR1	59.9	19.6	3.9	2.4	1.4	2.2	0.6	0.2	0.1	9.2	0.4	0.3	99.5
WyR1	58.5	19.1	3.8	2.4	1.4	2.1	0.5	0.2	0.0	11.9	0.3	0.3	100.1
WyR2	61.2	19.2	3.6	2.3	1.3	1.9	0.5	0.1	0.1	9.0	0.3	0.3	99.4
WyR2	60.7	19.2	3.6	2.3	1.3	1.9	0.5	0.1	0.1	9.7	0.3	0.3	99.5

Table 3-5. The chemical composition, expressed as weight percent of the major oxides, of the purified and sodium-exchanged, clay fractions. ICP/AES and Leco analyses. * indicate single dialysis (section 2.8.2).

	SiO_2	Al_2O_3	Fe_2O_3	MgO	CaO	Na_2O	K_2O	TiO_2	LOI	Tot C	Tot S	Sum
DnNa	44.9	26.2	9.5	0.9	0.0	1.3	1.3	1.2	14.0	0.2	0.0	99.7
RoNa	51.9	15.5	12.5	2.5	0.6	2.5	0.4	4.8	8.4	0.2	< .01	99.9
SkNa	51.6	18.7	13.1	2.1	0.0	1.6	2.0	0.9	9.6	0.1	0.0	99.8
StNa	50.5	18.3	12.0	1.9	0.4	2.5	0.5	3.5	9.3	0.1	0.0	99.5
HoNa	56.6	15.7	10.3	3.1	0.2	2.1	2.2	0.7	8.2	0.2	0.0	99.4
RöNa	49.1	21.1	11.9	2.6	0.2	1.5	2.7	0.9	9.6	0.1	< .01	99.8
ÖlNa	53.5	13.3	12.4	4.1	0.5	2.6	0.9	2.8	9.3	0.6	0.0	99.7
FrNa	52.6	22.1	6.9	2.3	0.1	1.8	3.1	1.0	9.5	0.8	0.2	99.6
Ku36Na	56.7	17.2	8.8	3.6	0.3	3.1	0.1	0.4	9.3	0.0	< .01	99.6
Ku37Na	53.6	18.7	10.6	2.3	0.2	2.4	0.1	0.5	11.7	0.1	< .01	100.1
Ku38Na	51.9	19.3	10.2	2.1	0.4	2.4	0.0	1.3	12.1	0.1	< .01	99.8
Ku39Na	56.0	18.7	8.5	3.3	0.2	3.0	0.2	0.5	9.7	0.0	< .01	100.1
Ku40Na	50.4	21.2	11.8	1.6	0.0	2.7	0.1	1.4	10.7	0.2	< .01	100.0
MiCa*	50.2	17.4	3.9	2.6	2.6	0.0	0.5	0.7	21.6	0.1	0.0	99.4
MiCa	51.0	17.9	3.9	2.6	2.6	0.0	0.5	0.7	20.4	0.1	0.0	99.7
MiNa*	53.0	18.5	4.0	2.7	1.9	1.2	0.5	0.7	17.4	0.2	0.0	100.1
MiNa	59.6	21.9	4.6	3.1	0.1	3.1	0.5	0.8	6.3	0.4	0.0	100.2
MxCa	57.4	19.9	3.6	2.3	2.6	0.1	0.1	0.1	13.7	0.2	0.0	99.8
MxCa	53.8	18.2	3.4	2.1	2.4	0.1	0.1	0.1	19.8	0.2	0.0	100.0
MxK	60.3	20.7	3.9	2.5	0.1	0.1	4.5	0.1	7.8	0.1	0.0	100.0
MxK	58.6	19.8	3.7	2.5	0.1	0.1	4.0	0.1	10.8	0.1	0.0	99.7
MxMg	56.8	19.6	3.6	3.9	0.0	0.1	0.1	0.1	15.3	0.1	0.0	99.7
MxMg	53.4	17.9	3.3	3.8	0.0	0.1	0.1	0.1	21.2	0.1	0.0	99.9
MxNa	61.0	21.3	3.9	2.5	0.1	2.6	0.1	0.1	8.5	0.2	0.0	100.1
MxNa	58.9	20.1	3.6	2.4	0.1	2.5	0.1	0.1	11.8	0.1	0.0	99.6

3.5.2 Specific carbon and sulfur analyses

The bulk materials were dried to constant weight at 105°C and the total carbon content was determined by stepped heating of the samples from 100 to 1,000°C using a Leco multiphase carbon analyzer (RC412) equipped with an IR-detector for CO_2.

The output from the detector was recorded continuously, which allows the sources of carbon to be differentiated by the temperature at which they oxidize/volatilize. CO_2 evolved below 550°C was allocated to organic matter, and CO_2 evolved above 550°C to carbonates. The results are reported as weight percentage C of the dry matter in Table 3-6.

Total sulfur was determined by combustion at 1,200°C in a Leco furnace. The sulfate content was determined by analysis of a separate sample, which had been ignited at 800°C. The presented sulfide content was calculated as the difference between total S and the sulfate S content. The sulfide fraction will include also elemental and organic sulfur, if present. The results are reported in Table 3-7.

Table 3-6. Carbon content of the bulk materials. T < 550°C and T > 550°C indicate carbon evolved below and above 550°C, respectively. The maximum possible $CaCO_3$ content was calculated by allocating C evolved above 550°C to Ca carbonate. All results in weight percent of the total dry mass.

	Material	Total C	Organic C T < 550°C	Carbonate C T > 550°C	max $CaCO_3$
Cz	DnR1	0.13	0.10	0.03	0.25
	RoR1	0.91	0.02	0.89	7.41
	SkR1	0.14	0.11	0.03	0.25
	StR1	0.10	0.06	0.04	0.32
De	HoR1	0.29	0.25	0.04	0.34
	RöR1	1.15	0.15	1.00	8.31
	ÖlR1	0.53	0.53	0.00	0.00
Ge	FrR1	0.60	0.60	0.00	0.00
Gr	MiR1	1.14	0.24	0.90	7.50
	MiR1	1.14	0.22	0.92	7.66
In	Ku36R1	0.20	0.02	0.18	1.50
	Ku36R1	0.23	0.10	0.13	1.08
	Ku37R1	0.77	0.40	0.37	3.08
	Ku37R1	0.78	0.58	0.20	1.67
	Ku38R1	0.43	0.17	0.26	2.17
	Ku38R1	0.51	0.40	0.11	0.92
	Ku39R1	0.03	0.02	0.01	0.10
	Ku39R1	0.04	0.03	0.01	0.06
	Ku40R1	0.26	0.24	0.02	0.17
	Ku40R1	0.26	0.22	0.04	0.33
Wy	WyR1	0.38	0.20	0.18	1.50
	WyR1	0.39	0.21	0.18	1.50
	WyR1	0.42	0.28	0.14	1.17
	WyR1	0.40	0.25	0.15	1.25
	WyNa	0.15	0.14	0.01	0.05

Table 3-7. Sulfur content in all bulk materials. The maximum pyrite content was calculated by allocating sulfide S to FeS_2. All figures in weight percent of total mass.

	Material	S in sulfate	S in sulfide	max Pyrite
Cz	RoR1	0.00	0.00	0.00
	SkR1	0.01	0.03	0.06
	StR1	0.00	0.00	0.00
	StR1	0.00	0.00	0.00
De	HoR1	0.04	0.00	0.00
	RöR1	0.01	0.00	0.00
	ÖlR1	0.39	0.51	0.96
Ge	FrR1	0.15	0.33	0.62
	FrR1	0.18	0.38	0.71
	FrR1	0.18	0.37	0.69
	FrR1	0.09	0.35	0.65
	FrR1	0.08	0.40	0.74
	mean Friedland R1			0.68
Gr	MiR1	0.42	0.22	0.41
	MiR1	0.38	0.29	0.54
	MiR1	0.38	0.25	0.47
	MiR1	0.38	0.27	0.51
	MiR1	0.39	0.30	0.57
	MiR1	0.39	0.20	0.38
	mean Deponit CA-N R1			0.48
In	Ku36R1	0.03	0.00	0.00
	Ku37R1	0.11	0.00	0.00
	Ku38R1	0.04	0.00	0.00
	Ku39R1	0.03	0.00	0.00
	Ku40R1	0.05	0.05	0.09
US	WyR1	0.20	0.13	0.24
	WyR1	0.22	0.16	0.30
	WyR1	0.27	0.04	0.08
	WyR1	0.14	0.14	0.26
	WyR1	0.23	0.16	0.31
	mean MX-80 R1			0.24

3.5.3 Free iron oxides in the clay fraction

Iron derived from so called free iron oxides, e.g. goethite, lepidocrocite, hematite, maghemite, can be extracted selectively using the CBD method /Mehra and Jackson 1960/. The method employs sodium dithionite ($Na_2S_2O_4$) for the reduction, sodium bicarbonate as a buffer at neutral pH, and sodium citrate as a chelating or complexing agent for ferrous/ferric iron. The basis of operation at a neutral pH without precipitation of FeS is the strong chelating action of citrate.

The treatment follows the recommendations of /Jackson 1975/. 0.3M Na-citrate and 1M $NaHCO_3$ were added at a ratio of 8:1 to the pre-weighed, dried clay sample in a centrifuge tube. The temperature was brought to 75–80°C in a water bath. Na-dithionite was added by

means of a spatula and the mixture was stirred constantly for one minute and then occasionally for 5 minutes. The addition of dithionite was repeated twice, i.e. three times until no reddish coloration of the clay was visible. After centrifugation the supernatant was collected in a volumetric flask. Fe was determined by ICP/AES.

3.6 Quantitative Greene-Kelly test

The samples were tested according to /Greene-Kelly 1953/ to differentiate between montmorillonite (octahedral charge > tetrahedral charge) and beidellite (octahedral charge < tetrahedral charge). The basis of the test is the loss of expansion and cation-exchange properties exhibited by montmorillonite but not by beidellite when saturated with lithium and heated. Thus, the irreversible collapse of a smectite mineral to c. 9.5 Å after Li-saturation and heating is the criterion for montmorillonite identification and is attributed to the neutralisation of the negative layer charge by migration of the lithium ions from interlayer positions to vacant octahedral sites /Hofman and Klemen 1950/.

Table 3-8. CBD extractable iron in the purified and sodium exchanged clay fractions expressed as Fe_2O_3. The total iron from Table 3-5 is shown together with the calculated fraction of CBD extractable iron. * The RoR1 analysis was made on bulk material.

	Material	CBD extractable Fe_2O_3 Weight-%	Total Fe_2O_3 Weight-%	Fraction CBD extractable Fe_2O_3
Cz	DnNa	2.5	9.5	0.26
	RoR1*	2.5	12.5	0.20
	SkNa	1.4	13.1	0.11
	StNa	0.6	12.0	0.05
De	HoNa	0.3	10.3	0.03
	RöNa	3.5	11.9	0.29
	ÖlNa	1.2	12.4	0.10
Ge	FrNa	0.3	6.9	0.05
Gr	MiNa	0.3	4.6	0.06
In	Ku36Na	0.6	8.8	0.07
	Ku37Na	1.6	10.6	0.15
	Ku38Na	0.4	10.2	0.04
	Ku39Na	0.8	8.5	0.09
	Ku40Na	2.4	11.8	0.20
US	Wy-Na	0.1	3.6	0.02

The experimental procedure follows the recommendations of /Lim and Jackson 1986/. The bentonite samples were washed three times with aqueous 3 M LiCl and twice with 0.01 M LiCl in 90% alcohol. Oriented mounts were prepared by smearing the thick paste on glass slides

(preferably silica slides). The clay mounts were allowed to dry slowly at room temperature, and were then heated at 250°C overnight. After cooling the Li-clays were placed in a desiccator containing glycerol for solvation, and heated at 90°C for 16 hours. The clay mounts were X-ray scanned using the same instrumental settings as described above. The expansion behavior is expected to give a qualitative indication of the original layer charge location.

The method was extended by measuring the CEC as described in section 3.3 after Li-saturation and heating according to the Green-Kelly test and the CEC were compared with that of the non-treated sample. A change in exchange capacity is assumed to reflect a change of the charge emanating from the octahedral sheet, which is expected to be electrically neutralized by Li uptake. The remaining charge can consequently be assumed to origin from the tetrahedral sheet. The bulk samples were treated once with 3 M LiCl solution, washed with de-ionized water and the clay fraction was separated by centrifugation. The clay fraction was again treated with 3 M LiCl solution and washed with water just until incipient dispersion. The sample was placed in a porcelain crucible and heated to 250°C over night. The sample was ground and dried at 70°C, and the CEC was determined by the Cu-trien method (section 3.3).

Table 3-9. CEC of Li exchanged clay fractions before and after treatment according to the Green-Kelly test. All figures in eq/kg dry mass.

		Original Cu-CEC	Cu-CEC after heating (Green-Kelly)			CEC loss
		mean	no 1	no 2	mean	
Cz	DnLi	0.40	0.14	0.09	0.12	0.28
	RoLi	0.74	0.32	0.36	0.34	0.41
	SkLi	0.47		0.31	0.31	0.16
	StLi	0.76	0.53	0.48	0.50	0.26
	HoLi	0.58	0.24	0.24	0.24	0.34
	RöLi	0.40	0.31	0.24	0.27	0.13
Da	ÖlLi	0.67	0.36	0.41	0.38	0.29
Ge	FrLi	0.34	0.10	0.21	0.15	0.19
Gr	MiLi	0.86	0.17	0.21	0.19	0.67
In	Ku36Li	1.00	0.17	0.21	0.19	0.81
	Ku37Li	0.88	0.52	0.49	0.50	0.37
	Ku38Li	0.90	0.57	0.53	0.55	0.34
	Ku39Li	0.99	0.25	0.21	0.23	0.76
	Ku40Li	0.88	0.63	0.61	0.62	0.27
US	WyStLi	0.88	0.03	0.05	0.04	0.84
	WyL1Li	0.88	0.01	0.01	0.01	0.87
	WyL2Li	0.86	0.06	0.08	0.07	0.79
	WyLi	0.86	0.08	0.07	0.07	0.79

4 Physical tests, techniques and results

4.1 Grain size

Grain size of soil materials may be split in at least two different concepts. One being the size of the more or less dry grains, which may be conglomerates of smaller particles only held together under dry conditions. The other is the size of the particles after dispersion of the material in water. For many soils, the difference is negligible, but for bentonite materials, the difference is fundamental since the grains will deform, disperse and in some respect dissolve in contact with water, depending on the conditions. The size of the dry grains has some importance with respect to air evacuation during block production and dust problems, but the original size has in principle no effect on the function of a buffer. What might be called the fundamental (dispersed in water) grain-size distribution has been determined in this study.

A Sedigraph 5000 ET particle analyzer (Micromeritics) was used and the instrument measures the particle size distribution using a finely collimated beam of low energy X-rays which passes through a container with the suspended sample to a detector. The change in intensity of the X-ray beam is recorded during the progress of the sedimentation and this X-ray pulse count is used to derive the particle size distribution expressed as the mass percent at given particle diameters.

Bulk samples were dispersed in 0.5% sodium pyrophosphate by ultra-sonic treatment for 15 minutes and left on a magnetic stirrer for at least 2 hours prior to analysis. Previously Na-saturated and dialyzed samples were dispersed in de-ionized water only. Cumulative particle size curves were recorded over the size range 60–1 μm. The resulting graphs are shown in Figure 4-1 to Figure 4-4.

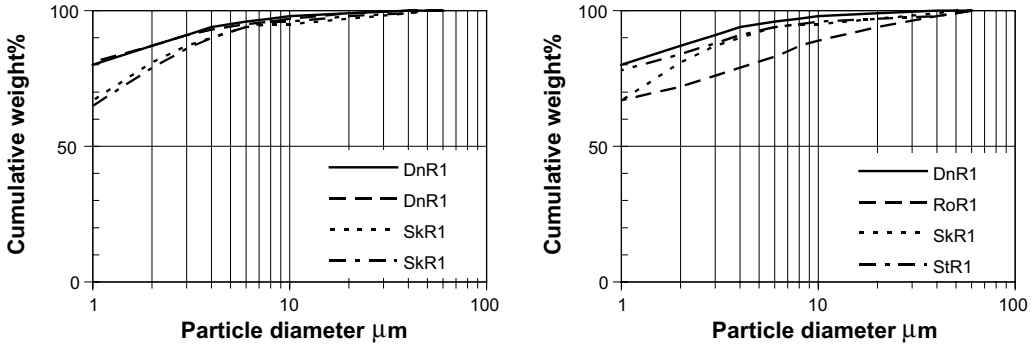

Figure 4-1. *Grain size distribution of the Czech reference materials. Illustration of the repeatability of the Dnesice and Skalna materials (left), and single scans of the Dnesice, Rokle, Skalna and Strance materials (right).*

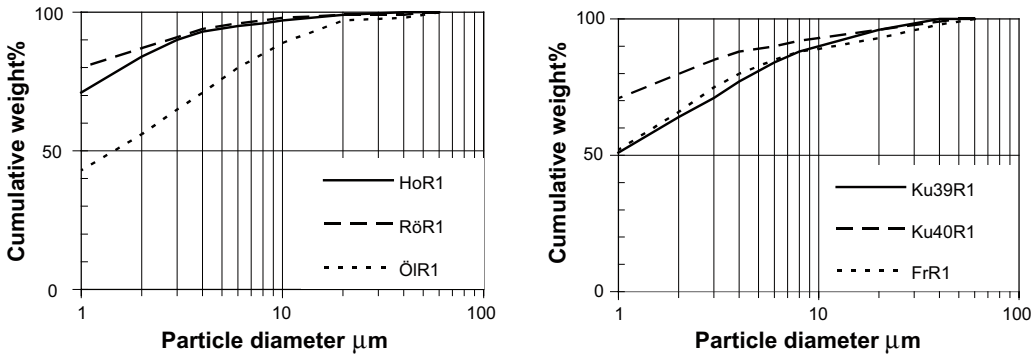

Figure 4-2. *Grain size distribution of the Danish Holmehus, Rösnäs and Ölst reference materials (left), and the Indian Kutch 8939 and 8940 reference materials and the German Friedland reference material (right).*

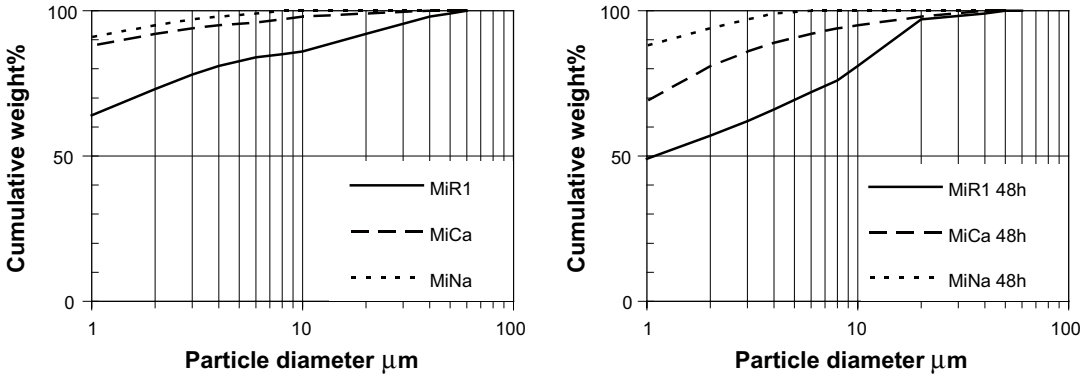

Figure 4-3. *Grain size distribution of the Milos Deponit CA-N material and the corresponding purified and ion-exchanged calcium and sodium materials (left). Results from the same materials after 24 h rest (right).*

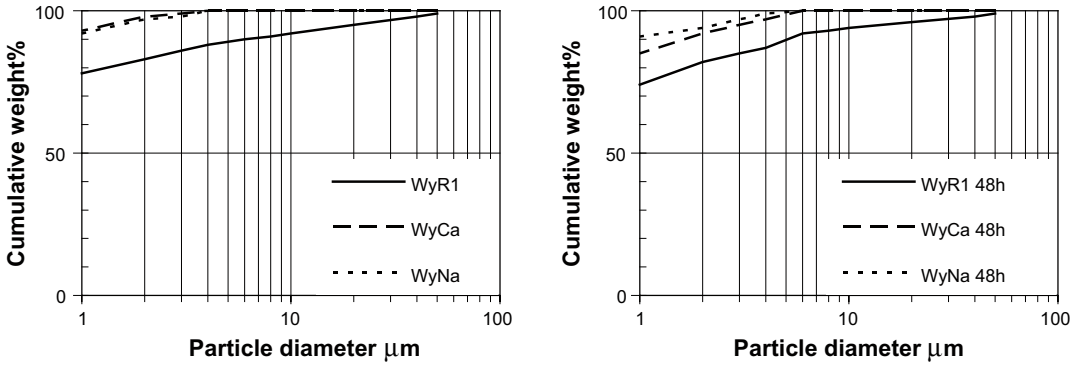

Figure 4-4. *Grain size distribution of the Wyoming MX-80 reference material and the purified and the corresponding ion-exchanged calcium and sodium materials (left). Results from the same materials after 24 h rest (right).*

4.2 Grain density

Traditionally, grain density is determined in pycnometers, but for swelling clays this is problematic and volumetric flasks were used instead. The mass of dry and water filled 50 ml flasks was individually determined by means of an analytical balance, and the volume of the flasks was calculated based on the water density at the ambient temperature. Approximately 15 g of the different bentonite samples were dried at 105°C for 24 h in a ventilated oven in order to remove adsorbed water. The samples were taken from the oven and quickly poured into the volumetric flasks, which were sealed, cooled to room temperature and weighed. Since contact with pure water leads to massive swelling of the bentonite, the tests series were run with kerosene, 1.0 or 3.0 M NaCl solutions, and in some cases also with 1.0 M $CaCl_2$ solution. A sufficient portion of the test liquid was poured into the flasks in order to compleately covered the test material, and the flasks were again stoppered. The flasks were repeatedly shaken and rotated in order to facilitate the escape of air from the bentonite. After 24 h the flasks were again rotated and thereafter filled up to the graduation mark with additional test liquid. The total mass of the flasks, including bentonite sample and liquid was determined. Two reference flasks filled with only the actual test liquid were used parallel to the test samples in order to determine the liquid density at the ambient temperature. The grain density (D_s) was calculated from:

$$D_s = \frac{m_s}{V_{tot} - \frac{m_{tot} - m_{s+f}}{D_l}}$$

where m_s is the mass of the solids, V_{tot} is the total volume, m_{tot} is the total mass, m_{s+f} is the mass of the solids and flask, and D_l is the density of the liquid. The precision of the calculated grain density is mainly determined by the by the calibration of the volumetric flasks, and by the leveling of the liquid menisci, since the masses can be determined with high precision. The scatter for a specific liquid/solid was generally within the range of ± 10 kg/m^3. The results are reported in Table 4-1.

4.3 Specific surface area

The determinations of specific surface area were made by use of BET standard techniques on a Micromeritics ASAP 2400 instrument, in which the samples were degassed under vacuum, weighed and cooled by external liquid nitrogen. Principally, the nitrogen gas pressure is successively increased from vacuum to 0.995 atm, which leads to physico-sorption on the material surfaces, and an adsorption isotherm is recorded. The nitrogen pressure is reduced back to vacuum and a desorption isotherm is recorded. Specific surface area, pore volume and pore size distribution can be derived from the results, but only the specific surface area is reported here. The MX-80, Deponit CA-N, and the Friedland reference materials, and the corresponding purified and ion-exchanged Na and Ca forms were analyzed in this study (Figure 4-5).

The Wyoming MX-80 materials were also analyzed in the ”as received” state (milled), after wetting and drying in 105°C oven overnight (dried), and finally, after dispersion of 10 g in 1 L de-ionized water, freezing of the suspension at –20°C and subsequently freeze-drying at approximately 2 Pa pressure (freeze dried) (Figure 4-6). The latter material was characterized by an initially very fluffy structure in which the 10 g of clay had a volume of almost 1 L.

Table 4-1. Compilation of test results performed for all the analyzed reference materials in the various liquids. Figures show the grain density in kg/m^3.

Origin	Sample	kerosene	1 M CaCl2	1 M NaCl	3 M NaCl
Cz	DnR1	2,634		2,765	
	RoR1	2,788		2,920	
	SkR1	2,687		2,786	
	StR1	2,680		2,841	
De	HoR1	2,757		2,796	
	RöR1	2,712		2,814	
	ÖlR1	2,731		2,805	
Ge	FrR1	2,751	2,772	2,785	2,776
	FrR1	2,745	2,781	2,789	2,776
Gr	MiR1	2,638	2,763	2,751	2,740
	MiR1	2,637	2,784	2,751	2,729
In	Ku36R1	2,691		2,862	
	Ku37R1	2,716		2,860	
	Ku38R1	2,701		2,880	
	Ku39R1	2,731		2,907	
	Ku40R1	2,750		2,937	
US	WyR1	2,621	2,761	2,776	2,754
	WyR1	2,625	2,777	2,777	2,752

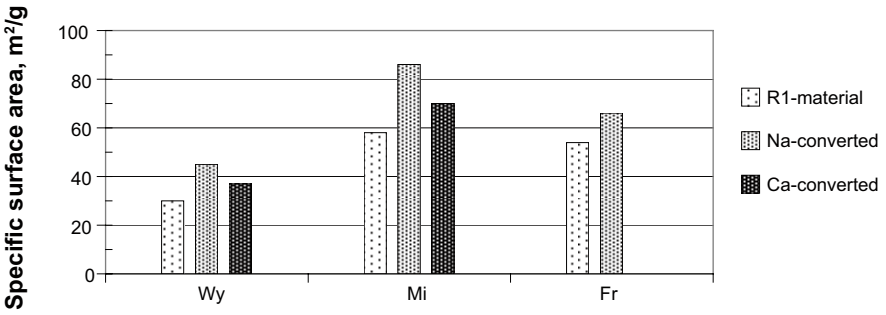

Figure 4-5. *Specific surface area according to BET measurements of the MX-80 material (Wy), the Deponit CA-N material (Mi), and the Friedland material (Fr), respectively. All three materials were analyzed as delivered (R1-material), after purification and ion exchange to sodium state (Na-converted), and the Wy and Mi material were also ion exchanged to calcium state (Ca-converted).*

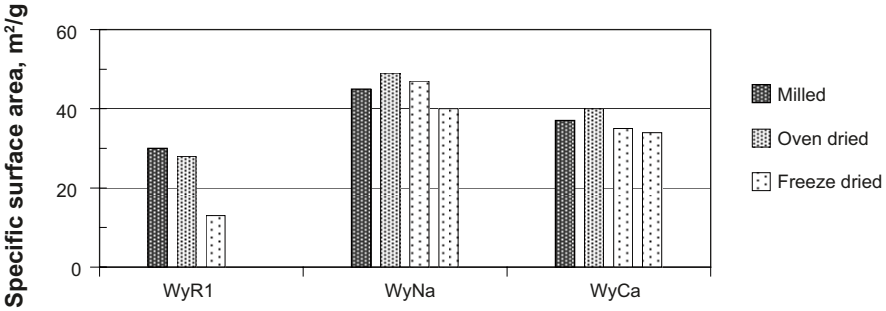

Figure 4-6. *Specific surface area according to BET measurements of the MX-80 material in the reference state (WyR1), after purification and ion-exchange to sodium state (WyNa) and to calcium state (WyCa). All three materials were pretreated by milling (Milled), oven-drying (Oven dried) and freeze-drying (Freeze dried), respectively.*

4.4 Swellling pressure

4.4.1 General

In bentonite, the conditions are extraordinary compared to other soil materials due to the electrically negatively charged montmorillonite layers and the charge compensating cations in the interlayer space (Figure 3-1), and an analogue with salt is relevant to some extent.

Ions in a water solution reduce the water chemical potential, and a concentration difference between solutions normally leads to water transport from the high potential (low concentration) to the low potential volume. In parallel, ions will diffuse from the high concentration to low concentration volume, and the equilibrium condition, i.e. equal chemical potentials, leads to uniform ion concentration.

In bentonite, water molecules can be intercalated between the individual montmorillonite layers to create an interlayer ionic solution. However, the cations cannot freely diffuse away from the mineral surface because of the demand for electrical neutrality. Water will consequently be transported into the inter-layer space, if water with a higher chemical potential is available, and the interlayer distance will increase, which is synonymous with bentonite swelling. This water uptake will continue until the chemical potentials equal, which in the case of a pure water source theoretically leads to infinite swelling /Kryut 1952/. The extent of water uptake in bentonite may thereby be orders of magnitude larger and have a different character compared to other soil materials.

In a fixed total volume, the water uptake into the interlayer space will reduce the volume of initially larger pores. The uptake is forced to stop when the total available pore volume is completely filled with introduced water. At this full water saturation condition, water will

continue to move in order to level the interlayer ion concentration in the system. The interlayer distances will thus increase in interlayer space with high ion concentration on the expense of interlayer space with low concentration, and the final distances will be a function of the local montmorillonite layer charge. The remaining difference in ion concentration, between the high concentration interlayer solution and the water supplying solution, leads to an osmotic pressure build-up in the clay (swelling pressure), which equals the chemical potential of water in the system. The homogenization of the pore size, due to the leveling of the chemical potential, may be partly counteracted by mechanically stable structures, e.g. in volumes with complicated stacking of the montmorillonite layers, or in clusters of accessory minerals. In extreme cases the pore-water in such clusters may eventually be in equilibrium with the water supplying solution, without influence from the surrounding charge compensating cations in the montmorillonite.

The degree of final pore size homogeneity has been analyzed and extensively discussed in literature, and quite different conceptual and quantitative models have been proposed. The conditions are of importance since the pore-size distribution governs e.g. the possible transport of colloids. The degree of homogeneity may to some extent be revealed by the hydraulic conductivity. The main reason for determination of this property is though the potential material transport by advective flow.

The volume of a KBS-3 deposition hole and the corresponding buffer mass are predetermined, and the mean interlayer cation concentration can consequently be calculated. The total pore volume in the buffer in one deposition hole is around 5,250 liters, and the bentonite mass is around 19,250 kg. Several bentonites in this study have CEC values around 0.75 eq/kg clay material, which gives a total cation content of around 14,430 equivalents in each borehole. The mean cation concentration in such a system is consequently almost 3 M for monovalent ions if it is in equilibrium with pure water.

However, the concentration of the charge compensating cations is not evenly distributed between the 2:1 layers, but decreases approximately exponentially with distance from the montmorillonite surfaces. The ion concentration profile, and thereby the resulting osmotic pressure, may ideally be calculated by use of the Poisson-Boltzmann equation for monovalent ions. At buffer density (2,000 kg/m^3 at full water saturation) the osmotic pressure in combination with hydration of the cations and montmorillonite surfaces are expected to generate swelling pressures in the range of 5 to 10 MPa for the CEC of 0.75 eq/kg /Karnland et al. 2005/.

4.4.2 Experimental

Small sample holders (4.8 cm^3) were used in order to measure the swelling pressure of a single sample successively exposed to pure water, and the test solutions (Figure 4-7). The purpose with the time consuming successive exposure was to ensure that the swelling pressure changes were only dependant on the solution concentration, and not on artifacts in density determination. The small scale was used in order to reach equilibrium reasonably fast.

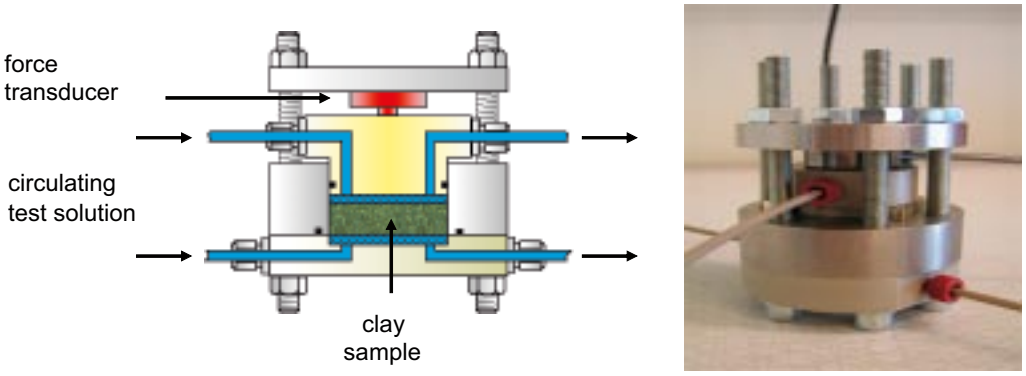

Figure 4-7. *Schematic drawing and photo of the sample holder for swelling pressure and hydraulic conductivity tests series.*

The dense samples were compacted in a special device to the intended densities and thereafter placed in the cylindrical sample holders, while the low density samples were compacted directly in the sample holders. The piston, pressure transducer and upper lid were attached and fixed in order to give the pre-defined density. De-ionized water was slowly circulated intermittently behind the bottom filters, in order to start the water saturation of the samples from the bottom side, and thereby let original air out through the upper filters. After approximately one week, the water was intermittently circulated also in the upper filters. At equilibrium, i.e. at constant measured swelling pressure, the water was changed to 0.1 M chloride solution with the same cation as the dominating cations in the clay (Na^+ or Ca^{2+}), pending a new equilibrium. The concentration of the external solutions was thereafter increased in steps at pressure equilibrium, generally to 0.3, 1.0 and 3.0 M. Finally, the concentration was changed back to 0.1 M or 0.3 M in order to check the reversibility. Results from one exposure sequence in one of the Indian Kutch 8940 samples are shown in Figure 4-8 as an example. The pressure increase after e.g. 30 to 37 days represents the effect of the water pressure increase during hydraulic conductivity measurement.

The swelling pressure in bentonite increases approximately exponentially with increasing sample density. The density determination is consequently critical, especially at high densities.

The sample holders was therefore disconnected after each test and the samples were removed and split in order to determine the water ratio (w), and sample density (D_d) according to:

$$w = \frac{m_w}{m_s}$$

Where m_w is the mass loss due to drying for 24 h in 105°C, and m_s is the remaining solid mass.

The dry density (D_d), defined as the mass of the solids divided by the total volume, was calculated from water ratio data according to:

$$D_d = \frac{D_s \cdot D_w}{D_s \cdot w + D_w}$$

where D_s is the density of the solid grains (separately determined in section 4.2), and D_w is the density of water (1,000 kg/m^3).

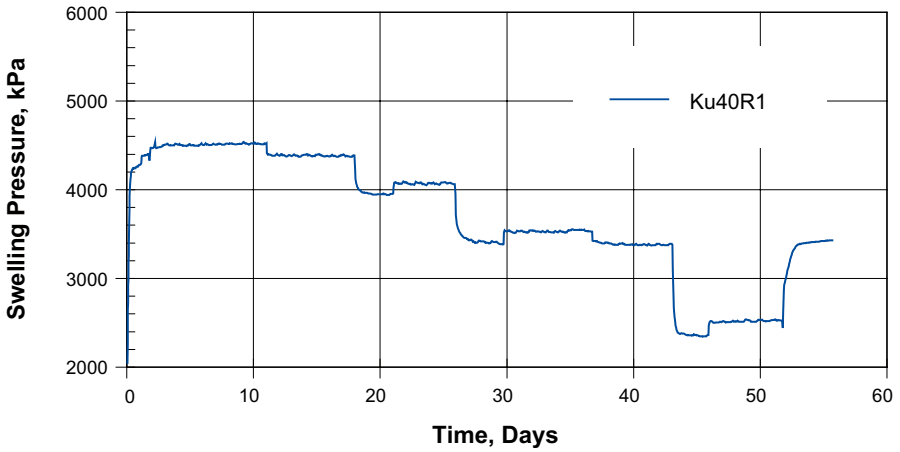

Figure 4-8. *Example of swelling pressure evolution during the successive exposure to pure water 0.1, 0.3. 1.0, 3.0, 0.3 M NaCl in the Indian Kutch 3940 sample at a dry density of 1,371 kg/m^3 (Table 4-6).*

Since the samples can be considered fully water saturated, the saturated density (D_m) was determined by submerging one half of the sample into paraffin oil. The dry density may be calculated from the saturated density according to:

$$D_d = \frac{D_m - D_w}{1 - \frac{D_w}{D_s}}$$

The presented dry density values are generally calculated from the water ratio determinations and checked against the measured saturated density values. The release of confining pressure during the dismantling of the test cells lead unavoidably to a minor water uptake from the filters. Fast and similar handling during the dismantling of the samples was the only countermeasure taken to minimize this possible artifact. The equilibrium pressure conditions from all materials as a function of sample density are shown in Table 4-2 to Table 4-7 and in Figure 4-9 to Figure 4-14.

Table 4-2. Swelling pressures in the Czech reference materials. The first column shows clay dry density (D_d) in kg/m³ and the following columns show the $CaCl_2$ concentrations (moles/L) in the test solutions successively in contact with the samples. Pressure values in kPa.

Material	D_d, kg/m³	H_2O	0.1 M	0.3 M	1.0 M	3.0 M	0.1 M
DnR1	849	10					
	1,386	360	340	320	270	210	330
	1,342	280	270	270	250	200	260
RoR1	816	50					
	1,156	523					
	1,474	7,150					
SkR1	936	43	36	36	36	28	36
	1,274	563	524	511	480	350	540
	1,565	6,300	6,270	6,260	6,100	5,400	6,300
StR1	949	83	75	75	75	74	75
	1,236	200	170	160	145	110	170
	1,618	5,500	5,300	5,200	4,700	3,600	4,900

Table 4-3. Swelling pressures in two of the Danish reference materials Holmehus and Rösnäs. The first column shows dry clay density (D_d) in kg/m³ and the following columns show the NaCl concentrations (moles/L) in the test solutions successively in contact with the samples. Pressure values in kPa.

Material	D_d, kg/m³	H_2O	0.1 M	0.3 M	1.0 M	3.0 M	0.1 M
HoR1	757	113	31	29	24	10	31
	1,264	970	720	700	630	410	760
	1,570	6,400	6,100	6,100	6,050	5,350	6,900
RöR1	901	15	5	5	5	5	15
	1,237	230	195	190	175	150	195
	1,595	3,100	3,000	2,900	2,800	2,500	3,000

Table 4-4. Swelling pressures in the Friedland reference material and the corresponding purified and sodium exchanged clay fraction. The first column shows dry clay density (D_d) in kg/m^3 and the following columns show the NaCl concentrations (mole/L) in the test solutions successively in contact with the samples. Pressure values in kPa.

Material	D_d, kg/m^3	H_2O	0.1 M	0.3 M	1.0 M	3.0 M
FrR1	816	45				
	1,174	110	85	75	50	35
	1,437	400	375	350	275	210
	1,576	1,400	1,250	1,200	1,000	850
FrNa	1,070	240	175	140	115	100
	776	80	40	20	5	4
	1,188	500	400	350	250	190
	1,432	1,640	1,400	1,300	1,100	875
	1,649	4,100	3,900	3,700	3,500	3,100
	1,774	8,960	8,700	8,600	8,300	7,700

Table 4-5. Swelling pressures in the Milos Deponit CA-N reference material and the corresponding purified and Na^+ and Ca^{2+} exchanged clay fraction. The first column shows dry clay density (D_d) in kg/m^3 and the following columns show the $CaCl_2$ concentrations (moles/L) in the test solutions successively in contact with the MiR1 and MiCa samples, and the NaCl concentrations in the test solutions in successive contact with the MiNa sample. Pressure values in kPa.

Matrial	D_d, kg/m^3	H_2O	0.1 M	0.3 M	1.0 M	3.0 M	0.1 M	1.0 M	0.1 M
MiR1	544	15	10						
	852	50	30	30	30	25			
	1,189	1,000	930	870	600	270			
	1,454	4,350	4,200	3,950	3,070	1,900			
	1,541	7,250	7,100	6,900	5,670	4,450			
	1,627	12,100	11,950	11,850	11,300	10,100			
MiNa	444	245	100	55	35	30	100	30	100
	794	600	380	185	90	60	365	90	360
	1,252	2,540	2,460	1,870	1,320	400	2,180	1,270	2,160
	1,532	12,360	11,730	11,370	10,810	9,380	11,480	10,680	11,500
	1,627	22,100	20,640	20,400	19,920	18,130	20,540	19,780	20,700
MiCa	522	13	0	0	0	0	0		
	807	95	80	80	70	45	80		
	1,225	1,680	1,600	1,510	1,150	360	1,570		
	1,547	12,320	12,060	11,900	11,250	9,300	12,000		
	1,628	23,000	22,700	22,500	21,800	19,500	22,800		
	1,653	28,850	26,500	26,200	25,500	23,000	26,500		

Table 4-6. Swelling pressures in the Indian reference materials Kutch 8936, 8939 and 8940, and in the purified and sodium exchanged clay fraction of the Kutch 8940 material. The first column shows dry clay density (D_d) in kg/m³ and the following columns show the NaCl concentrations (moles/L) in the test solutions successively in contact with the samples. Pressure value in kPa.

Material	D_d, kg/m³	H_2O	0.3 M	1.0 M	3.0 M	0.3 M
Ku36R1	1,229	1,360				
	1,425	6,800				
Ku39R1	1,245	1,570				
	1,420	5,540				
Ku40R1	1,272	1,040				
	1,464	5,900				
Ku40Na	830	404	110	32	10	47
	1,169	1,660	1,140	780	290	880
	1,371	4,400	4,000	3,400	2,500	3,430
	1,520	13,800	13,600	13,100	12,100	12,900

Table 4-7. Swelling pressures in the Wyoming MX-80 R1 reference material and the corresponding purified and sodium and calcium exchanged clay fraction. The first column shows dry clay density (D_d) in kg/m³ and the following columns show the NaCl concentrations (moles/L) in the test solutions successively in contact with the WyR1 and WyNa samples, and the $CaCl_2$ concentrations in the tests solutions in successive contact with the WyCa samples. Pressure values in kPa.

Material	D_d, kg/m³	H_2O	0.1 M	0.3 M	1.0 M	3.0 M	0.3 M	1.0 M	0.1 M
WyR1	517	61	35	23	16	12	23		
	761	156	123	68	37	26	79		
	1,202	1,020	1,000	800	550	100	770		
	1,461	4,190	4,240	4,000	3,150	1,240	3,690		
	1,539	7,590	7,590	7,380	6,340	4,550	6,910		
	1,641	12,470	12,350	12,170	11,520	10,220	12,020		
WyNa	458	232	115	70	44	38	115	43	112
	766	621	428	210	85	53	450	84	438
	1,249	2,248	2,125	1,634	1,074	213	2,025	1,079	1,985
	1,555	9,850	9,340	9145	8,270	6,520	9,240	8,230	9,210
	1,615	16,000	15,400	14,900	14,240	12,600	14,900	14,100	14,960
	1,717	27,600	26,500	25,980	25,430	23,910	26,000	25,290	26,000
WyCa	502	12	9	8	8	4	8		
	789	87	69	63	51	12	66		
	1,275	1,650	1,540	1,430	970	246	1,530		
	1,580	11,285	11,040	10,800	9,870	7,980	10,880		
	1,658	21,770	21,530	21,270	20,720	17,900	21,390		
WyMg	744	90							
	1,209	1,800							
	1,564	13,400							
WyK	778	195							
	1,154	600							
	1,567	5,300							

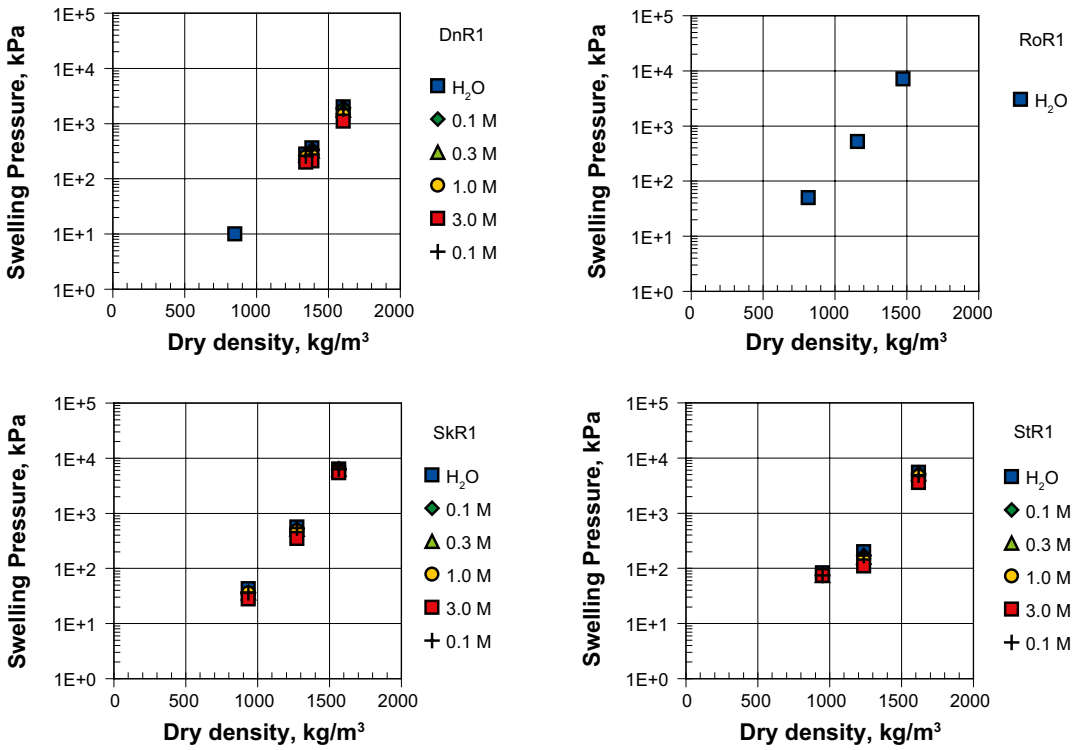

Figure 4-9. *Swelling pressures in the Czech reference materials Dnesice, Rokle, Skalna and Strance. The legends show the $CaCl_2$ concentrations in the test solutions successively in contact with the samples.*

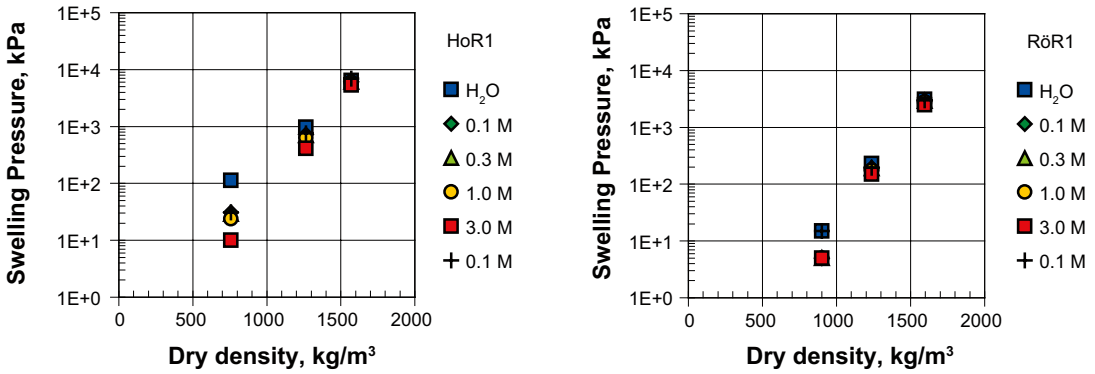

Figure 4-10. *Swelling pressures in the Danish reference materials Holmehus and Rösnäs. The legends show the NaCl concentrations in the test solutions successively in contact with the samples.*

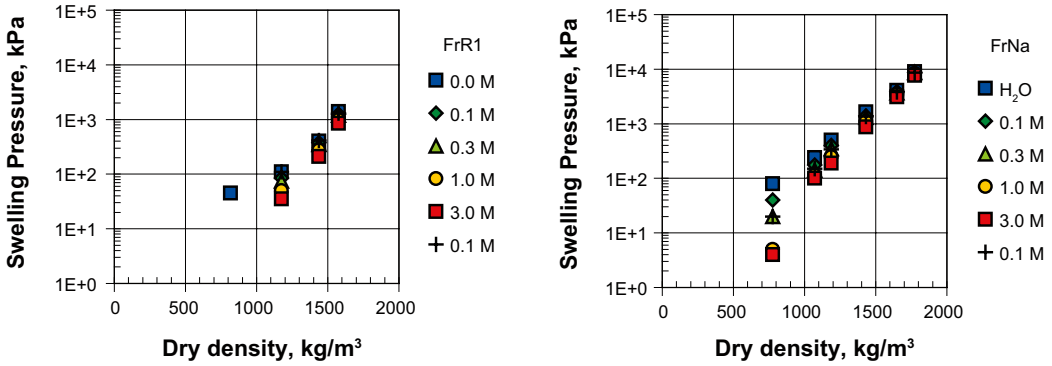

Figure 4-11. *Swelling pressures in the Friedland reference material (left) and the corresponding sodium exchanged and purified FrNa material. The legends show the NaCl concentrations in the test solutions successively in contact with the samples*

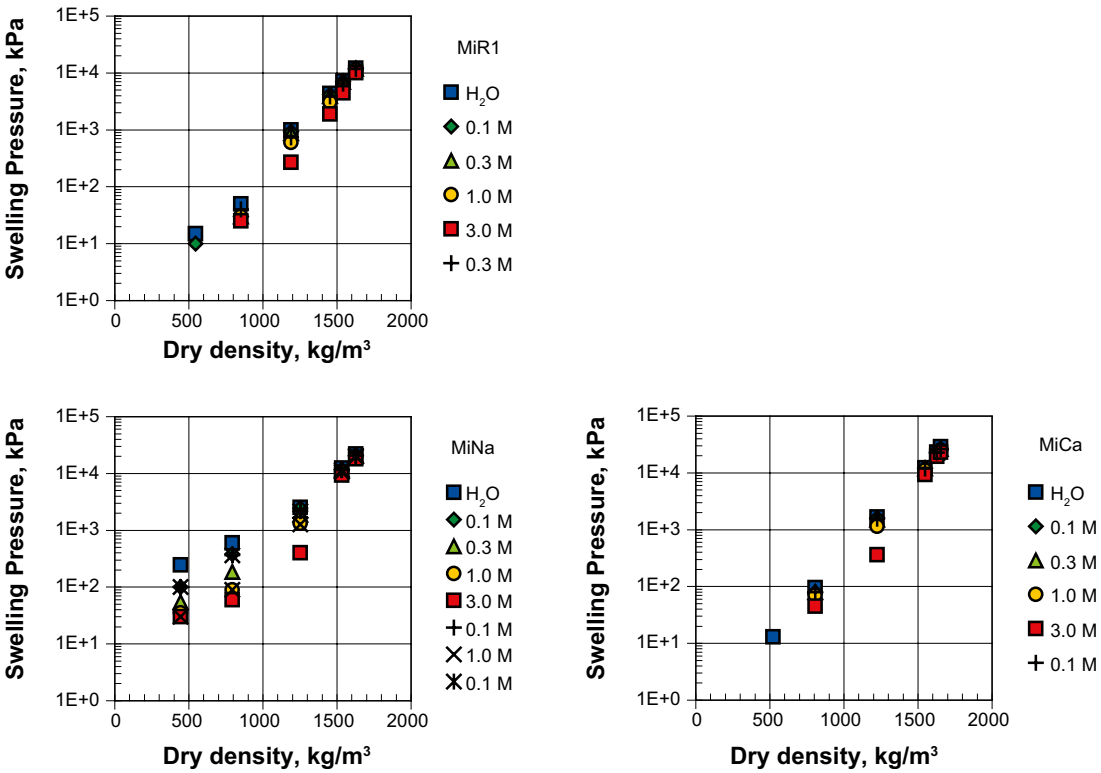

Figure 4-12. *Swelling pressures in the Milos Deponit CA-N reference material (upper) and the corresponding calcium (left) and sodium (right) converted and purified materials. The legends show the $CaCl_2$ concentrations in the solutions successively in contact with the MiR1 and MiCa samples, and the NaCl concentrations in the solutions successively in contact with the MiNa samples.*

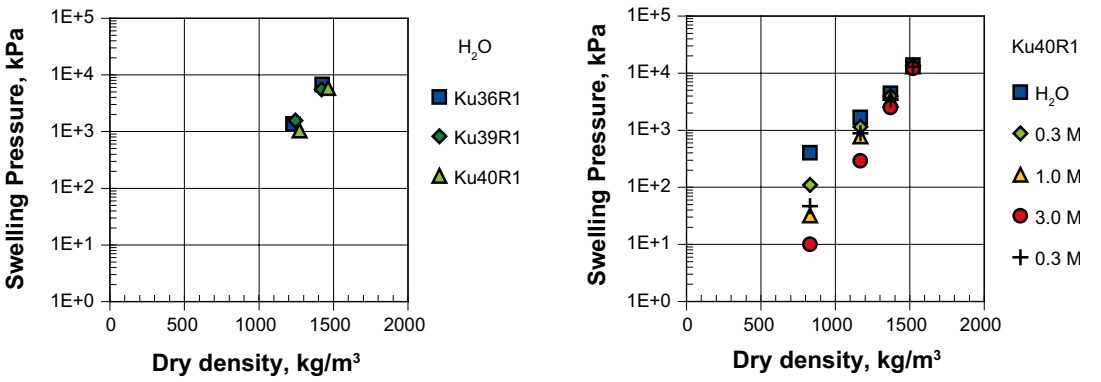

Figure 4-13. *Swelling pressures in the Indian Kutch 8936, 8939 and 8940 material in contact with pure water (left), and in the purified and sodium exchanged clay fraction of the Kutch 8940 material (right). The legend in the right diagram shows the NaCl concentrations in the test solutions successively in contact with the Kutch 8940 material.*

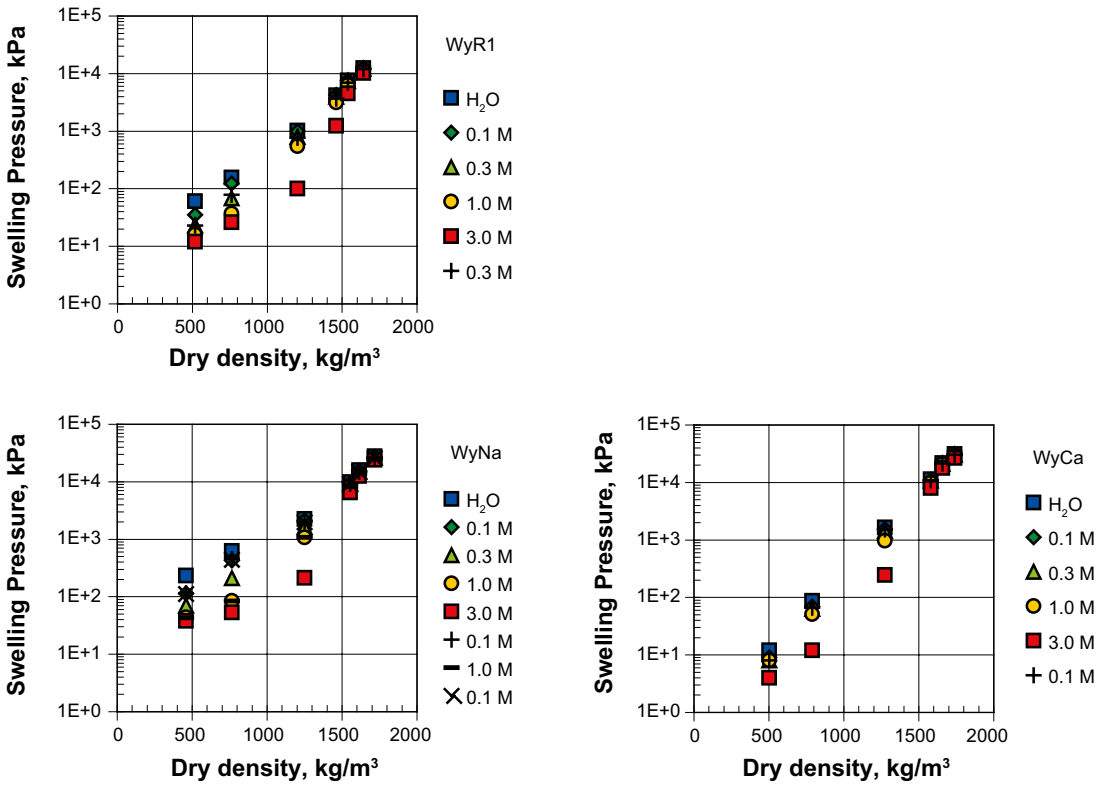

Figure 4-14. *Swelling pressure in the Wyoming MX-80 reference material (upper) and the corresponding sodium (lower left) and calcium (lower right) converted and purified materials. The legends show the NaCl concentrations in the test solutions in successive contact with the MxR1 and MxNa materials and $CaCl_2$ concentrations in the solutions in successive contact with the MxCa material.*

4.5 Hydraulic conductivity

The hydraulic conductivity was measured in parallel with the swelling pressures. At each pressure equilibrium condition, the pressure in the bottom filter of the sample holders (Figure 4-7) was increased and the hydraulic conductivity was calculated from the volume of percolated solution according to Darcy's law. The changes in hydraulic conductivity due to the saline solutions can thereby be correlated directly to the swelling pressure change. The pressure gradient should ideally be low in order not to consolidate the sample, and as a role of thumb, it should not exceed half of the measured swelling pressure. This demand was not fulfilled in some of the low density samples exposed to high saline conditions. All results are shown in Table 4-8 to Table 4-13 and Figure 4-15 to Figure 4-20.

Table 4-8. Hydraulic conductivity in the Czech reference materials. The first column shows dry clay density (D_d) in kg/m³ and the following columns show the $CaCl_2$ concentrations (moles/L) in the test solutions successively in contact with the samples. Hydraulic conductivity values in m/s.

Material	D_d, kg/m³	H_2O	0.1 M	0.3 M	1.0 M	3.0 M
DnR1	849					
	1,386	4.5E–12	4.5E–12	4.4E–12	4.0E–12	2.7E–12
	1,342	4.0E–12	4.5E–12	5.0E–12	5.0E–12	4.0E–12
	1,604	3.5E–13	3.5E–13	3.5E–13	3.5E–13	2.0E–13
RoR1	816	2.7E–07				
	1,156	3.0E–11				
	1,474	1.3E–13				
SkR1	936	9.0E–09	4.5E–09	4.7E–09	4.7E–09	6.0E–08
	1,274	3.5E–12	3.5E–12	4.0E–12	4.0E–12	2.7E–12
	1,565	1.3E–13	1.2E–13	1.1E–13	1.1E–13	7.0E–14
StR1	949	5.0E–08	5.0E–08	5.0E–08	5.0E–08	8.0E–08
	1,236	9.0E–11	8.0E–11	6.0E–11	7.0E–11	2.0E–10
	1,618	1.2E–13	1.0E–13	1.2E–13	1.2E–13	8.0E–14

Table 4-9. Hydraulic conductivity in the Danish reference materials. The fist column shows dry clay density (D_d) in kg/m³ and the following columns show the NaCl concentrations (moles/L) in the test solutions successively in contact with the samples. Hydraulic conductivity values in m/s.

Material	D_d	H_2O	0.1 M	0.3 M	1.0 M	3.0 M
HoR1	757	2.0E–11	2.0E–10	3.0E–10	3.0E–10	4.0E–10
	1,264	5.0E–13	9.0E–13	7.0E–13	7.0E–13	7.0E–13
	1,570	1.0E–13	7.0E–14	7.0E–14	7.0E–14	5.0E–14
RöR1	901	5.0E–10	8.0E–09	8.0E–08	6.0E–08	3.0E–08
	1,237	2.0E–11	2.2E–11	2.3E–11	2.0E–11	1.3E–11
	1,595	6.0E–13	6.5E–13	6.2E–13	5.7E–13	3.0E–13

Table 4-10. Hydraulic conductivity in the Friedland reference material and the corresponding purified and sodium exchanged clay fraction. The first column shows dry clay density (D_d) in kg/m³ and the following columns show the NaCl concentrations (mole/L) in test solutions successively in contact with the samples. Hydraulic conductivity values in m/s.

Material	D_d	H_2O	0.1 M	0.3 M	1.0 M	3.0 M
FrR1	816					
	1,437	5.0E–12	4.0E–12	4.0E–12	7.0E–12	7.0E–12
	1,174	2.0E–11	1.5E–11	2.0E–11	3.0E–11	4.0E–11
	1,576	1.0E–12	1.2E–12	1.4E–12	2.0E–12	1.7E–12
FrNa	1,070	1.5E–11	3.0E–11	4.0E–11	7.0E–11	4.0E–10
	776	3.0E–09	2.0E–10	1.0E–10	5.0E–09	2.0E–08
	1,188	2.0E–12	2.0E–12	5.0E–12	1.0E–11	4.0E–11
	1,432	4.0E–13	5.0E–13	6.0E–13	7.0E–13	1.0E–12
	1,649	2.0E–13	3.0E–13	3.0E–13	4.0E–13	4.0E–13
	1,774	6.0E–14	6.0E–14	6.0E–14	7.0E–14	8.0E–14

Table 4-11. Hydraulic conductivity in the Milos Deponit CA-N reference material and the corresponding purified and sodium and calcium exchanged clay fraction. The first column shows dry clay density (D_d) in kg/m³ and the following columns show the $CaCl_2$ concentrations (moles/L) in test solutions successively in contact with the MiR1 and MiCa samples, and the NaCl concentrations in the test solutions successively in contact with the MiNa samples. Hydraulic conductivity values in m/s.

Material	D_d	H_2O	0.1 M	0.3 M	1.0 M	3.0 M
MiR1	544	2.6E–10				
	852	4.3E–11				
	1,189	1.0E–12	1.2E–12	1.1E–12	1.1E–12	1.0E–12
	1,454	8.0E–14	8.0E–14	7.0E–14	7.0E–14	6.0E–14
	1,541	5.0E–14	4.0E–14	4.0E–14	4.0E–14	4.0E–14
	1,627	2.0E–14	2.0E–14	2.0E–14	1.5E–14	1.0E–14
MiNa	444	2.5E–12	3.0E–12	4.0E–12	5.0E–11	2.0E–09
	794	3.0E–13	3.0E–13	5.0E–13	6.0E–12	3.0E–09
	1,252	5.0E–14	3.0E–14	3.0E–14	4.0E–14	5.0E–14
	1,532	1.0E–14	5.0E–15	5.0E–15	5.0E–15	1.0E–14
	1,627	5.0E–15	5.0E–15	5.0E–15	5.0E–15	5.0E–15
MiCa	522					
	807	2.0E–10	6.0E–10	5.0E–10	5.0E–10	3.0E–09
	1,225	1.0E–13	9.0E–14	9.0E–14	9.0E–14	1.0E–13
	1,547	2.0E–14	2.0E–14	2.0E–14	1.0E–14	1.0E–14
	1,628	2.0E–14	2.0E–14	2.0E–14	1.0E–14	1.0E–14
	1,653	1.0E–14	5.0E–15	5.0E–15	5.0E–15	5.0E–15

Table 4-12. Measured hydraulic conductivity in the three Indian reference materials Kutch 8936, 8939 and 8940. The first column shows dry clay density (D_d) in kg/m³ and the following columns show the NaCl concentrations (moles/L) in the test solutions successively in contact with the samples. Hydraulic conductivity values in m/s.

Material	D_d	H_2O	0.3 M	1.0 M	3.0 M
Ku36R1	1,194	1.24E–13			
	1,425	4.40E–14			
Ku39R1	1,245	1.60E–13			
	1,420	5.00E–14			
Ku40R1	1,272	1.30E–13			
	1,464	3.30E–14			
Ku40Na	833	1.1E–12	1.5E–12		
	1,169	1.6E–13	2.0E–13	2.0E–13	
	1,371	3.0E–14	4.0E–14	5.0E–14	6.0E–14
	1,520	2.0E–14	3.0E–14	2.0E–14	2.0E–14

Table 4-13. Hydraulic conductivity in the Wyoming MX-80 R1 reference material and the corresponding purified and sodium and calcium exchanged clay fraction. The fist column shows dry clay density (D_d) in kg/m³ and the following columns show the NaCl concentrations (moles/L) in test solutions successively in contact with the WyR1 and WyNa samples, and the $CaCl_2$ concentrations in the test solutions successively in contact with the WyCa samples. Hydraulic conductivity values in m/s.

Material	D_d	H_2O	0.1 M	0.3 M	1.0 M	3.0 M
WyR1	517	5.0E–12	6.0E–12			
	761	2.0E–12	1.0E–12	3.0E–12	3.0E–12	
	1,202	3.0E–13	2.0E–13	3.0E–13	6.0E–13	
	1,461	5.0E–14	5.0E–14	6.0E–14	5.0E–14	1.0E–13
	1,538	4.0E–14	3.0E–14	2.0E–14	2.0E–14	4.0E–14
	1,641	2.0E–14	2.0E–14	2.0E–14	2.0E–14	2.0E–14
WyNa	458	2.4E–12	3.0E–12	4.0E–12	1.0E–10	3.0E–10
	766	6.0E–13	2.5E–13	4.5E–13	4.0E–12	5.0E–11
	1,249	5.0E–14	3.5E–14	3.5E–14	5.5E–14	1.2E–13
	1,555	1.6E–14	1.0E–14	1.0E–14	1.0E–14	1.0E–14
	1,615	8.0E–15	5.0E–15	5.0E–15	5.0E–15	5.0E–15
	1,717	5.0E–15	5.0E–15	5.0E–15	5.0E–15	5.0E–15
WyCa	789				1.5E–08	1.0E–08
	1,275	1.0E–13	1.0E–13	1.0E–13	1.0E–13	2.0E–13
	1,580	2.0E–14	2.0E–14	2.0E–14	2.0E–14	1.0E–14
	1,658	1.0E–14	1.0E–14	8.0E–15	8.0E–15	8.0E–15
	1,740	1.0E–14	1.0E–14	5.0E–15	5.0E–15	6.0E–15

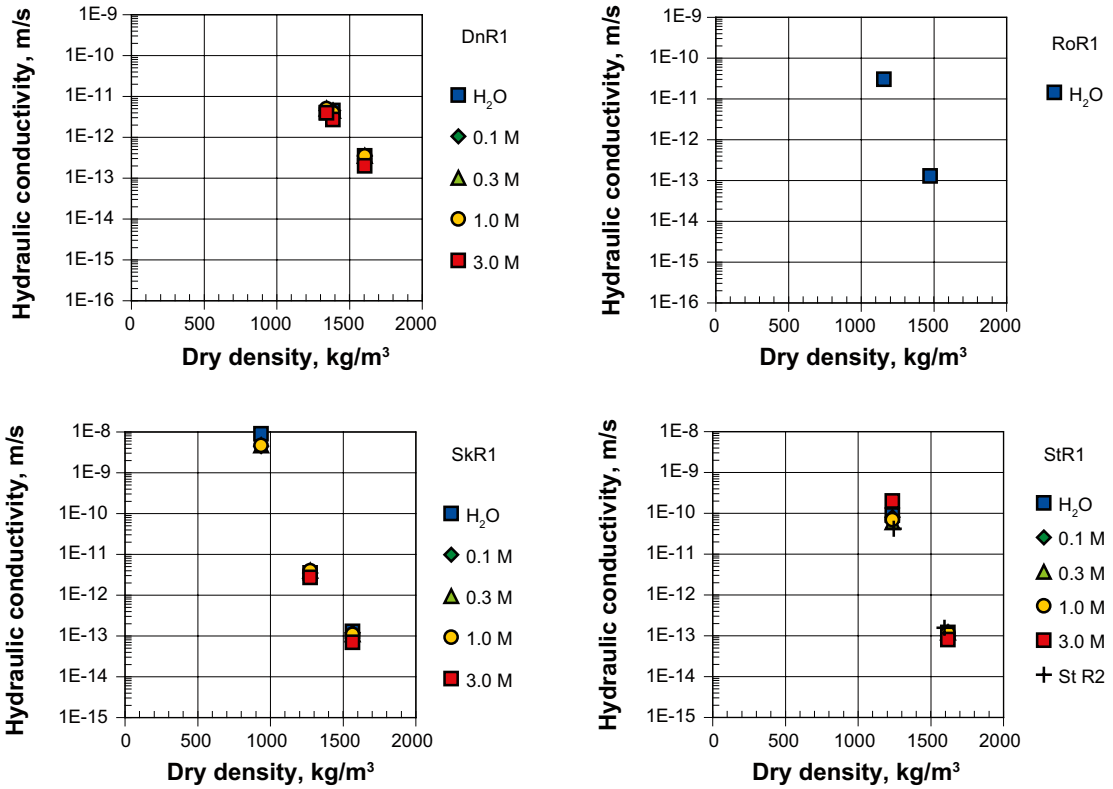

Figure 4-15. *Hydraulic conductivity in the Czech reference materials Dnesice, Rokle, Skalna and Strance. The legends show the $CaCl_2$ concentration in the solutions in successive contact with the samples. StR2 represents a doublet sample with pure water.*

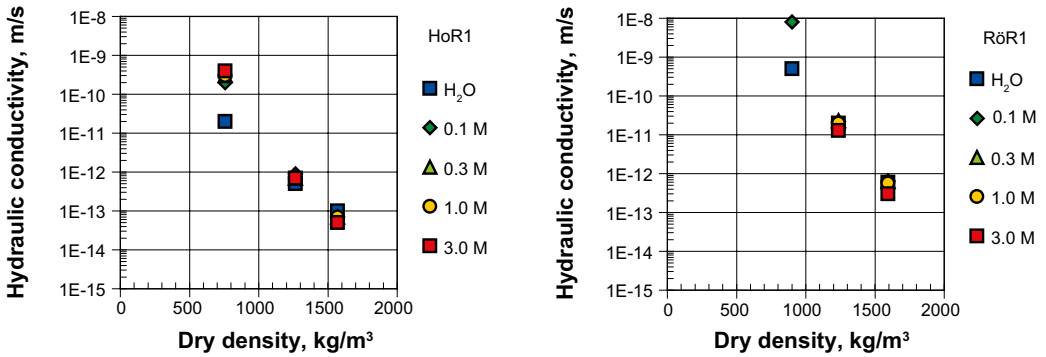

Figure 4-16. *Hydraulic conductivity in the Danish Holmehus and Rösnäs reference materials. The legends show the NaCl concentrations in the test solutions in successive contact with the samples.*

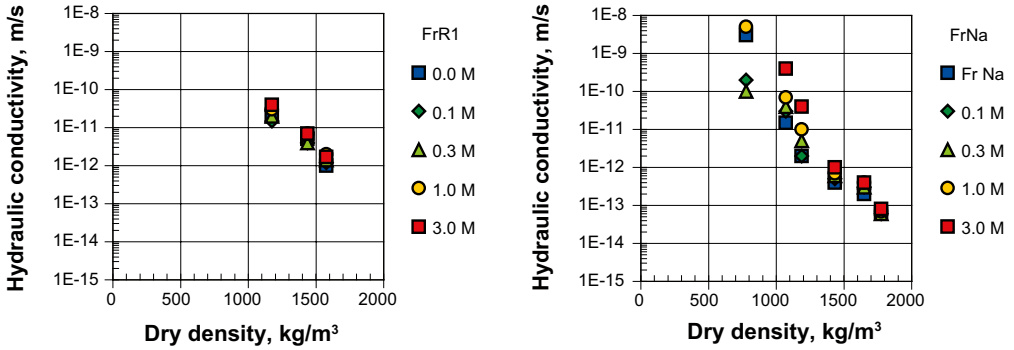

Figure 4-17. *Hydraulic conductivity in the Fridland reference material (left) and the corresponding sodium exchanged and purified material (right). The legends show the NaCl concentrations in the test solutions successively in contact with the samples.*

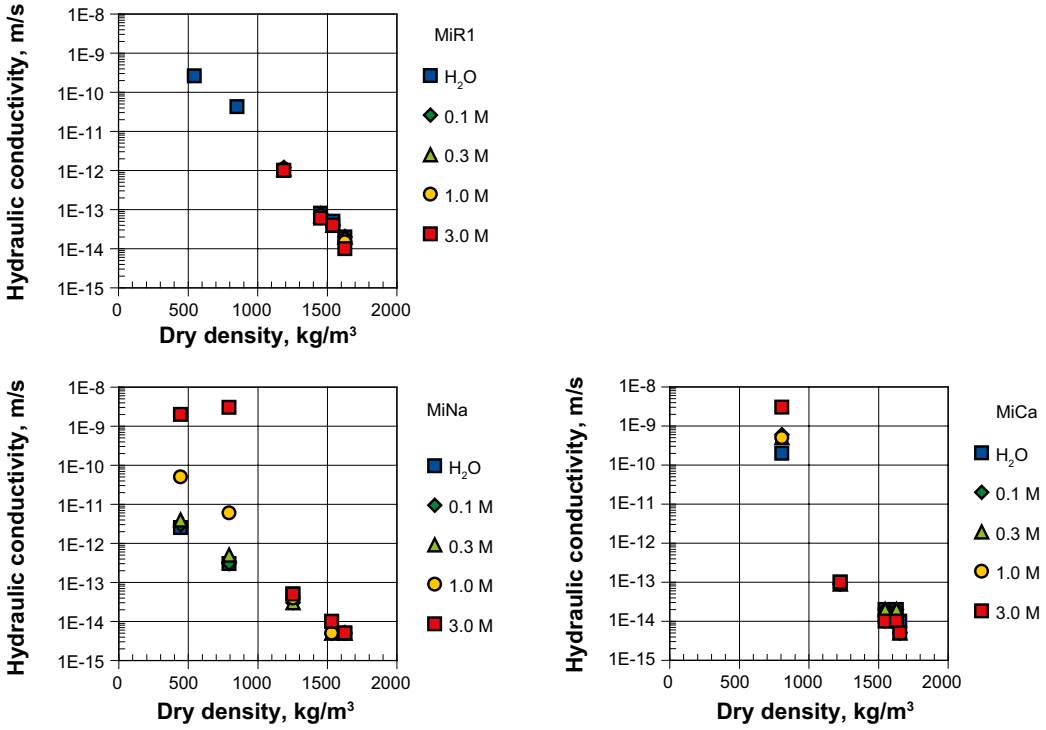

Figure 4-18. *Hydraulic conductivity in the Milos Deponit CA-N reference material (upper) and the corresponding sodium (left) and calcium (right) exchanged and purified material (right). The legends show the $CaCl_2$ concentrations in the test solutions successively in contact with the MiR1 and MiCa samples, and the NaCl concentrations in the test solutions successively in contact with the MiNa sample.*

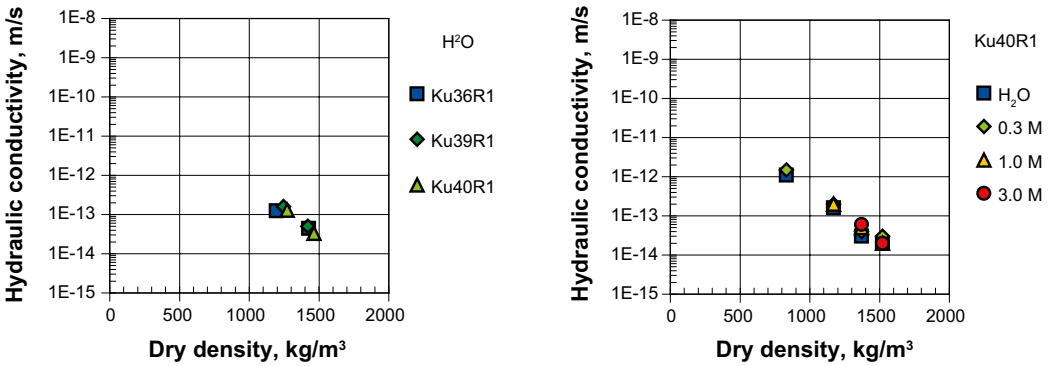

Figure 4-19. *Hydraulic conductivity in the Indian Kutch 8936, 8939 and 8940 reference material (left), and in the purified and sodium exchanged clay fraction of the Kutch 8940 material (right). The right legend shows the NaCl concentrations in the test solutions successively in contact with the samples.*

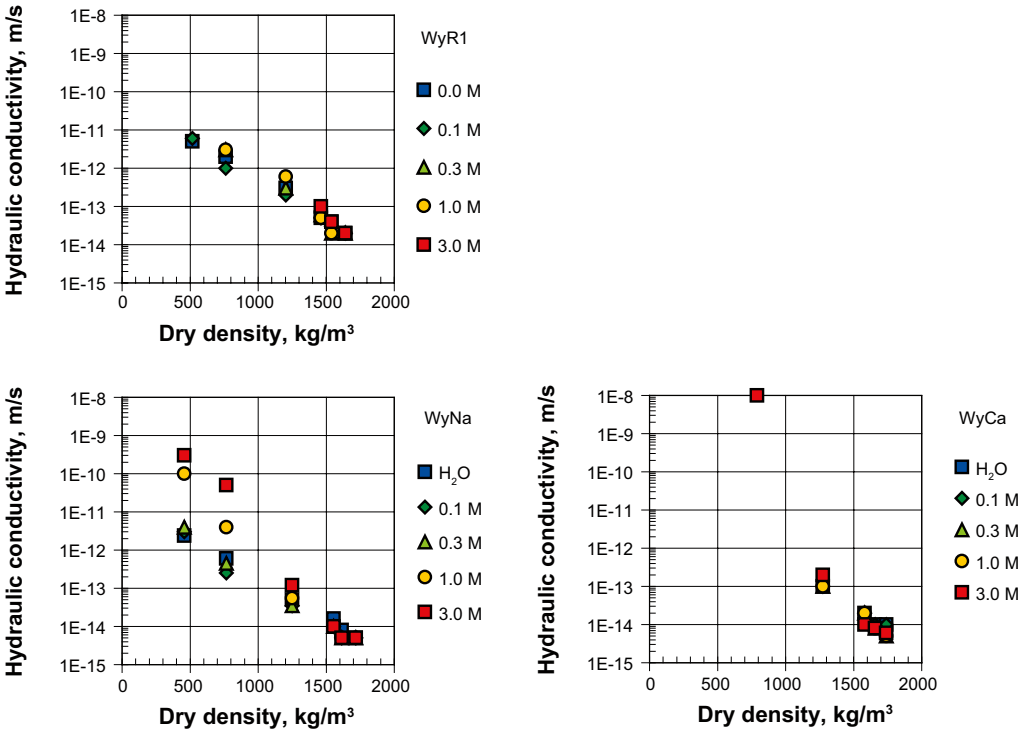

Figure 4-20. *Hydraulic conductivity in the Wyoming MX-80 reference material (upper) and the corresponding sodium (left) and calcium (right) exchanged and purified material (right). Legends show the NaCl concentrations in the solutions successively in contact with the WyR1 and WyNa samples, and the $CaCl_2$ concentration in the test solutions successively in contact with WyCa samples.*

5 Calculations and discussion

5.1 Mineralogical properties

5.1.1 Rietveld analyses of powder XRD

The mineralogical composition of the reference materials were evaluated from the XRD diffractograms (Figure 3-2 to Figure 3-8) by use of the Siroquant quantitative XRD software. The modeling is based on the Rietveld refinement method of least squares fit of calculated to measured XRD profiles /Rietweld 1969/. The method is described in general and used for montmorillonite in /Tailor
and Matulis 1994/.

The present analyses were made in a standardized way, including identification of present minerals by peak positions, and a subsequent modeling by use of the Siroquant mineral database. The basal spacing and the orientation of the 2:1 mineral were free to adjust to the recorded-values from modeling start. Thereafter, the general rules of modeling as described in the manual were followed.

The main minerals were identified manually by their typical peaks in the XRD diffractograms, and less obvious but possible mineral phases were checked by comparison with synthetic patterns created from the database including artificial rotation and structure variation. It is of course important not to overlook the existence of a mineral phase in the identification since this will introduce an error equal to the content of the mineral. Hoverer, the number of possible but uncertain mineral phases was minimized, due to the risk for accidental fit with scatter in the diffractograms. The calculated content of such an accidental fit will always be small, but such artifacts will apparently reduce the content of existing phases. This also implies that phases with content below 1% must be considered uncertain, unless they appear repeatedly. The calculated results are still shown with one decimal in order to indicate a possible presence of a mineral (Table 5-1 to Table 5-7).

The distinction between different feldspars is uncertain since they represent solid solutions and the plagioclase phases are presented as a sum although the modeling was made with albite and anorthite as starting phases.

Illite is a special problem in the analyses since the illite 2:1 structure may be almost identical to that of the swelling 2:1 mineral. The calculated illite content may well represent the actual content if the illite is a discrete phase, and if the difference from the swelling 2:1 mineral is reveal by the diffractograms. This is though not always the case, especially if the illite is present in illite/smectite mixed layer structures (I/S). The Siroquant quantification of both illite and montmorillonite has therefore to be completed by additional analyses (section 5.1.5 and 5.1.6). In the present study, adjustments of the Siroquant results were made in Czech DnR1, SkR1, Danish HoR1, RöR1 and in the German FrR1 materials. In all the other materials, the discrepancy in illite content between the analyses did not motivate any correction.

The swelling 2:1 mineral is generally presented in Table 5-1 to Table 5-7 as montmorillonite since this is the database mineral used for the quantifications. However, in order to be more precise some of the minerals should be termed beidellite according to the calculated structural formulas (section 5.1.5).

Table 5-1. Results from the Siroquant analyses of the Czech reference materials Dnesice (DnR1), Rokle (RoR1), Skalna (SkR1) and Strance (StR1). The montmorillonite and illite results in the DnR1, SkR1 and StR1 materials are adjusted according to section 5.1.5. Values within parenthesis show the original Siroquant results. Mineral phases expressed as weight percent of the total materials.

Phase	DnR1	RoR1	SkR1	StR1
Montmorillonite	21 (39.6)	69.4	50 (70.8)	66 (70.4)
Illite	25 (6.5)	5.4	24 (3.4)	5 (1.2)
Kaolin	38.9	3.1	11.3	7.9
Anatase	0.1	1.9	0.0	1.9
Biotite	0.0	1.5	0.0	0.0
Calcite	0.0	5.2	0.0	0.1
Chlorite	0.0	0.1	0.0	1.3
Cristobalite	0.0	0.5	0.0	0.2
Goethite	3.7	2.0	1.0	2.7
Gypsum	1.1	1.4	0.6	0.0
Hematite	0.0	0.3	0.1	0.0
Magnesite	0.4	0.7	0.7	0.3
Magnetite	0.2	0.1	0.1	0.1
Microcline	0.0	0.0	0.0	0.0
Muscovite	3.2	2.8	8.0	2.0
Orthoclase	0.0	0.4	0.0	0.0
Plagioclase	0.7	0.2	0.1	0.1
Pyrite	0.8	1.1	0.6	0.9
Quartz	3.4	2.5	1.8	9.5
Rutile	0.8	0.6	0.5	0.7
Siderite	0.2	0.3	0.5	0.2
Tridymite	0.3	0.5	0.2	0.3

Table 5-2. Results from the Siroquant analyses of the Danish reference materials Holmehus (HoR1), Rösnäs (RöR1) and Ölst (ÖlR1). The montmorillonite and illite results in the HoR1 and RöR1 materials are adjusted according to section 5.1.5. Values within parenthesis show the original Siroquant results. Mineral phases expressed as weight percent of the total materials.

Phase	HoR1	RöR1	ÖlR1
Montmorillonite	59 (76.6)	34 (45.5)	58.8
Illite	25 (6.8)	32 (20.2)	10.7
Kaolin	0.1	7.1	1.2
Calcite	0.2	8.6	0.1
Chlorite	0.0	0.0	2.2
Clinoptilolite	0.2	1.2	9.3
Cristobalite	0.0	0.1	0.6
Goethite	0.5	3.5	0.3
Gypsum	1.4	0.0	0.6

Phase	HoR1	RöR1	ÖlR1
Hematite	0.4	0.7	0.4
Magnetite	0.1	0.4	0.3
Microcline	0.0	0.0	0.0
Muscovite	5.5	5.0	1.9
Orthoclase	0.0	0.0	0.0
Plagioclase	0.1	0.2	11.5
Pyrite	1.1	1.0	1.1
Quartz	5.8	5.4	0.6
Rutile	0.4	0.0	0.0
Tridymite	0.7	1.0	0.3

Table 5-3. Results from the Siroquant analyses of the four diffractograms from the Friedland material. The montmorillonite and illite results are adjusted according to section 5.1.5. Values within parenthesis show the original Siroquant results. Mineral phases expressed as weight percent of the total materials. FrR1m indicate results from the calculated mean diffractogram, and the FrR1 indicate the calculated mean results from the Siroquant determinations. Mineral phases expressed as weight percent of the total materials. Plus and minus denote the maximum deviations from mean values.

Phase	FrR1a	FrR1b	FrR1c	FrR1m	FrR1	plus	minus
Montmorillonite	34 (34.7)	29 (32.7)	25 (30.1)	32 (35.2)	30 (33.2)	4 (2.0)	5 (3.1)
Illite	26 (25.5)	26 (22.7)	26 (21.0)	26 (23.2)	26 (23.1)	– (2.4)	– (2.1)
Kaolin	8.9	13.4	8.8	11.7	10.7	2.7	1.9
Anatase	0.0	0.0	0.0	0.0	0.0	0.0	0.0
Calcite	0.0	0.2	0.1	0.1	0.1	0.2	0.1
Cristobalite	0.1	0.0	0.3	0.0	0.1	0.2	0.1
Goethite	0.0	0.0	1.0	0.0	0.3	0.7	0.2
Gypsum	0.7	1.2	0.6	0.1	0.7	0.6	0.6
Hematite	0.5	0.0	0.7	0.1	0.3	0.4	0.3
Lepidocrocite	0.1	0.1	0.4	0.1	0.2	0.2	0.1
Magnetite	0.1	0.1	0.8	0.1	0.3	0.5	0.2
Microcline	0.0	0.0	0.0	0.0	0.0	0.0	0.0
Muscovite	6.8	6.4	10.2	5.4	7.2	3.0	1.8
Orthoclase	0.0	0.0	0.0	0.0	0.0	0.0	0.0
Plagioclase	1.2	0.8	0.2	2.3	1.1	1.2	0.9
Pyrite	1.4	0.9	1.7	0.9	1.2	0.5	0.3
Quartz	18.7	20.2	22.1	19.8	20.2	1.9	1.5
Rutile	0.7	0.4	0.7	0.5	0.6	0.1	0.2
Siderite	0.1	0.5	0.9	0.1	0.4	0.5	0.3
Tridymite	0.3	0.2	0.3	0.2	0.3	0.1	0.1

Table 5-4. Results from the Siroquant analyses of the four diffractograms from the Milos Deponit CA-N material. MiR1m indicate results from the calculated mean diffractogram, and the MiR1 indicate the calculated mean results from the all the Siroquant determinations. Mineral phases expressed as weight percent of the total materials. Plus and minus denote the maximum deviations from mean values.

Phase	MiR1a	MiR1b	MiR1c	MiR1m	MiR1	plus	minus
Montmorillonite	79.5	80.6	82.5	83.1	81.4	1.7	1.9
Illite	5.1	4.5	4.8	4.1	4.6	0.5	0.5
Anatase	0.2	0.0	0.0	0.0	0.1	0.1	0.0
Biotite	0.0	0.0	0.0	0.0	0.0	0.0	0.0
Calcite	6.2	6.0	3.6	5.3	5.3	0.9	1.7
Cristobalite	0.7	0.7	0.5	0.6	0.6	0.1	0.1
Dolomite	1.3	1.1	1.4	1.3	1.3	0.1	0.2
Goethite	1.5	1.7	1.4	1.4	1.5	0.2	0.1
Gypsum	0.2	0.5	0.6	0.2	0.4	0.2	0.2
Hematite	0.3	0.0	0.2	0.1	0.2	0.1	0.1
Lepidocrocite	0.2	0.2	0.4	0.2	0.3	0.2	0.1
Magnetite	0.1	0.1	0.1	0.1	0.1	0.0	0.0
Microcline	0.2	0.0	0.5	0.0	0.2	0.3	0.2
Muscovite	1.4	2.1	0.7	1.3	1.4	0.7	0.7
Orthoclase	0.0	0.0	0.0	0.0	0.0	0.0	0.0
Plagioclase	1.0	0.1	0.7	0.1	0.5	0.5	0.4
Pyrite	1.2	1.2	1.0	1.0	1.1	0.1	0.1
Quartz	0.1	0.5	0.5	0.4	0.4	0.1	0.3
Rutile	0.0	0.0	0.7	0.4	0.3	0.4	0.3
Siderite	0.4	0.4	0.2	0.2	0.3	0.1	0.1
Tridymite	0.6	0.4	0.3	0.2	0.4	0.2	0.2

Table 5-5. Results from the Siroquant analyses of the Indian reference materials. Mineral phases expressed as weight percent of the total material.

Phase	Ku36R1	Ku37R1	Ku38R1	Ku39R1	Ku 40R1
Montmorillonite	79.8	86.4	79.1	78.9	87.0
Illite	10.4	0.6	1.2	1.3	1.0
Anatase	0.2	0.6	1.0	1.2	0.9
Calcite	0.5	1.0	0.5	1.0	0.0
Cristobalite	0.0	0.0	0.0	0.3	0.4
Goethite	0.7	1.3	1.4	1.0	1.3
Gypsum	0.3	0.7	1.4	0.6	2.2
Hematite	0.4	0.3	0.0	0.8	0.0
Lepidocrocite	0.4	0.3	0.6	0.6	0.5
Maghemite	2.7	0.4	0.7	1.4	0.4
Magnesite	0.0	0.5	0.4	0.7	0.3
Magnetite	0.1	0.1	0.9	0.9	0.1
Microcline	0.0	0.0	0.0	1.6	0.4
Muscovite	0.1	2.4	4.6	2.5	0.1
Orthoclase	0.0	0.0	0.5	0.0	0.4
Plagioclase	0.2	0.6	0.5	1.8	1.0
Pyrite	0.9	0.5	0.5	1.1	0.3
Quartz	0.0	1.6	3.9	0.0	0.5
Rutile	0.5	0.6	0.4	0.1	0.2
Tridymite	0.5	1.0	1.9	3.2	2.5
Vaterite	0.0	0.5	0.0	0.1	0.3
Heulandite	2.0				

Table 5-6. Results from the Siroquant analyses of the four diffractograms from the Wyoming MX-80 material. WyR1m indicate results from the calculated mean diffractogram, and the WyR1 indicate the calculated mean results from all the Siroquant determinations. Mineral phases expressed as weight percent of the total materials. Plus and minus denote the maximum deviations from mean values.

Phase	WyR1a	WyR1b	WyR1c	WyR1m	WyR1	plus	minus
Montmorillonite	85.8	81.1	82.3	84.9	83.5	2.3	2.4
Illite	0.6	0.7	0.6	0.7	0.7	0.1	0.0
Anatase	0.4	0.3	0.0	0.1	0.2	0.2	0.2
Calcite	0.1	0.5	0.1	0.2	0.2	0.3	0.1
Cristobalite	0.7	0.8	0.1	0.0	0.4	0.4	0.4
Goethite	0.0	0.6	0.2	0.0	0.2	0.4	0.2
Gypsum	0.5	1.1	1.3	0.7	0.9	0.4	0.4
Hematite	0.0	0.1	0.0	0.1	0.1	0.0	0.0
Lepidocrocite	0.7	0.9	0.8	0.4	0.7	0.2	0.3
Magnetite	0.1	0.2	0.1	0.1	0.1	0.1	0.0
Microcline	0.4	0.3	2.4	0.0	0.8	1.6	0.8
Muscovite	1.5	3.2	3.2	3.4	2.8	0.6	1.3
Orthoclase	0.4	1.9	0.0	0.3	0.7	1.2	0.6
Plagioclase	4.2	1.8	3.0	2.6	2.9	1.3	1.1
Pyrite	0.5	0.6	0.6	0.5	0.6	0.0	0.1
Quartz	2.6	3.6	2.5	2.5	2.8	0.8	0.3
Tridymite	1.3	2.6	2.9	0.6	1.9	1.1	1.3

Table 5-7. Results from the Siroquant analyses of the five consignments of the Wyoming MX-80 material. The consignments were delivered around 1980 (WySt), 1995 (WyL1), 1999 WyL2), 2001 (WyR1) and WyR2). Wym denotes the mean value of the six analyzed samples. Plus and minus denote the maximum deviations from mean values. Mineral phases expressed as weight percent of the total material.

Phase	WySt	WyL1	WyL2	WyR1	WyR1m	WyR2	Wym	plus	minus
Montmorillonite	82.5	79.5	79.8	82.7	83.9	80.0	81.4	2.5	1.9
Illite	0.7	0.8	0.7	0.8	0.8	0.7	0.8	0.1	0.1
Anatase	0.4	0.1	0.2	0.3	0.0	0.2	0.2	0.2	0.2
Calcite	1.3	0.0	0.0	0.1	0.0	0.0	0.2	1.1	0.2
Cristobalite	0.2	1.4	2.5	0.6	0.7	0.0	0.9	1.6	0.9
Goethite	0.0	0.0	0.1	0.0	0.0	0.6	0.1	0.5	0.1
Gypsum	1.4	0.7	0.9	0.7	0.8	1.1	0.9	0.5	0.2
Hematite	0.5	0.9	0.1	0.2	0.4	0.0	0.4	0.5	0.3
Lepidocrocite	0.3	0.5	0.9	0.4	0.4	0.5	0.5	0.4	0.2
Magnetite	0.4	0.1	0.1	0.1	0.1	0.1	0.2	0.3	0.1
Microcline	0.0	0.3	0.0	0.0	0.0	0.0	0.1	0.2	0.0
Muscovite	2.4	5.1	2.6	3.5	4.4	2.5	3.4	1.7	1.0
Orthoclase	0.0	0.0	0.0	0.0	0.0	0.2	0.0	0.2	0.0
Plagioclase	4.6	2.4	4.0	3.2	2.3	4.7	3.5	1.2	1.2
Pyrite	0.8	0.6	0.6	0.6	0.3	0.9	0.6	0.3	0.3
Quartz	2.6	2.5	3.8	3.0	2.8	3.2	3.0	0.8	0.5
Tridymite	1.7	5.0	3.8	3.9	3.1	5.1	3.8	1.3	2.1

The precision of the analysis technique was tested by the repeated XRD scans and subsequent Siroquant analyses of the Milos Deponit CA-N, the Friedland clay and the Wyoming MX-80 batch R1 materials shown in Table 5-3, Table 5-4 and Table 5-6. It is obvious that the general repeatability is relatively good, especially since some of the scatter may represent actual variation in the mineralogy. Problems with accuracy are more difficult to grasp and at the same time it may be more crucial to overlook. The following technique was used to detect major mistakes. The mineral sets from all Siroquant analyses were used to calculate the total chemical composition of the analyzed materials. The calculation was made by use of the ideal chemical formula for each identified mineral, except in the case of montmorillonite, where instead the calculated structural formulas were used (Table 5-8 toTable 5-10). Finally, the calculated results were compared with the results from the ICP/AES analyses of the bulk materials. The calculations and comparisons are presented in Appendix 2.

Bad correlation surely indicates bad accuracy, unfortunately the opposite is not guaranteed since a good correlation may be accidental. The estimated error based on this study is that the amount of swelling minerals may be determined within ±5%, or better depending on the mineral composition. Such accuracy is supported by literature data /Taylor and Matulis 1994/. An error of this size does not affect the buffer properties significantly according to the physical test results. The general impression is that the XRD/Rietveld technique is well suited for standard analyses of buffer material.

However, the distinction between illite and montmorillonite has to be checked by supplementary analyses. Further, it has to be pointed out that the accuracy is estimated to be in the range of ±1 weight-percent for several minerals depending on the quality of the diffractograms and the mineral structure. Consequently, minerals of special interest also at a relatively low content have to be supplementary analyzed. This may be illustrated by the pyrite contents, which according to the XRD/Siroquant analysis results were 1.2, 1.1 and 0.6 weight-percent, respectively in the Friedland, Deponit CA-N and MX-80 materials, and the elemental analysis gave sulfide-S values corresponding to 0.68, 0.48, and 0.24 weight-percent pyrite.

5.1.2 CEC analyses

The slightly modified technique for measuring CEC by exchange with Cu(II)-trien complex gives very repeatable results, which generally are in reasonably good agreement with the results from analyses of extractable cations and with the calculated CEC from the structural formulas. Consequently, also the measured distribution of charge compensating cations likely reflects the conditions in the original clay materials quite well. Figure 5-1 illustrates all measured CEC results.

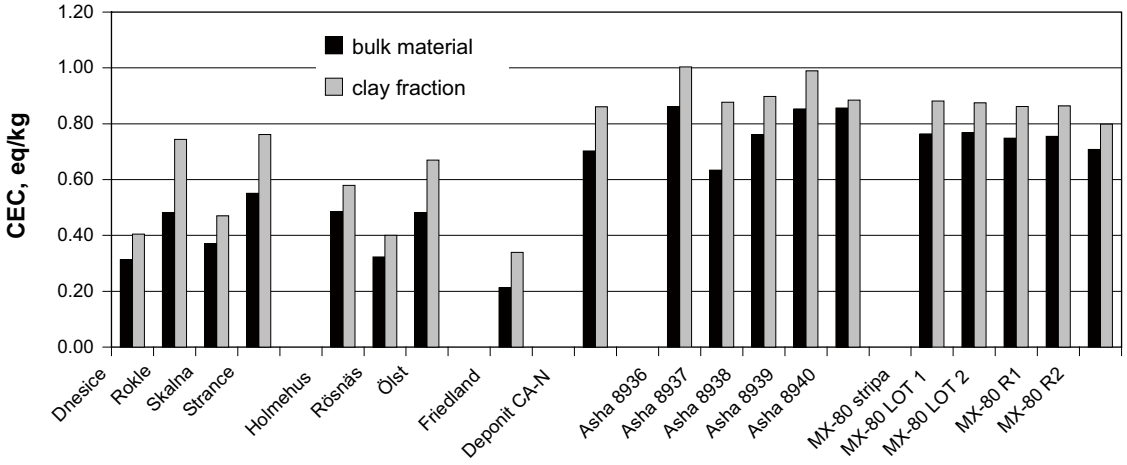

Figure 5-1. *Mean CEC of the bulk material and the clay fraction from all analyzed materials. CEC determined by use of the Cu-trien method.*

5.1.3 Sulfur and carbon analyses

The analyses of carbon and sulfur show that none of the examined clays have a very high content of organic carbon or sulfides. The Friedland clay had maximum values of 0.6 and 0.4 weight percent organic carbon and sulfide, respectively, which was the highest content of carbon and the second highest of sulfide of all analyzed materials.

5.1.4 Free iron oxides

The extraction of free iron from the clay fractions was made for two reasons; one was to improve the input data to the calculation of the mean structural formulas of the 2:1 swelling minerals, and the other was to determine the amount of iron phases which may be quite reactive, and serve as cementing agents under certain conditions. The present study has deliberately not paid attention to the oxidation state of iron, partly due to other ongoing studies concerning this topic. All iron was consequently treated as Fe(III) in the structural calculations.

5.1.5 ICP/AES and formula calculation

The raw data from the ICP/AES analyses of the clay fraction (Table 3-5) were used to calculate the structural formulas of the montmorillonite component in the materials, respectively. The calculation was made in accordance with /Newman 1987/, and with the addition of the following items:

- The materials were purified and ion exchanged to sodium state in accordance with section 2.8.2.
- The small remnants of sulfur and carbon present in the clay fractions were assumed to derive from calcium minerals ($CaSO_4$ and $CaCO_3$), and the calcium content was consequently reduced accordingly.
- No traces of feldspars or other potassium-bearing non-clay minerals were detected in the clay fractions by XRD. The remaining potassium content in the Na converted clay fractions was therefore considered fixed in the clay structure and should consequently, by definition, be termed illite. The silica and aluminum content was adjusted accordingly before the calculation of the montmorillonite structure, based on the K^+ content by assuming ideal illite structure with a layer charge of 1.5 per O_{24} unit cell. The calculated illite content is shown as weight-percent under the abridgment “illite calc” in Table 5-8 to Table 5-10.
- The content of iron was adjusted by the determined value of extractable iron in the clay fraction (Table 3-8).
- The content of aluminum and silica was adjusted in the samples containing kaolin, using the ideal kaolin structure and the content determined by the Siroquant modeling of the powder diffractograms.

The basic calculation technique was checked by use of data from /Newman 1987/ and from /Müller-Vonmoos and Kahr 1983/ and the reported montmorillonite structures were fully reproduced. All structure calculations, including input data and adjustments are shown in Appendix 3, and the concluding results are shown in Table 5-8 to Table 5-10. The CEC of the swelling 2:1 mineral (CEC mont calc) was calculated from the total layer charge by division by the molar unit cell weight. The CEC of the clay fraction (CEC clay calc) was calculated by compensating for the mass of accessory minerals in the clay fraction and assuming that the accessory minerals do not contribute to the CEC. For comparison, also the measured CEC (CEC clay meas) values for the clay fractions are shown.

A general problem in the calculation of the mineral structure is how to handle titanium, which may be part of the clay structure or in clay sized Ti-minerals e.g. anatase or rutile. Identification of such minerals by XRD is not possible if the grain size is too small. Further, the titanium may occupy sites both in the octahedral (preferably) and in the tetrahedral layers. The position of titanium is of no major importance, but whether Ti is included in the structure or not affects the calculated charge distribution. In the Rokle clay, which has the highest Ti content of all examined samples, the charge changes from 85% in tetrahedral position to 32% by including the titanium or not. However, the effect on total charge is moderate, corresponding to a change in CEC of 0.05 eq/kg. Including Ti or not, has a negligible effect on most of the analyzed materials due to the relatively low Ti content. Titanium is included in all the calculations in the presented data, since this leads to maximum tetrahedral charge, which may be considered as less favorable for use in a repository buffer /Karnland and Birgersson 2006/.

Table 5-8. Calculated structural formula for the swelling 2:1 component in the Czech Danish and German materials. The element figures show number of atoms per O_{24} cell, unit cell weight in grams /mole, charge refers to unit charge per cell, and the CEC is given in eq/kg.

	DnNa	RoNa	SkNa	StNa	HoNa	RöNa	ÖlNa	FrNa
Si	6.89	7.36	7.39	7.18	7.84	7.28	7.55	7.49
Al	1.11	0.64	0.61	0.82	0.16	0.72	0.45	0.51
Sum tetrahedral	8.00	8.00	8.00	8.00	8.00	8.00	8.00	8.00
Al	1.37	1.74	1.56	1.80	1.83	1.74	1.51	1.75
Ti	0.32	0.54	0.14	0.42	0.09	0.16	0.33	0.19
Fe3+	1.94	1.14	1.81	1.37	1.33	1.47	1.31	1.26
Fe2+	0.00	0.00	0.00	0.00	0.00	0.00	0.00	0.00
Mg	0.49	0.55	0.66	0.44	0.80	0.89	0.95	0.90
Sum octahedral	4.11	3.97	4.17	4.02	4.05	4.26	4.09	4.11
Ca	0.00	0.00	0.00	0.00	0.00	0.00	0.00	0.00
Mg	0.00	0.00	0.00	0.00	0.00	0.00	0.00	0.00
K	0.00	0.00	0.00	0.00	0.00	0.00	0.00	0.00
Na	0.94	0.74	0.63	0.78	0.71	0.68	0.78	0.90
Sum interlayer	0.94	0.74	0.63	0.78	0.71	0.68	0.78	0.90
O	24.00	24.00	24.00	24.00	24.00	24.00	24.00	24.00
H	4.00	4.00	4.00	4.00	4.00	4.00	4.00	4.00
Unit cell weight	805	779	792	785	776	786	783	782
Tetr charge	–1.11	–0.64	–0.61	–0.82	–0.16	–0.72	–0.45	–0.51
Octa charge	0.17	–0.10	–0.02	0.05	–0.55	0.04	–0.34	–0.39
Total charge	–0.94	–0.74	–0.63	–0.78	–0.71	–0.68	–0.78	–0.90
Tetra charge, %	118	87	97	106	22	106	57	56
CEC mont calc	1.17	0.95	0.80	0.99	0.92	0.86	1.00	1.15
CEC clay calc	0.41	0.87	0.50	0.85	0.68	0.50	0.88	0.55
CEC clay meas	0.40	0.76	0.47	0.76	0.57	0.40	0.67	0.34
Illite calc, %	26	5	26	6	26	35	11	40

Table 5-9. Calculated structural formula for the 2:1 mineral component in the Greece and Indian materials. The element figures show number of atoms per O_{24} cell, unit cell weight in grams /mole, charge refers to unit charge per cell, and the CEC is given in eq/kg.

	MiCa1	MiCa2	MiNa1	MiNa2	Ku36Na	Ku37Na	Ku38Na	Ku39Na	Ku40Na
Si	7.84	7.83	7.85	7.73	7.71	7.54	7.30	7.62	7.13
Al	0.16	0.17	0.15	0.27	0.29	0.46	0.70	0.38	0.87
Sum tetrahedral	8.00	8.00	8.00	8.00	8.00	8.00	8.00	8.00	8.00
Al	2.86	2.87	2.88	2.88	2.44	2.60	2.50	2.56	2.62
Ti	0.08	0.08	0.08	0.09	0.04	0.05	0.13	0.05	0.15
Fe3+	0.43	0.43	0.42	0.43	0.83	0.95	1.03	0.79	1.00
Fe2+	0.00	0.00	0.00	0.00	0.00	0.00	0.00	0.00	0.00
Mg	0.59	0.58	0.59	0.58	0.73	0.48	0.44	0.67	0.33
Sum octahedral	3.96	3.96	3.98	3.98	4.04	4.08	4.11	4.07	4.10
Ca	0.39	0.39	0.19	0.00	0.02	0.00	0.01	0.00	0.00
Mg	0.00	0.00	0.00	0.00	0.00	0.00	0.00	0.00	0.00
K	0.00	0.00	0.00	0.00	0.00	0.00	0.00	0.00	0.00
Na	0.01	0.01	0.35	0.82	0.82	0.65	0.66	0.79	0.75
Sum interlayer	0.40	0.40	0.53	0.82	0.85	0.65	0.67	0.79	0.75
O	24.00	24.00	24.00	24.00	24.00	24.00	24.00	24.00	24.00
H	4.00	4.00	4.00	4.00	4.00	4.00	4.00	4.00	4.00
Unit cell weight	732	732	740	751	763	764	769	762	771
Tetr charge	–0.16	–0.17	–0.15	–0.27	–0.29	–0.46	–0.70	–0.38	–0.87
Octa charge	–0.63	–0.61	–0.57	–0.55	–0.58	–0.19	0.02	–0.42	0.11
Total charge	–0.80	–0.79	–0.72	–0.82	–0.87	–0.65	–0.68	–0.79	–0.75
Tetra charge, %	20	22	21	33	33	71	104	48	115
CEC mont calc	1.09	1.07	0.97	1.09	1.14	0.85	0.88	1.04	0.98
CEC clay calc	1.02	1.01	0.91	1.02	1.13	0.84	0.88	1.02	0.97
CEC clay meas	0.80	0.80	0.87	0.82	1.00	0.88	0.90	0.99	0.88
Illite calc, %	6	6	6	6	1	1	0	2	1

The calculated structural formulas (Appendix 3) of the swelling component are most likely of varying quality, mainly depending on the mineralogical composition of the clay fraction composition. The extremes would be the illite and kaolin rich Dnesice material on one hand and MX-80, Deponit CA-N and some of the Kutch materials on the other. The match between measured and calculated CEC may be seen as one indicator of the quality of the calculated structural formula. Further, comparison between the calculated and measured element content of the bulk material (Appendix 2) is indicative, since the mineral for which the structural formula was calculated makes up a substantial part of the bulk material.

Table 5-10. Calculated structural formula for the 2:1 mineral component in the materials originating from the Wyoming MX-80 material. The element figures show number of atoms per O_{24} cell, unit cell weight in grams /mole, charge refers to unit charge per cell, and the CEC is given in eq/kg.

	WyCa	WyCa2	WyMg1	WyMg2	WyK	WyK2	WyNa	WyNa2
Si	7.92	7.98	7.91	7.96	7.93	7.96	7.89	7.95
Al	0.08	0.02	0.09	0.04	0.07	0.04	0.11	0.05
Sum tetrahedral	8.00	8.00	8.00	8.00	8.00	8.00	8.00	8.00
Al	3.13	3.13	3.09	3.07	3.10	3.09	3.10	3.11
Ti	0.01	0.01	0.01	0.01	0.01	0.01	0.01	0.01
Fe	0.37	0.37	0.37	0.36	0.37	0.37	0.38	0.36
Mg	0.48	0.47	0.52	0.55	0.48	0.49	0.49	0.47
Sum octahedral	3.99	3.99	4.00	4.00	3.97	3.96	3.98	3.95
Ca	0.27	0.25	0.00	0.00	0.00	0.00	0.00	0.00
Mg	0.00	0.00	0.29	0.28	0.00	0.00	0.00	0.00
K	0.00	0.00	0.00	0.00	0.62	0.61	0.00	0.00
Na	0.02	0.01	0.02	0.01	0.02	0.03	0.65	0.65
Sum interlayer	0.29	0.27	0.31	0.30	0.64	0.64	0.65	0.65
O	24.00	24.00	24.00	24.00	24.00	24.00	24.00	24.00
H	4.00	4.00	4.00	4.00	4.00	4.00	4.00	4.00
Unit cell weight	730	730	738	737	754	754	745	744
Tetr charge	–0.08	–0.02	–0.09	–0.04	–0.07	–0.04	–0.11	–0.05
Octa charge	–0.49	–0.50	–0.51	–0.54	–0.57	–0.60	–0.54	–0.60
Total charge	–0.56	–0.52	–0.60	–0.58	–0.64	–0.64	–0.65	–0.65
Tetra charge, %	13	4	15	7	12	7	17	8
CEC mont calc	0.77	0.71	0.82	0.79	0.85	0.85	0.87	0.88
CEC clay calc	0.76	0.70	0.81	0.78	0.84	0.84	0.86	0.87
CEC clay meas	0.77	0.77	0.79	0.79	0.84	0.84	0.86	0.86
Illite calc, %	1	1	1	1	1	1	1	1

5.1.6 Illite and montmorillonite quantification

There are several techniques available aiming at quantifying the amount of illite in swelling soils materials. The one used in section 5.1.5, based on the content of fixed potassium in the clay fraction, is precise but time consuming due to the need for careful ion exchange. The results do not give direct information about the illite structure or the stacking order of illite in mixed layer illit/smectite (I/S) structures, but the method reveals the maximum possible amount of illite in the materials, which is the key issue for use in a repository.

In contrast, the Siroquant modeling, as used in this study, only reveals illite present as a separate mineral phase, and illite in mixed layers may be mistaken for montmorillonite. Consequently, the difference in illite content between the Siroquant and fixed potassium methods likely represents illite present in illite/smectite mixed layers. In order to be pessimistic from a repository perspective, the montmorillonite content as determined by the Siroquant analyses has to be adjusted for possible presence of mixed layer illite according to:

Montmorillonite content = Montmorillonite(Siroquant) + illite(Siroquant) – illite(K^+)

Where *Montmorillonite(Siroquant)* and *illite(Siroquant)* represents the montmorillonite and illite contents determined by the Siroquant analyses, and *illite(K^+)* represents the illite content determined by the fixed potassium method.

Table 5-11 compiles selected measured data concerning illite content in the various materials. The first result column (I) shows the Siroquant evaluated weight percentage of a separate illite phase in the bulk material (I(sep) in tot). The second column (II) shows the Siroquant evaluated weight percentage of montmorillonite in the bulk materials (I/S in tot), which may contain illite in mixed layers. The third column (III) shows the evaluated weight percentage of illite in the I/S mixed layers (I in I/S) based on XRD results (section 3.2.2 /Moore and Renolds, 1989/). The fourth column (IV) shows the calculated weight percentage of mixed layer illite in total material (I(I/S) in tot) as calculated from column II and III according to:

I(I/S) in tot = I/S in tot · (I in I/S – I in I/S (Sm))

where *I in I/S (Sm)* is a correction constant, measured in pure smectite.

Table 5-11. Illite content in the examined reference samples. The column abridgements are explained in the text above. * indicate optimized calculated value since no evaluation was possible from XRD results. All figures in percent.

	Column Method Phase	I SQ I(sep) in tot	II SQ I/S in tot	III M&R I in I/S	IV SQ/M&R I(I/S) in tot	V ICP/AES I (K) in cf	VI Stoke d < 2my	VII I(sep+I/S)	IIX I (K) total
Cz	DnMg eg	7	40	55*	18	26	95	25	25
	RoMg eg	5	69	10	1	5	77	6	4
	SkMg eg	3	71	30	15	26	93	18	24
	StMg eg	1	70	13	3	6	84	4	5
Da	HoMg eg	9	75	19	8	26	98	17	25
	RöMg eg	20	46	36	12	35	97	32	34
	ÖlMg eg	11	59	13	2	11	79	13	9
Ge	FrMg eg	23	33	28	6	40	66	29	26
Gr	MiR1 eg	5	81	10	1	6	83	6	5
	MiCa eg	5	81	5	–3	6	83	2	5
	MiMg eg	5	81	8	–1	6	83	4	5
	MiK eg	5	81	12	2	6	83	7	5
	MiNa eg	5	81	4	–4	6	83	1	5
	MiNa eg	5	81	9	0	6	83	5	5
In	Ku36Mg eg	2	86	13	3	1	83	5	1
	Ku37Mg eg	1	86	17	7	1	83	8	1
	Ku38Mg eg	1	79	19	8	0	83	9	0
	Ku39Mg eg	1	79	7	–2	0	83	–1	0
	Ku40Mg eg	1	87	13	3	1	83	4	1
US	WyR1 eg	1	83	6	–2	1	83	–1	1
	WyCa eg	1	83	6	–3	1	83	–2	1
	WyMg eg	1	83	6	–3	1	83	–2	1
	WyK eg	1	83	13	4	1	83	5	1
	WyNa eg	1	83	8	–1	1	83	0	1
Ref	Sm eg			9					

The fifth (V) column shows the total maximum weight percentage illite as calculated from the fixed potassium content in the sodium-exchanged clay fraction. The sixth (VI) column shows the clay fraction in weight percent of total material. The seventh (VII) column shows the total weight percentage illite, based on the XRD results, and the eight column (IIX) shows the total weight percentage illite based on the potassium content (ICP/AES analyses). The results are surprisingly concordant, taking into account the complexness of the materials and analyses.

5.2 Physical properties

5.2.1 Grain density and specific area

Figure 5-2 (left) shows that the grain densities evaluated in kerosene were significantly lower compared to those evaluated in the salt solutions. Supporting tests by use of tetrachoromethane (CCl_4) and benzine gave similar results as kerosene. The limited swelling of the vermiculite admits measurements in pure water, and supporting measurements were therefore made with vermiculate in kerosene, 1.0 M NaCl solution and pure water (Figure 5-2, right). The general conclusion from all results (Table 4-1) is that there is a significant and systematic difference in evaluated grain densities between measurements in kerosene, carbon tetrachloride etc. on the one hand and water and saline solutions on the other.

Figure 5-3 shows that the measured density difference with kerosene and saline solutions is significantly smaller in the Friedland material (FrR1) compared to the MX-80 material (WyR1) and the Deponit CA-N material (MiR1). The content of swelling 2:1 minerals is around 30 weight-percent in the FrR1 material and around 80 weight-percent in the WyR1 and MiR1 materials, indicating that the interaction between the swelling mineral and the liquid is the cause of the difference in evaluated grain density.

The results may reflect a real difference in grain density due to the exposure to the various liquids as illustrated in e.g. Figure 5-3. Alternatively, the results reflect different density changes in the liquids due to contact with the clay, which is a frequently proposed explanation for various observed related phenomena. The matter influences the evaluation of the degree of saturation and other geotechnical entities, and of course on the conceptual view of montmorillonite hydration.

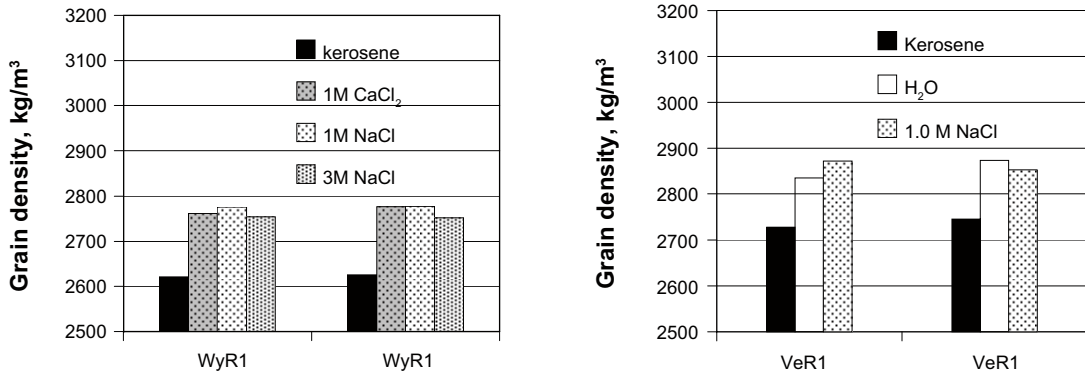

Figure 5-2. *Measured grain density for duplicate samples of MX-80 material (WyR1) in kerosene, 1.0 M $CaCl_2$, 1.0 M NaCl and 3.0 M NaCl solutions, assuming no change in the liquid densities (left), and measured grain density of vermiculite duplicate samples in kerosene, pure water and in 1.0 M NaCl solution, assuming no change in the liquid densities (right).*

Starting with the change in liquid density, an apparent water density may be calculated from the results in Table 4-1, assuming a fixed grain density e.g. equal to that measured in kerosene. Figure 5-4 (left) shows the apparent water density results versus clay density for MX-80 material as an example. Figure 5-4 (right) shows analogues with NaCl and $CaCl_2$ solutions, in which apparent water densities are calculated, assuming no change in salt density at dissolution /CRC 1973/. The increase in apparent water density in montmorillonite at buffer density (~ 7%) is larger than what can be explained by the hydration of the charge compensating cations alone (2 to 4%).

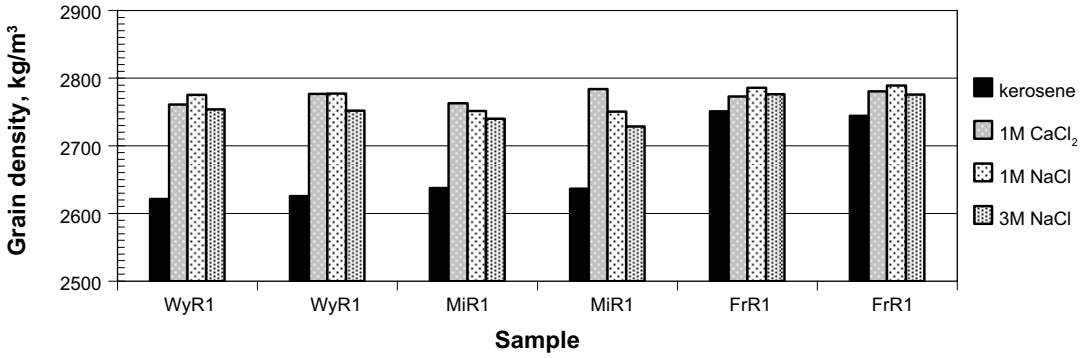

Figure 5-3. *Results from grain density determinations of the MX-80 (WyR1), Deponit CA-N (MiR1) and Friedland (FrR1) bulk materials performed in kerosene, 1.0 M and 3.0 M NaCl solutions, and 1.0 M $CaCl_2$ solution, assuming no change in the liquid densities.*

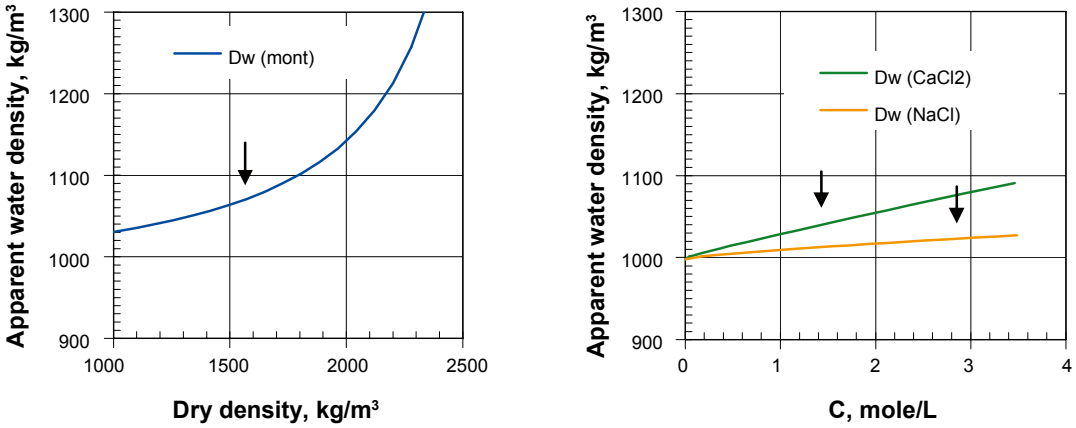

Figure 5-4. *Left; apparent water density (dotted line) versus sample density based on the assumption that the grain density is constant. Arrow indicates buffer density. Right; apparent water density in NaCl (solid line) and $CaCl_2$ (dotted line) solutions assuming that the salt density is not change at dissolution. Arrows indicate the mean concentration of sodium and calcium charge compensating ions, respectively, in MX-80 at buffer density.*

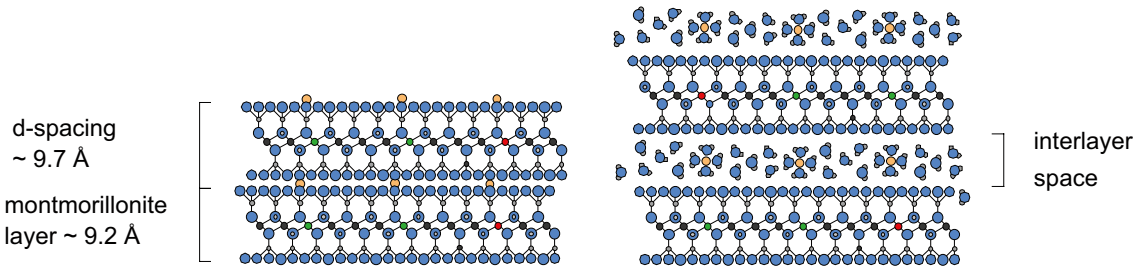

Figure 5-5. *Schematic structure of dry montmorillonite (left) and hydrated montmorillonite (right).*

The alternative explanation, based on a true difference in grain density in the various liquids, may be justified by the following discussion. The BET measurements of the specific surface area (section 4.3) by use of N_2 generally show specific surface areas of 20 to 40 m^2/g. Comparison with the total theoretical surface area of around 750 m^2/g indicate that the dry clay is dominated by interlayer contacts with tens of layers in close contact, and that the interlayer volume is not accessible for the nitrogen gas (Figure 5-5, left). The clay structure, in the dehydrated state and if sodium is the charge compensating cation, is close to that of paragonite, in which the d-spacing is around 9.7 Å. The calcium analogue is clintonite, which has approximately the same d-spacing, while the potassium variants illite and muscovite have d-spacing of over 10 Å /Brindley and Brown 1980/.

Using a non- or low-polar liquid, the structure will be the same as in the dry state, since the liquid is not able to separate the individual 2:1 layers (Figure 5-5 left). In the case of pure water or saline solutions, the charge compensating cations in the inter-layer volume will hydrate, which leads to separation of the individual 2:1 layers (Figure 5-5 right). The 2:1 layers thereby occupy a volume similar to that of pyrophyllite in which the d-spacing is around 9.3 Å. The layer charge density in the MX-80 montmorillonite corresponds to one unit charge per 73 $Å^2$ base area (CEC = 0.85 eq/kg). The volume of one such "unit charge entity" in a non-polar liquid consequently occupies:

$9.7 \cdot 73 \sim 708$ $Å^3$

In the hydrated system, the volume of one "unit charge entity" consists of the individual volumes of the 9.3 Å thick layer and of the released cation:

$9.3 \cdot 73 + 4\pi\ (1.02)^3/3 \sim 679 + 4 = 683$ $Å^3$

The density change at hydration for pure montmorillonite is consequently approximately 4%, corresponding to around 3%, in the MX-80 material, since the montmorillonite content is around 80%. The measured mean grain density values 2,623 kg/m^3 in kerosene and 2,766 kg/m^3 in the saline solutions correspond to a density change of 5.5%. Consequently, the combined effects of a grain density change (~ 3%) and the small change in liquid density due to hydration of the charge compensating cations may explain the measured difference in grain density.

The mineral density (Ds(XxNa)) of the swelling minerals in the fifteen materials was also calculated from the total mass of the elements in the O_{24} cell (Table 5-8 to Table 5-10) and the cell volume (Table 5-12). The b dimension of the cell may be determined from the XRD analyses by use of the hkl (0.6.0) reflections. Theoretically, also the "a" and "c" dimensions may be determined by use of e.g. the (0.0.1) and (0.2.0) reflections. However, hydration effects (0.0.1) and overlap with other peaks (0.2.0) make such interpretation delicate in the present diffractograms, and literature data likely lead to results that are more reliable. An "a" dimension of 5.21 and a "c" dimension of 9.3 Å was therefore used /Brindley and Brown 1980/. The resulting densities were used to calculate also the density of the total reference materials (Ds(XxR1)) by taking into account the mineral composition given in table Table 5-3 to Table 5-7, and by assuming that the accessory minerals had ideal composition. For comparison also the measured grain density of the total materials are shown, both 1 M NaCl solution (Ds(1.0M)) and in kerosene (Ds(ker)). Figure 5-6 shows the compiled results. Adjustment of the "c" dimension to 9.5 Å in the calculated densities give an optimal fitting to the values measured in 1.0 M NaC, and the corresponding figure for kerosene is 10.1 Å. The difference between the XRD based value (9.3 Å) and the evaluated (9.5 Å) may be considered reasonable, taking into account the uncertainties concerning both the unit cell masses and cell volumes.

Table 5-12. Compilation of data concerning grain density in the various examined materials. Column (0.6.0) shows the position in °2θ of the (0.6.0) peaks, column "a" and "c" shows the literature data of the unit cell dimensions, "b" shows the calculated dimension based on the (0.6.0) peaks, "mole w" shows the calculated molar mass of the O_{24} cell. Ds(XxNa) shows the calculated density of the swelling minerals, Ds(XxR1) shows the calculated mean density of all the minerals in the reference materials, Ds(1.0 M) shows the density of the reference materials measured in 1.0 M NaCl solution, and Ds(ker) shows the density of the reference materials measured in kerosene.

	Material	Peak (0.6.0) °2θ	Cell a Å	b Å	c Å	V Å3	mole w g	Calc Ds(XxNa) kg/m³	Calc Ds(XxR1) kg/m³	Meas Ds(1.0 M) kg/m	Meas Ds(ker) kg/m
Cz	DnNa	62.20	5.21	8.96	9.30	434	805	3,081	2,814	2,765	2,634
	RoNa	61.76	5.21	9.01	9.30	437	779	2,962	2,946	2,920	2,788
	SkNa	61.89	5.21	9.00	9.30	436	792	3,017	2,895	2,786	2,687
	StNa	61.89	5.21	9.00	9.30	436	785	2,991	2,949	2,841	2,680
De	HoNa	61.92	5.21	8.99	9.30	436	776	2,958	2,877	2,796	2,757
	RöNa	62.12	5.21	8.97	9.30	434	786	3,004	2,862	2,814	2,712
	ÖlNa	61.63	5.21	9.03	9.30	437	783	2,972	2,796	2,805	2,731
Ge	FrNaa	62.00	5.21	8.98	9.30	435	782	2,984	2,828	2,785	2,751
	FrNab	61.95	5.21	8.99	9.30	436	782	2,982	2,800	2,789	2,745
	FrNac	61.82	5.21	9.00	9.30	436	782	2,976	2,850	2,772	2,751
	FrNam	61.80	5.21	9.01	9.30	436	782	2,975	2,809	2,781	2,745
Gr	MiNaa	61.96	5.21	8.99	9.30	435	732	2,791	2,816	2,751	2,638
	MiNab	61.96	5.21	8.99	9.30	435	732	2,792	2,814	2,751	2,637
	MiNac	61.98	5.21	8.98	9.30	435	732	2,792	2,819	2,763	2,638
	MiNam	61.95	5.21	8.99	9.30	435	732	2,791	2,816	2,784	2,637
In	Ku36Na	61.89	5.21	9.00	9.30	436	763	2,907	2,947	2,862	2,691
	Ku37Na	61.96	5.21	8.99	9.30	435	764	2,915	2,930	2,860	2,716
	Ku38Na	62.10	5.21	8.97	9.30	435	769	2,940	2,942	2,880	2,701
	Ku39Na	61.81	5.21	9.01	9.30	436	762	2,901	2,930	2,907	2,731
	Ku40Na	61.82	5.21	9.00	9.30	436	771	2,933	2,916	2,937	2,750
US	WyNaa	62.09	5.21	8.97	9.30	435	737	2,816	2,804	2,776	2,621
	WyNab	62.10	5.21	8.97	9.30	435	737	2,816	2,799	2,777	2,625
	WyNac	62.05	5.21	8.97	9.30	435	737	2,814	2,788	2,761	2,621
	WyNam	61.99	5.21	8.98	9.30	435	737	2,812	2,789	2,777	2,625

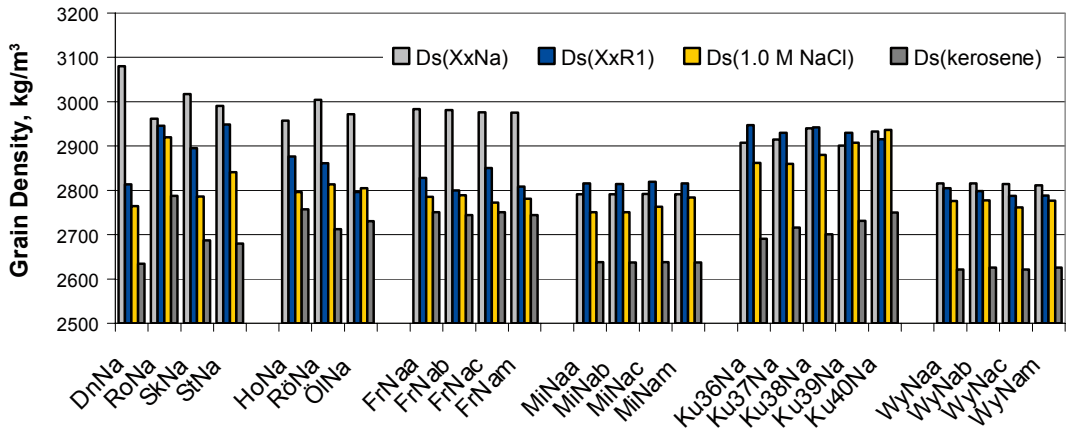

Figure 5-6. *Compilation of grain density data concerning all the examined materials. Ds(XxNa) shows the calculated density of the swelling minerals, Ds(XxR1) shows the calculated mean density of all the minerals in the reference materials, Ds(1.0 M) shows the density of the reference materials measured in 1.0 M NaCl solution, and Ds(ker) shows the density of the reference materials measured in kerosene.*

5.2.2 Swelling pressure and hydraulic conductivity

The mineralogical analyses show that there are major differences in many respects between the 15 analyzed materials. The montmorillonite content ranges from around 30 weight-percent of the total mass in the Fridland clay to over 80 weight-percent in the Wyoming MX-80, Milos Deponit CA-N and Kutch materials. This leads to a difference in swelling pressure of approximately one order of magnitude (Figure 5-7 left) although the clay fraction is almost the same. The lower swelling pressure in the Friedland clay may be explained by a larger mean distance between the individual swelling mineral layers, simply because they are less frequent at the same total density. The effect may be compensated by an increase of the total density. However, this will affect i.a. the rheological properties of the buffer material.

Figure 5-7 left also illustrates the difference between di- and-mono valent charge compensating cations. Both the total charge and the charge distribution are similar in the MX-80 and Deponit CA-N materials. Still, at low sample density the calcium dominated Deponit CA-N material has a swelling pressure equal to the low-grade sodium dominated Friedland clay. After complete ion exchange of all three clays to sodium state, the swelling pressures in the WyNa and MiNa materials are almost identical Figure 5-7 (right). The high content of non-swelling minerals also in the clay fraction, i.a. 40% illite based on the fixed potassium content, is the cause of the lower swelling pressure in the FrNa material.

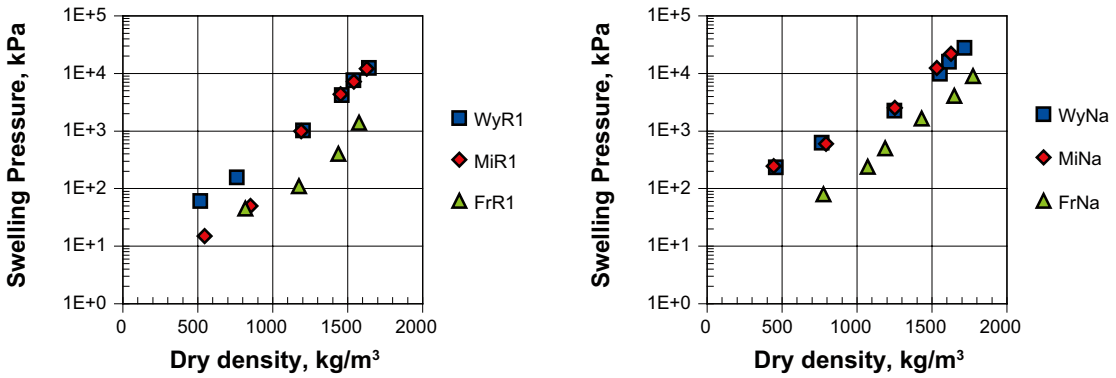

Figure 5-7. *Measured swelling pressures in the Wyoming MX-80, Milos Deponit CA-N and the Friedland clay in equilibrium with pure water (left). The same original materials purified and ion-exchange to Na^+ state in equilibrium with pure water (right).*

Figure 5-8 (left) shows the almost identical effects of a complete ion exchange to a calcium state of the purified MX-80 (WyCa) and Deponit CA-N (MiCa) materials. Finally, Figure 5-8 (right) shows the effects of equilibrium with saline solutions. The drop in swelling pressure due to increasing solution concentration is very systematic and may be explained by osmotic effects for sodium conditions /Karnland et al. 2005/. Because of the osmotic origin, the pressure effects are expected to be fully reversible, which was also measured and is illustrated with crosses and plus signs in Figure 5-8 right. The pressure drop as a response of equilibrium with saline solutions is less pronounced in calcium-dominated systems, which is illustrated in Figure 4-12 and Figure 4-14.

One basic demand on repository buffer material and, to a less extent, on tunnel backfilling material is to reduce groundwater flow. The highly compacted high-quality bentonites have a hydraulic conductivity in the range of $1*10^{-14}$ to 10^{-13} m/s, which is lower than reported for e.g. fracture-free granite /Bear 1988/, /Dixon et al. 2001/. Generally, the hydraulic conductivity increased approximately exponentially with decreasing sample density, and the fact that the product of swelling pressure and hydraulic conductivity is almost constant over a wide range of densities indicates that there is a close relationship in the origin of the two properties. Consequently, the discussion above, concerning swelling pressure, has relevance to some extent also for the hydraulic conductivity.

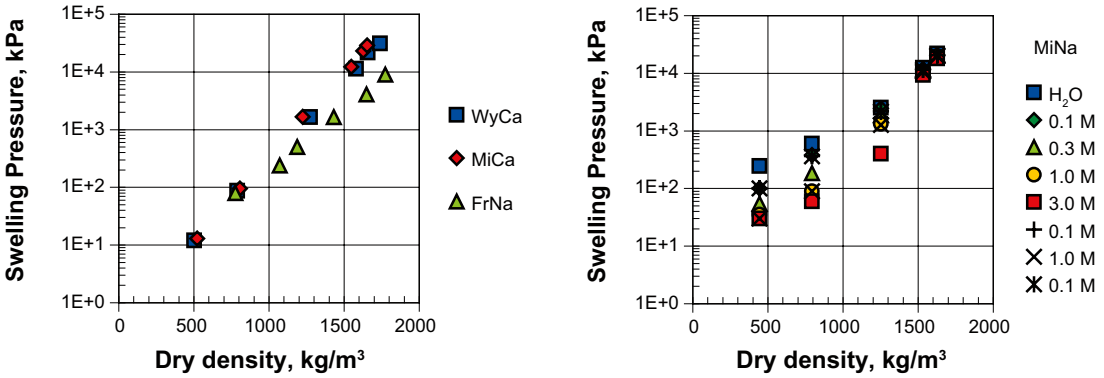

Figure 5-8. *Measured swelling pressures in Mx Ca, Mi Ca and Fr Na materials in equilibrium with pure water (left). Mi Na materiel successively in equilibrium with pure water, 0.1 M, 0.3 M, 1.0 M, 3.0 M, 0.1 M, 1.0 M and finally 0.1 M NaCl solutions (right).*

6 Conclusions

Determination of the mineral composition of a clay material is not a straight forward analysis, which is illustrated by the fact that there are scientific contests in clay mineral analysis /Omotoso et al. 2006/. The new computer tools, based on i.a. Rietveld technique for analysis of XRD data, have though improved the mineral identification, and have led to a breakthrough for mineral quantification. Still, the complexness of many clay materials makes the quantitative analyses complicated and the results have to be verified, and often revised, by supporting methods.

The mineralogical investigation in this study shows that all the analyzed swelling minerals have a dioctahedral structure, revealed both by the position of the (060) XRD reflection /Brindley and Brown 1980/, and by the calculations of the 2:1 mineral structures. However, the materials differ significantly with respect to the:

- Amount and type of accessory minerals.
- Dominating charge compensating cation.
- Dominating charge location in the swelling 2:1 minerals.
- Content of iron, titanium etc. in the clay fraction.

The content of illite as a separate phase seems to be determined relatively correct by the Siroquant modeling, but the content of mixed layer illite/smectite is strongly underestimated. However, quantification of the illite/smectite from XRD data, by combination of the Siroquant and Moore and Reynolds techniques, led to results fairly well in agreement with results based on the fixed potassium method.

As an example of Siroquant quantification Figure 6-1 shows the analyzed mineral content in Wyoming MX-80 bentonite from five consignments representing more than 20 years of production. The relatively constant quality is due to blending of material from different bentonite horizons or localities, a technique used by most producers of bentonite (Figure 2-1). However, there is a significant variation in the content of minor accessory minerals, partly depending on lack of quality demands on specific accessory minerals in many commercial products. Calcite is a typical example, which is evidently present (~ 1%) in the Stripa consignment, but almost absent in the other examined consignments.

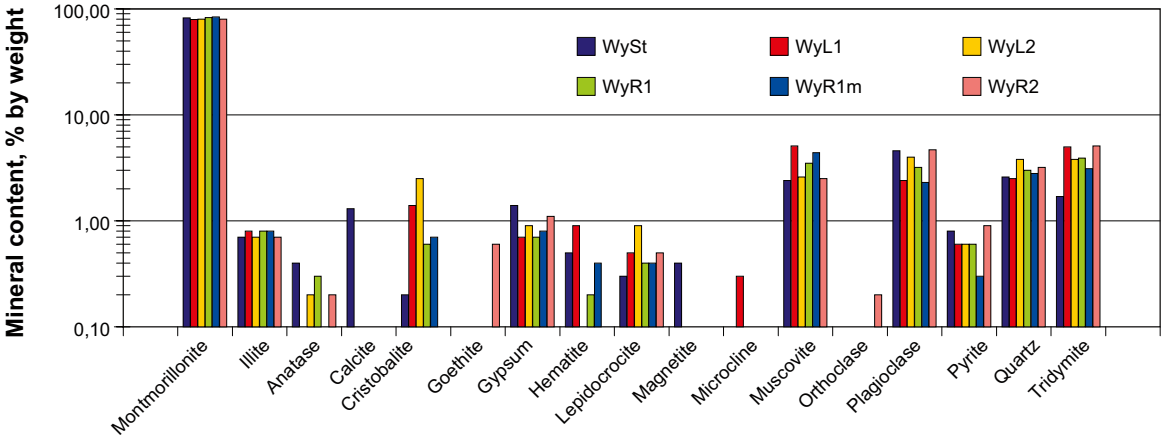

Figure 6-1. *Siroquant results showing the mineral content in the five consignments representing over 20 years of production of MX-80 bentonite. The Stripa (WySt) material represents material delivered around 1980, and the others were delivered 1995 (WyL1), 1999 (WyL2), and 2001 (WyR1 and WyR2). Note the logarithmic scale.*

A significant discrepancy in grain (mineral) density was found between measurements in kerosene and water solutions. A significant water density increase may be evaluated from these results by assuming the grain density constant at the value measured in kerosene. Alternatively, the results may be interpreted as a true difference in grain (2:1 mineral) density caused by the intercalation of water, but not of kerosene, between the individual 2:1 mineral layers. The volume of the solid is thereby reduced in the case of water. The concept of a change in grain density is supported by literature XRD data and by the major difference between BET measured and theoretical specific surface area. This difference indicate that there are tens of stacked 2:1 layers in close contact after dehydration, and that the interlayer volume is not accessible for N_2.

The charge location in the swelling 2:1 mineral seems not to affect the sealing properties significantly. As an example, the Kutch 8940 material is a pronounced beidellite, i.e. the tetrahedral charge dominates, and the Wyoming MX-80 is a corresponding montmorillonite according to the structure calculations. Still, the measured swelling pressures and hydraulic conductivities are similar in the KuNa and the WyNa materials, although there is a tendency for higher swelling pressure at high densities in the Kutch beidellite type material.

On the other hand, the sealing properties varied strongly between some of the tested materials, mainly because of different content of swelling 2:1 minerals, but also as a function of the type of charge compensating cations and the concentration of the test solutions. However, at high densities, only the materials with low content of swelling 2:1 minerals have sealing properties that makes them inappropriate as buffer material. These materials still have a considerable sealing capacity and may well be suited for use in other parts of a repository. A final but important conclusion is that there are bentonite materials with quite different geological origin, which have the same suitable basic mineralogical characteristics and thereby the same sealing properties.

7 References

Bear J, 1988. Dynamics of Fluids in Porous Media. Dover Publications, Inc. ISBN 0-486-65675-6.

Belyayeva N I, 1967. Rapid method for the simultaneous determination of the exchange capacity and content of exchangeable cations in solonetzic soils. Soviet Soil Science. 1409–1413.

Brindley G W, Brown G, (eds.) 1980. Crystal Structures of Clay Minerals and their X-ray Identification. Mineralogical Society Mon. No. 5. London 495 p.

Christidis G, Scott P W Marcopoulos T, 1995. Origin of the bentonite deposits of Eastern Milos, Aegean, Greece: Geological, Mineralogical and Geochemical Evidence. Clays and Clay Minerals, Vol 43, p 63 – 77.

CRC, 1973. Handbook of Chemistry and Physics. CRC Press, The Chemical Rubber Co. Cleveland, Ohio.

Decher A, Bechtel A, Echle W, Friedrich G, Hoernes S, 1996. Stable isotope geochemistry of bentonites from the island of Milos (Greece). Chemical Geology, Volume 129, Number 1, 14 June 1996, pp 101–113(13) Elsevier.

Dixon D A, Chandler N A, Stroes-Gascoyne S, Kozak E, 2001. The isothermal buffer-Rock-Concrete plug interaction test: Final Report. Report No: 06819-REP-01200-10056-R00, Atomic Energy of Canada Limited.

Drever J I, 1973. The preparation of oriented clay mineral specimen for X-ray diffraction analysis by a filter-membrane peel technique. American Mineralogist 58, 553–554.

Elzea J M, Murrey H H, 1989. Trace element composition of the Cretaceous Clay Spur bentonite and implications for its alteration history. 9th Int. Clay Conference, Strasbourg.

Elzea J M, Murrey H H, 1990. Cretaceous Clay Spur bentonite in Wyoming and Montana. Applied Clay Science, 1990, No 3.

Greene-Kelly R, 1953. The identification of montmorillonoids in clays. J.Soil Sci. 4, 223–237.

Henning K-H, Kasbohm J, 1998. Mineralbestand und Genese feinkörniger quartärer und präquartärer Sedimente in NE-Deutschland unter besonderer Berücksichtigung des “Friedländer Tones”.- Berichte der DTTG, Bd. 6: S. 147–167; Greifswald.

Hofmann, U, Klemen R, 1950. Verlust der Austauschfähigkeit von Lithiumionen an Bentonit durch Erhitzung. Z. anorg. Chemie 262, 95–99.

Jackson M L, 1975. Soil chemical analysis – advanced course. Madison, Department of Soil Science, University of Wisconsin, author

Karnland O, Birgersson M, 2006. Montmorillonite stability – With special respect to KBS-3 conditions. SKB TR-06-11, Svensk Kärnbränslehantering AB.

Karnland O, Muurinen A, Karlsson F, 2005. Bentonite swelling pressure in NaCl solutions – Experimentally determined data and model calculations. Advances in Understanding Engineered Clay Barriers, Alonso & Ledesma (eds), 2005 Taylor & Francis Group, London, ISBN 04 1536544 9.

Karnland O, Sandén T, Johannesson L-E, Eriksen T E, Jansson M, Wold S, Pedersen K, Mutamedi M, Rosborg B, 2000. Long Term Test of Buffer Material – Final Report on the pilot parcels. SKB TR-00-22, Svensk Kärnbränslehantering AB.

Konta J, 1986. Textural variation and composition of bentonite derived from basaltic ash. Clays and Clay Minerals*;* June 1986; v. 34; no. 3; p. 257–265

Kryut H R, 1952. Colloid Sience, edited by Kruyt. Chapter VI, Overbeek J Th G, p 245. Elsevier Publishing Company.

Lim C H, Jackson M L, 1986. Expandable Phyllosilicate Reactions with Lithium on Heating. Clays and Clay Minerals 34, 346–352.

Meier L P, Kahr G, 1999. Determination of the cation exchange capacity (CEC) of clay minerals using the complexes of copper(II) ion with triethylenetetraamine and tetraethylenepentamine. Clays and Clay Minerals 47, 386–388.

Mehra O P, Jackson M L, 1960. Iron oxide removal from soils and clays by a dithionite-citrate system buffered with sodium bicarbonate. Clays and Clay Minerals. 7th National Conference. Pergamon Press. 317–327.

Moore D M, Reynolds R C, 1989. X-ray Diffraction and the Identification and Analysis of Clay Minerals. Oxford University Press. 332 p.

Müller-Vonmoos M, Kahr G, 1983. Mineralogiche untersuchungen von Wyoming bentonit MX-80 und Montegel. Technicher Bericht 83-12, Nagra, Schweiz.

Newman A C D, Brown G, 1987. The Chemical Constitution of Clays, Mineralogical Society. Monograph No.6, ed. A.C.D. Newman, 1987.

Omotoso O, McCarty D K, Hillier S, Kleeberg R, 2006. Some successful approaches to quantitative mineral analysis as revealed by the 3rd Reynolds cup contest. Clay and Clay Minerals, Vol 54, No6, 748–760.

Polemio M, and Rhodes J D, 1977. Determining cation exchange capacity: a new method for calcareous and gypsiferous soils. SSSA J 41:524-528.

Přikryl R, Woller F, 2002. Going underground: A new market for Czech bentonite in nuclear waste disposal. Industrial Minerals 415: 72–77. (ISSN 0019-8544)

Rietveld H M, 1969. A profile refinement method for nuclear and magnetic structures. J. Appl. Cryst., 2, 65–71.

Shah N R, 1997. Indian bentonite – focus on the Kutch region. Industrial Minerals, no. 359, pp 43–47.

Slaughter M, Early J W, 1965. Mineralogy and Geological Significance of the Mowry Bentonites, Wyoming. Geol.Soc. Am. Spec. Pap., 83.

Taylor J C, Matulis C E, 1994. A new method for Rietveld Clay Analyses. Part I. Use of a universal measured standard profile for Rietveld quantification of montmorillonite. Powder Diffraction, 9 119–123.

Appendix 1


Holmehus


Rösnäs


Ölst


Asha 8936


Asha 8937


Asha 8938


Asha 8939


Asha 8940


Mx-80


Friedland

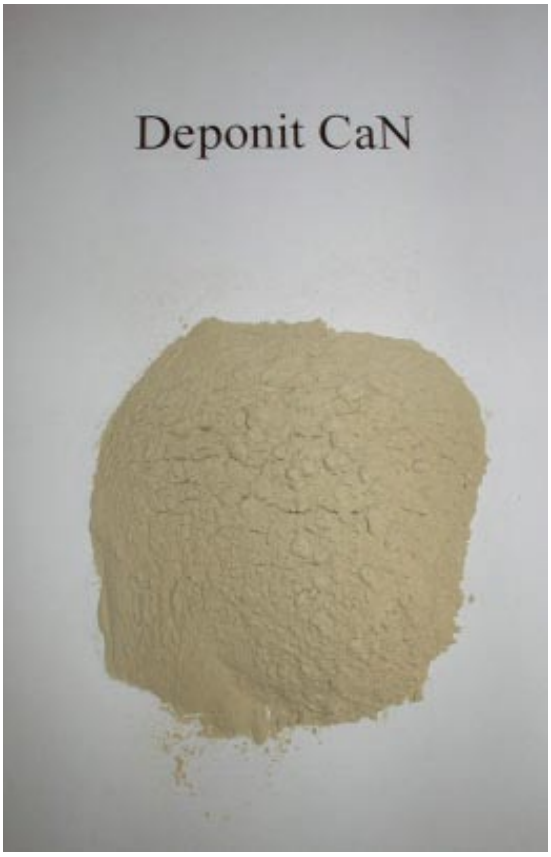
Deponit CaN

Appendix 2

Task Dnesice
Date 2007-03-14
Chi-sqr 2.92
R factor 0.39
Path C:\SQ files\Czech\Dnesice\Dnesice.tsk

Composition Table for Oxides.

		SiO2	Al2O3	TiO2	Fe2O3	MgO	CaO	K2O	Na2O	CO2	SO3	H2O
Phase												
Montmorillonite	39.6	21.88	7.96	1.02	5.21	0.91	0.68	0.05	0.02			
Illite	6.5	3.27	2.35					0.59				
Kaolin	38.9	18.1	15.35									
Albite	0.6	0.43	0.12						0.07			
Anatase	0.1			0.11								
Anorthite	0.1	0.06	0.05				0.03					
Biotite	0											
Calcite	0						0			0		
Chlorite	0	0.01	0.01			0.01						0
Cristobalite	0	0										
Goethite	3.7				3.33							0.38
Gypsum	1.1						0.35				0.5	0.22
Hematite	0				0.03							
Magnesite	0.4					0.19				0.21		
Magnetite	0.2				0.21							
Microcline	0	0.02	0.01					0.01				
Muscovite	3.2	1.46	1.23					0.38				0.15
Orthoclase	0	0.02	0.01					0.01				
Pyrite	0.8				0.55						1.1	
Quartz	3.4	3.43										
Rutile	0.8			0.77								
Siderite	0.2				0.12					0.06		
Tridymite	0.3	0.25										

		SiO2	Al2O3	TiO2	Fe2O3	MgO	CaO	K2O	Na2O	CO2	SO3	H2O	Sum
Calc	Dnesice	48.93	27.09	1.9	9.45	1.11	1.06	1.04	0.09	0.27	1.6	0.75	92.54
Meas	Dnesice	44.09	25.24	1.3	9.93	1.12	0.71	1.38	0.07	0.40	0.05		84.29
Calculated	**Dnesice**	**52.87**	**29.27**	**2.05**	**10.21**	**1.20**	**1.15**	**1.12**	**0.10**	**0.29**	**1.73**		100
Measured	**Dnesice**	**52.31**	**29.94**	**1.54**	**11.78**	**1.33**	**0.84**	**1.64**	**0.08**	**0.48**	**0.06**		100
	Difference	**0.57**	**–0.67**	**0.51**	**–1.57**	**–0.13**	**0.30**	**–0.51**	**0.01**	**–0.19**	**1.67**		0

Task Rokle
Date 2007-03-14
Chi-sqr 1.91
R factor 0.31
Path C:\SQ files\Czech\Rokle\Rokle.tsk

Composition Table for Oxides.

		SiO2	Al2O3	TiO2	Fe2O3	MgO	CaO	K2O	Na2O	CO2	SO3	H2O
Phase												
Montmorillonite	69.4	39.73	10.96	3.94	7.8	2.21	1.41	0.08	0.03			
Illite	5.4	2.71	1.95					0.49				
Kaolin	3.1	1.45	1.23									
Albite	0	0.03	0.01						0			
Anatase	1.9			1.88								
Anorthite	0.2	0.07	0.06				0.03					
Biotite	1.5											
Calcite	5.2						2.92			2.29		
Chlorite	0.1	0.04	0.02			0.04						0.01
Cristobalite	0.5	0.5										
Goethite	2				1.78							0.2
Gypsum	1.4						0.44				0.63	0.28
Hematite	0.3				0.3							
Magnesite	0.7					0.32				0.35		
Magnetite	0.1				0.14							
Microcline	0	0.03	0.01					0.01				
Muscovite	2.8	1.28	1.09					0.34				0.13
Orthoclase	0.4	0.25	0.07					0.06				
Pyrite	1.1				0.71						1.43	
Quartz	2.5	2.54										
Rutile	0.6			0.58								
Siderite	0.3				0.22					0.12		
Tridymite	0.5	0.49										

		SiO2	Al2O3	TiO2	Fe2O3	MgO	CaO	K2O	Na2O	CO2	SO3	H2O	Sum
Calc	Rokle	49.12	15.4	6.4	10.95	2.57	4.8	0.98	0.03	2.76	2.06	0.62	95.07
Meas	Rokle	46.6	12.86	4.06	12.97	2.64	5.84	0.98	0.16	3.67	0.03		89.81
Calculated	**Rokle**	**51.67**	**16.20**	**6.73**	**11.52**	**2.70**	**5.05**	**1.03**	**0.03**	**2.90**	**2.17**		100
Measured	**Rokle**	**51.89**	**14.32**	**4.52**	**14.44**	**2.94**	**6.50**	**1.09**	**0.18**	**4.09**	**0.03**		100
	Difference	**–0.22**	**1.88**	**2.21**	**–2.92**	**–0.24**	**–1.45**	**–0.06**	**–0.15**	**–1.18**	**2.14**		0

Task Skalna
Date 2007-03-14
Chi-sqr 2.31
R factor 0.36
Path C:\SQ files\Czech\Skalna\Skalna.tsk

Composition Table for Oxides.

		SiO2	Al2O3	TiO2	Fe2O3	MgO	CaO	K2O	Na2O	CO2	SO3	H2O
Phase												
Montmorillonite	70.8	41.69	11.36	0.95	10.06	2.02	1.23	0.17				
Illite	3.4	1.72	1.24					0.31				
Kaolin	11.3	5.26	4.46									
Albite	0	0.02	0.01						0			
Anatase	0			0								
Anorthite	0.1	0.05	0.04				0.02					
Biotite	0											
Calcite	0						0			0		
Chlorite	0	0.01	0.01			0.01						0
Cristobalite	0	0.05										
Goethite	1				0.89							0.1
Gypsum	0.6						0.2				0.29	0.13
Hematite	0.1				0.08							
Magnesite	0.7					0.33				0.36		
Magnetite	0.1				0.1							
Microcline	0	0.02	0.01					0.01				
Muscovite	8	3.63	3.08					0.95				0.36
Orthoclase	0	0.02	0.01					0.01				
Pyrite	0.6				0.42						0.85	
Quartz	1.8	1.85										
Rutile	0.5			0.46								
Siderite	0.5				0.36					0.2		
Tridymite	0.2	0.23										

		SiO2	Al2O3	TiO2	Fe2O3	MgO	CaO	K2O	Na2O	CO2	SO3	H2O	Sum
Calc	Skalna	54.55	20.22	1.41	11.91	2.36	1.45	1.45	0	0.56	1.14	0.59	95.05
Meas	Skalna	53.26	18.38	1.02	11.32	2.17	1.08	2.51	0.15	0.40	0.10		90.39
Calculated	**Skalna**	**57.39**	**21.27**	**1.48**	**12.53**	**2.48**	**1.53**	**1.53**	**0.00**	**0.59**	**1.20**		100
Measured	**Skalna**	**58.92**	**20.33**	**1.13**	**12.52**	**2.40**	**1.19**	**2.78**	**0.17**	**0.45**	**0.11**		100
	Difference	**–1.53**	**0.94**	**0.36**	**0.01**	**0.08**	**0.33**	**–1.25**	**–0.17**	**0.14**	**1.09**		0

Task Strance m
Date 2007-03-14
Chi-sqr 1.93
R factor 0.22
Path C:\SQ files\Czech\Strance\Strance m.tsk

Composition Table for Oxides.

		SiO2	Al2O3	TiO2	Fe2O3	MgO	CaO	K2O	Na2O	CO2	SO3	H2O
Phase												
Montmorillonite	70.4	39.27	12.37	2.82	9.47	2.26	0.92	0.04	0.03			
Illite	1.2	0.59	0.43					0.11				
Kaolin	7.9	3.66	3.11									
Albite	0	0.02	0.01						0			
Anatase	1.9			1.94								
Anorthite	0.1	0.06	0.05				0.03					
Biotite	0											
Calcite	0.1						0.07			0.06		
Chlorite	1.3	0.43	0.24			0.48						0.17
Cristobalite	0.2	0.2										
Goethite	2.7				2.41							0.27
Gypsum	0						0.01				0.01	0
Hematite	0				0.03							
Magnesite	0.3					0.12				0.13		
Magnetite	0.1				0.13							
Microcline	0	0.03	0.01					0.01				
Muscovite	2	0.92	0.78					0.24				0.09
Orthoclase	0	0.03	0.01					0.01				
Pyrite	0.9				0.58						1.17	
Quartz	9.5	9.48										
Rutile	0.7			0.68								
Siderite	0.2				0.12					0.07		
Tridymite	0.3	0.29										

		SiO2	Al2O3	TiO2	Fe2O3	MgO	CaO	K2O	Na2O	CO2	SO3	H2O	Sum
Calc	Strance m	54.98	17.01	5.44	12.74	2.86	1.03	0.41	0.03	0.26	1.18	0.53	95.94
Meas	Strance	52.44	15.06	2.89	12.61	2.06	1.59	0.66	0.1	0.44	0.00		87.85
Calculated	**Strance m**	**57.31**	**17.73**	**5.67**	**13.28**	**2.98**	**1.07**	**0.43**	**0.03**	**0.27**	**1.23**		100
Measured	**Strance**	**59.69**	**17.14**	**3.29**	**14.35**	**2.34**	**1.81**	**0.75**	**0.11**	**0.50**	**0.00**		100
	Differerence	**–2.39**	**0.59**	**2.38**	**–1.07**	**0.64**	**–0.74**	**–0.32**	**–0.08**	**–0.23**	**1.23**		0

Task HoR1
Date 2007-03-14
Chi-sqr 2.48
R factor 0.38
Path C:\SQ files\Danish\Ho\HoR1.tsk

Composition Table for Oxides.

		SiO2	Al2O3	TiO2	Fe2O3	MgO	CaO	K2O	Na2O	CO2	SO3	H2O
Phase												
Montmorillonite	74.8	47.12	10.99	0.7	7.9	2.6	0.49	0.28	1.15			
Illite	9.3	4.67	3.36					0.85				
Kaolin	0.1											
Albite	0	0.02	0.01						0			
Anorthite	0.2	0.1	0.08				0.05					
Calcite	0.1						0.08			0.06		
Chlorite	0	0.01	0.01			0.01						0
Clinoptilolite	0.2	0.15	0.03				0.01	0	0.01			0.05
Cristobalite	0	0										
Goethite	0.2				0.16							0.02
Gypsum	1.5						0.5				0.71	0.32
Hematite	0.2				0.19							
Magnetite	0.1				0.11							
Microcline	0	0.02	0.01					0.01				
Muscovite	5.1	2.3	1.95					0.6				0.23
Orthoclase	0	0.02	0.01					0.01				
Pyrite	1				0.69						1.39	
Quartz	5.8	5.83										
Rutile	0.3			0.3								
Tridymite	0.7	0.74										

		SiO2	Al2O3	TiO2	Fe2O3	MgO	CaO	K2O	Na2O	CO2	SO3	H2O	Sum
Calc	HoR1	60.98	16.45	1	9.05	2.61	1.13	1.75	1.16	0.06	2.1	0.62	96.29
Meas	Holmehus	58.12	15.82	0.81	9.11	3.19	0.67	2.91	1.27	1.03	0.15		93.08
Calculated	**HoR1**	**63.33**	**17.08**	**1.04**	**9.40**	**2.71**	**1.17**	**1.82**	**1.20**	**0.06**	**2.18**		100
Measured	**Holmehus**	**62.44**	**17.00**	**0.87**	**9.79**	**3.43**	**0.72**	**3.13**	**1.36**	**1.10**	**0.16**		100
	Differernce	**0.89**	**0.09**	**0.17**	**–0.39**	**–0.72**	**0.45**	**–1.31**	**–0.16**	**–1.04**	**2.02**		0

Task RöR1
Date 2007-03-14
Chi-sqr 2.49
R factor 0.39
Path C:\SQ files\Danish\Rö\RöR1.tsk

Composition Table for Oxides.

		SiO2	Al2O3	TiO2	Fe2O3	MgO	CaO	K2O	Na2O	CO2	SO3	H2O
Phase												
Montmorillonite	45.5	26.96	8.43	0.76	4.7	1.58	0.77	0.06	0.11			
Illite	20.2	10.15	7.29					1.84				
Kaolin	7.1	3.29	2.8									
Albite	0	0.03	0.01						0			
Anorthite	0.2	0.07	0.06				0.03					
Calcite	8.6						4.82			3.78		
Chlorite	0	0.01	0.01			0.02						0.01
Clinoptilolite	1.2	0.72	0.15				0.05	0.02	0.03			0.24
Cristobalite	0.1	0.07										
Goethite	3.5				3.14							0.35
Gypsum	0						0.01				0.01	0
Hematite	0.7				0.66							
Magnetite	0.4				0.45							
Microcline	0	0.03	0.01					0.01				
Muscovite	5	2.24	1.9					0.59				0.22
Orthoclase	0	0.03	0.01					0.01				
Pyrite	1				0.66						1.32	
Quartz	5.4	5.4										
Rutile	0			0								
Tridymite	1	1.02										

		SiO2	Al2O3	TiO2	Fe2O3	MgO	CaO	K2O	Na2O	CO2	SO3	H2O	Sum
Calc	RöR1	50.02	20.67	0.76	9.61	1.6	5.68	2.53	0.14	3.78	1.33	0.82	96.12
Meas	Rösnäs	45.38	18.47	0.88	9.57	2.41	5.61	2.78	0.36	4.62	0.03		90.11
Calculated	**RöR1**	**52.04**	**21.50**	**0.79**	**10.00**	**1.66**	**5.91**	**2.63**	**0.15**	**3.93**	**1.38**		100
Measured	**Rösnäs**	**50.36**	**20.50**	**0.98**	**10.62**	**2.67**	**6.23**	**3.09**	**0.40**	**5.13**	**0.03**		100
	Difference	**1.68**	**1.01**	**–0.19**	**–0.62**	**–1.01**	**–0.32**	**–0.45**	**–0.25**	**–1.20**	**1.36**		0

Task ÖlR1
Date 2007-03-14
Chi-sqr 2.25
R factor 0.39
Path C:\SQ files\Danish\Öl\ÖlR1.tsk

Composition Table for Oxides.

Phase		SiO2	Al2O3	TiO2	Fe2O3	MgO	CaO	K2O	Na2O	CO2	SO3	H2O
Montmorillonite	58.8	34.81	7.92	2	7.08	2.87	0.3	0.21	0.89			
Illite	10.7	5.45	1.84	0.35	1.22	0.45		0.93				
Kaolin	1.2											
Albite	11.3	7.79	2.2						1.34			
Anorthite	0.2	0.06	0.06				0.03					
Calcite	0.1						0.06			0.05		
Chlorite	2.2	0.67	0.38		0.89							0.29
Clinoptilolite	9.3	5.61	1.15				0.36	0.15	0.2			1.85
Cristobalite	0.6	0.63										
Goethite	0.3				0.26							0.03
Gypsum	0.6						0.19				0.28	0.12
Hematite	0.4				0.36							
Magnetite	0.3				0.29							
Microcline	0	0.03	0.01					0.01				
Muscovite	1.9	0.88	0.74					0.23				0.09
Orthoclase	0	0.03	0.01					0.01				
Pyrite	1.1				0.74						1.49	
Quartz	0.6	0.56										
Rutile	0			0								
Tridymite	0.3	0.29										

		SiO2	Al2O3	TiO2	Fe2O3	MgO	CaO	K2O	Na2O	CO2	SO3	H2O	Sum
Calc	ÖlR1	56.81	14.31	2.35	10.84	3.32	0.94	1.54	2.43	0.05	1.77	2.38	94.36
Meas	Ölst	53.57	13.99	3.06	11.1	3.6	2.26	1.56	1.82	2.02	2.25		95.23
Calculated	**ÖlR1**	**60.21**	**15.17**	**2.49**	**11.49**	**3.52**	**1.00**	**1.63**	**2.58**	**0.05**	**1.88**		100
Measured	**Ölst**	**56.25**	**14.69**	**3.21**	**11.66**	**3.78**	**2.37**	**1.64**	**1.91**	**2.12**	**2.36**		100
	Difference	**3.95**	**0.47**	**–0.72**	**–0.17**	**–0.26**	**–1.38**	**–0.01**	**0.66**	**–2.07**	**–0.49**		0

Task FrR1a
Date 2007-03-09
Chi-sqr 2.54
R factor 0.4
Path C:\SQ files\Friedland\FrR1\FrR1a.tsk

Composition Table for Oxides.

Phase		SiO2	Al2O3	TiO2	Fe2O3	MgO	CaO	K2O	Na2O	CO2	SO3	H2O
Montmorillonite	34.7	21.24	6.08	0.65	2.83	1.14	0.05	0.13	0.93			
Illite	25.5	13.64	5.27	0.46	1.98	0.72		2.25				
Kaolin	8.9	4.16	3.53									
Albite (high)	0	0.02	0.01						0			
Albite (low)	1.1	0.73	0.21						0.13			
Anatase	0			0								
Anorthite	0.1	0.05	0.05				0.02					
Calcite 1	0						0.03			0.02		
Calcite 2	0						0.01			0		
Cristobalite	0.1	0.12										
Goethite	0				0							0
Gypsum	0.7						0.24				0.34	0.15
Hematite	0.5				0.51							
Lepidocrocite	0.1				0.07							0.01
Magnetite	0.1				0.11							
Microcline	0	0.02	0.01					0.01				
Muscovite	6.8	3.08	2.62					0.81				0.31
Orthoclase	0	0.02	0.01					0.01				
Pyrite	1.4				0.93						1.86	
Quartz	18.7	18.71										
Rutile	0.7			0.74								
Siderite	0.1				0.07					0.04		
Tridymite	0.3	0.26										

		SiO2	Al2O3	TiO2	Fe2O3	MgO	CaO	K2O	Na2O	CO2	SO3	H2O	Sum
Calc	FrR1a	62.05	17.79	1.85	6.5	1.86	0.35	3.21	1.06	0.06	2.2	0.47	96.93
Meas	Friedland	60.91	17.28	0.94	6.41	1.9	0.36	3.05	1.05	2.24	1.20		95.34
Calculated	**FrR1a**	**64.02**	**18.35**	**1.91**	**6.71**	**1.92**	**0.36**	**3.31**	**1.09**	**0.06**	**2.27**		100
Measured	**Friedland**	**63.89**	**18.12**	**0.99**	**6.72**	**1.99**	**0.38**	**3.20**	**1.10**	**2.35**	**1.26**		100
	Difference	**0.13**	**0.23**	**0.92**	**–0.02**	**–0.07**	**–0.02**	**0.11**	**–0.01**	**–2.29**	**1.01**		0

Task FrR1b
Date 2007-03-09
Chi-sqr 2.06
R factor 0.37
Path C:\SQ files\Friedland\FrR1\FrR1b.tsk

Composition Table for Oxides.

		SiO2	Al2O3	TiO2	Fe2O3	MgO	CaO	K2O	Na2O	CO2	SO3	H2O
Phase												
Montmorillonite	32.7	20.01	5.73	0.62	2.67	1.07	0.05	0.12	0.88			
Illite	22.7	12.14	4.69	0.41	1.76	0.64		2				
Kaolin	13.4	6.24	5.29									
Albite (high)	0	0.02	0.01						0			
Albite (low)	0.7	0.47	0.13						0.08			
Anatase	0			0								
Anorthite	0.1	0.05	0.04				0.02					
Calcite 1	0.2						0.12			0.09		
Calcite 2	0						0.01			0		
Cristobalite	0	0										
Goethite	0				0							0
Gypsum	1.2						0.4				0.58	0.26
Hematite	0				0.03							
Lepidocrocite	0.1				0.09							0.01
Magnetite	0.1				0.1							
Microcline	0	0.02	0.01					0.01				
Muscovite	6.4	2.9	2.46					0.76				0.29
Orthoclase	0	0.02	0.01					0.01				
Pyrite	0.9				0.6						1.21	
Quartz	20.2	20.22										
Rutile	0.4			0.44								
Siderite	0.5				0.32					0.18		
Tridymite	0.2	0.24										

		SiO2	Al2O3	TiO2	Fe2O3	MgO	CaO	K2O	Na2O	CO2	SO3	H2O	Sum
Calc	FrR1b	62.33	18.37	1.47	5.57	1.71	0.6	2.9	0.96	0.27	1.79	0.56	95.97
Meas	Friedland	60.91	17.28	0.94	6.41	1.9	0.36	3.05	1.05	2.24	1.20		95.34
Calculated	**FrR1b**	**64.95**	**19.14**	**1.53**	**5.80**	**1.78**	**0.63**	**3.02**	**1.00**	**0.28**	**1.87**		100
Measured	**Friedland**	**63.89**	**18.12**	**0.99**	**6.72**	**1.99**	**0.38**	**3.20**	**1.10**	**2.35**	**1.26**		100
	Difference	**1.06**	**1.02**	**0.55**	**–0.92**	**–0.21**	**0.25**	**–0.18**	**–0.10**	**–2.07**	**0.61**		0

Task FrR1c
Date 2007-03-09
Chi-sqr 1.69
R factor 0.39
Path C:\SQ files\Friedland\FrR1\FrR1c.tsk

Composition Table for Oxides.

		SiO2	Al2O3	TiO2	Fe2O3	MgO	CaO	K2O	Na2O	CO2	SO3	H2O
Phase												
Montmorillonite	30.1	18.42	5.27	0.57	2.46	0.99	0.04	0.11	0.81			
Illite	21	11.27	4.35	0.38	1.64	0.59		1.86				
Kaolin	8.8	4.09	3.47									
Albite (high)	0	0.03	0.01						0			
Albite (low)	0	0.03	0.01						0			
Anatase	0			0								
Anorthite	0.2	0.07	0.06				0.03					
Calcite 1	0						0			0		
Calcite 2	0.1						0.08			0.06		
Cristobalite	0.3	0.26										
Goethite	1				0.87							0.1
Gypsum	0.6						0.19				0.28	0.12
Hematite	0.7				0.66							
Lepidocrocite	0.4				0.36							0.04
Magnetite	0.8				0.8							
Microcline	0	0.03	0.01					0.01				
Muscovite	10.2	4.62	3.92					1.21				0.46
Orthoclase	0	0.03	0.01					0.01				
Pyrite	1.7				1.12						2.25	
Quartz	22.1	22.1										
Rutile	0.7			0.73								
Siderite	0.9				0.65					0.36		
Tridymite	0.3	0.32										

		SiO2	Al2O3	TiO2	Fe2O3	MgO	CaO	K2O	Na2O	CO2	SO3	H2O	Sum
Calc	FrR1c	61.27	17.11	1.68	8.56	1.58	0.34	3.2	0.81	0.42	2.53	0.72	97.50
Meas	Friedland	60.91	17.28	0.94	6.41	1.9	0.36	3.05	1.05	2.24	1.20		95.34
Calculated	**FrR1c**	**62.84**	**17.55**	**1.72**	**8.78**	**1.62**	**0.35**	**3.28**	**0.83**	**0.43**	**2.59**		100
Measured	**Friedland**	**63.89**	**18.12**	**0.99**	**6.72**	**1.99**	**0.38**	**3.20**	**1.10**	**2.35**	**1.26**		100
	Difference	**–1.05**	**–0.58**	**0.74**	**2.06**	**–0.37**	**–0.03**	**0.08**	**–0.27**	**–1.92**	**1.34**		0

Task FrR1m
Date 2007-03-09
Chi-sqr 2.18
R factor 0.33
Path C:\SQ files\Friedland\FrR1\FrR1m.tsk

Composition Table for Oxides.

		SiO2	Al2O3	TiO2	Fe2O3	MgO	CaO	K2O	Na2O	CO2	SO3	H2O
Phase		63.6	18.14	1.58	5.7	1.81	0.14	2.82	1.21	0.07	1.21	1.02
Montmorillonite	35.2	21.58	6.17	0.66	2.88	1.16	0.05	0.13	0.95			
Illite	23.2	12.44	4.81	0.42	1.81	0.65		2.05				0.75
Kaolin	11.7	5.42	4.6									
Albite (high)	0	0.02	0.01						0			
Albite (low)	2.2	1.54	0.44						0.27			
Anatase	0			0								
Anorthite	0.1	0.05	0.04				0.02					
Calcite 1	0.1						0.03			0.03		
Calcite 2	0						0.01			0		
Cristobalite	0	0										
Goethite	0				0							0
Gypsum	0.1						0.02				0.03	0.01
Hematite	0.1				0.13							
Lepidocrocite	0.1				0.12							0.01
Magnetite	0.1				0.1							
Microcline	0	0.02	0.01					0.01				
Muscovite	5.4	2.43	2.06					0.63				0.24
Orthoclase	0	0.02	0.01					0.01				
Pyrite	0.9				0.59						1.18	
Quartz	19.8	19.83										
Rutile	0.5			0.5								
Siderite	0.1				0.07					0.04		
Tridymite	0.2	0.24										

		SiO2	Al2O3	TiO2	Fe2O3	MgO	CaO	K2O	Na2O	CO2	SO3	H2O	Sum
Calc	FrR1m	63.59	18.15	1.58	5.7	1.81	0.13	2.83	1.22	0.07	1.21	1.01	96.29
Meas	Friedland	60.91	17.28	0.94	6.41	1.9	0.36	3.05	1.05	2.24	1.20		95.34
Calculated	**FrR1m**	**66.04**	**18.85**	**1.64**	**5.92**	**1.88**	**0.14**	**2.94**	**1.27**	**0.07**	**1.26**		100
Measured	**Friedland**	**63.89**	**18.12**	**0.99**	**6.72**	**1.99**	**0.38**	**3.20**	**1.10**	**2.35**	**1.26**		100
	Difference	**2.15**	**0.72**	**0.65**	**–0.80**	**–0.11**	**–0.24**	**–0.26**	**0.17**	**–2.28**	**0.00**		0

Task MiR1a
Date 2007-03-08
Chi-sqr 2.05
R factor 0.28
Path C:\SQ files\Greece\MiR1m\MiR1a.tsk

Composition Table for Oxides.

		SiO2	Al2O3	TiO2	Fe2O3	MgO	CaO	K2O	Na2O	CO2	SO3	H2O
Phase												
Montmorillonite	79.5	49.77	16.75	0.68	3.65	3	1.07	0.1	0.63			
Illite	5.1	2.55	1.83					0.46				
Albite (high)	0.9	0.58	0.17						0.1			
Albite (low)	0	0.02	0.01						0			
Anatase	0.2			0.2								
Anorthite	0.1	0.05	0.04				0.02					
Biotite	0											
Calcite	6.2						3.47			2.72		
Cristobalite	0.7	0.71										
Dolomite	1.3					0.29	0.4			0.63		
Goethite	1.5				1.35							0.15
Gypsum	0.2						0.05				0.07	0.03
Hematite	0.3				0.26							
Lepidocrocite	0.2				0.16							0.02
Magnetite	0.1				0.09							
Microcline	0.2	0.14	0.04					0.04				
Muscovite	1.4	0.61	0.52					0.16				0.06
Orthoclase	0	0.02	0.01					0.01				
Pyrite	1.2				0.77						1.55	
Quartz	0.1	0.11										
Rutile	0			0.01								
Siderite	0.4				0.26					0.14		
Tridymite	0.6	0.6										

		SiO2	Al2O3	TiO2	Fe2O3	MgO	CaO	K2O	Na2O	CO2	SO3	H2O	Sum
Calc	MiR1a	55.16	19.37	0.89	6.54	3.29	5.01	0.77	0.73	3.49	1.62	0.26	96.87
Meas	Deponit CA-N	48.27	15.67	0.7	4.56	2.92	5.37	0.78	0.65	3.7067	1.675		84.30
Calculated	**MiR1a**	**56.94**	**20.00**	**0.92**	**6.75**	**3.40**	**5.17**	**0.79**	**0.75**	**3.60**	**1.67**		100
Measured	**Deponit CA-N**	**57.26**	**18.59**	**0.83**	**5.41**	**3.46**	**6.37**	**0.93**	**0.77**	**4.40**	**1.99**		100
	Difference	**–0.32**	**1.41**	**0.09**	**1.34**	**–0.07**	**–1.20**	**–0.13**	**–0.02**	**–0.79**	**–0.31**		0

Task MiR1b
Date 2007-03-08
Chi-sqr 2.08
R factor 0.2
Path C:\SQ files\Greece\MiR1m\MiR1b.tsk

Composition Table for Oxides.

		SiO2	Al2O3	TiO2	Fe2O3	MgO	CaO	K2O	Na2O	CO2	SO3	H2O
Phase												
Montmorillonite	80.6	50.48	16.99	0.69	3.7	3.04	1.09	0.1	0.63			
Illite	4.5	2.24	1.61					0.41				
Albite (high)	0	0.01	0						0			
Albite (low)	0	0.01	0						0			
Anatase	0			0								
Anorthite	0.1	0.04	0.04				0.02					
Biotite	0											
Calcite	6						3.36			2.64		
Cristobalite	0.7	0.66										
Dolomite	1.1					0.24	0.33			0.53		
Goethite	1.7				1.48							0.17
Gypsum	0.5						0.15				0.22	0.1
Hematite	0				0.04							
Lepidocrocite	0.2				0.15							0.02
Magnetite	0.1				0.08							
Microcline	0	0.02	0.01					0.01				
Muscovite	2.1	0.96	0.82					0.25				0.1
Orthoclase	0	0.02	0.01					0.01				
Pyrite	1.2				0.77						1.55	
Quartz	0.5	0.45										
Rutile	0			0								
Siderite	0.4				0.3					0.16		
Tridymite	0.4	0.37										

		SiO2	Al2O3	TiO2	Fe2O3	MgO	CaO	K2O	Na2O	CO2	SO3	H2O	Sum
Calc	MiR1b	55.26	19.48	0.69	6.52	3.28	4.95	0.78	0.63	3.33	1.77	0.39	96.69
Meas	Deponit CA-N	48.27	15.67	0.7	4.56	2.92	5.37	0.78	0.65	3.7067	1.675		84.30
Calculated	**MiR1b**	**57.15**	**20.15**	**0.71**	**6.74**	**3.39**	**5.12**	**0.81**	**0.65**	**3.44**	**1.83**		100
Measured	**Deponit CA-N**	**57.26**	**18.59**	**0.83**	**5.41**	**3.46**	**6.37**	**0.93**	**0.77**	**4.40**	**1.99**		100
	Difference	**–0.11**	**1.56**	**–0.12**	**1.33**	**–0.07**	**–1.25**	**–0.12**	**–0.12**	**–0.95**	**–0.16**		0

Task MiR1c
Date 2007-03-08
Chi-sqr 2.09
R factor 0.24
Path C:\SQ files\Greece\MiR1m\MiR1c.tsk

Composition Table for Oxides.

		SiO2	Al2O3	TiO2	Fe2O3	MgO	CaO	K2O	Na2O	CO2	SO3	H2O
Phase												
Montmorillonite	82.5	51.68	17.39	0.71	3.79	3.11	1.11	0.1	0.65			
Illite	4.8	2.39	1.71					0.43				
Albite (high)	0.6	0.42	0.12						0.07			
Albite (low)	0	0.02	0						0			
Anatase	0			0								
Anorthite	0.1	0.05	0.04				0.02					
Biotite	0											
Calcite	3.6						2			1.57		
Cristobalite	0.5	0.47										
Dolomite	1.4					0.3	0.41			0.65		
Goethite	1.4				1.27							0.14
Gypsum	0.6						0.21				0.3	0.13
Hematite	0.2				0.21							
Lepidocrocite	0.4				0.38							0.04
Magnetite	0.1				0.09							
Microcline	0.5	0.35	0.1					0.09				
Muscovite	0.7	0.3	0.25					0.08				0.03
Orthoclase	0	0.02	0.01					0				
Pyrite	1				0.63						1.27	
Quartz	0.5	0.46										
Rutile	0.7			0.66								
Siderite	0.2				0.11					0.06		
Tridymite	0.3	0.33										

		SiO2	Al2O3	TiO2	Fe2O3	MgO	CaO	K2O	Na2O	CO2	SO3	H2O	Sum
Calc	MiR1c	56.49	19.62	1.37	6.48	3.41	3.75	0.7	0.72	2.28	1.57	0.34	96.39
Meas	Deponit CA-N	48.27	15.67	0.7	4.56	2.92	5.37	0.78	0.65	3.7067	1.675		84.30
Calculated	**MiR1c**	**58.61**	**20.35**	**1.42**	**6.72**	**3.54**	**3.89**	**0.73**	**0.75**	**2.37**	**1.63**		100
Measured	**Deponit CA-N**	**57.26**	**18.59**	**0.83**	**5.41**	**3.46**	**6.37**	**0.93**	**0.77**	**4.40**	**1.99**		100
	Difference	**1.35**	**1.77**	**0.59**	**1.31**	**0.07**	**–2.48**	**–0.20**	**–0.02**	**–2.03**	**–0.36**		0

Task MiR1m
Date 2007-03-08
Chi-sqr 2.12
R factor 0.19
Path C:\SQ files\Greece\MiR1m\MiR1m.tsk

Composition Table for Oxides.

		SiO2	Al2O3	TiO2	Fe2O3	MgO	CaO	K2O	Na2O	CO2	SO3	H2O
Phase												
Montmorillonite	83.1	52.04	17.51	0.71	3.82	3.14	1.12	0.1	0.65			
Illite	4.1	2.06	1.48					0.37				
Albite (high)	0	0.02	0.01						0			
Albite (low)	0	0.02	0.01						0			
Anatase	0			0								
Anorthite	0.1	0.05	0.04				0.02					
Biotite	0											
Calcite	5.3						2.98			2.33		
Cristobalite	0.6	0.59										
Dolomite	1.3					0.28	0.39			0.61		
Goethite	1.4				1.22							0.14
Gypsum	0.2						0.07				0.1	0.05
Hematite	0.1				0.09							
Lepidocrocite	0.2				0.13							0.02
Magnetite	0.1				0.09							
Microcline	0	0.02	0.01					0.01				
Muscovite	1.3	0.61	0.51					0.16				0.06
Orthoclase	0	0.02	0.01					0.01				
Pyrite	1				0.65						1.31	
Quartz	0.4	0.36										
Rutile	0.4			0.39								
Siderite	0.2				0.11					0.06		
Tridymite	0.2	0.23										

		SiO2	Al2O3	TiO2	Fe2O3	MgO	CaO	K2O	Na2O	CO2	SO3	H2O	Sum
Calc	MiR1m	56.02	19.58	1.1	6.11	3.42	4.58	0.65	0.65	3.00	1.41	0.27	96.52
Meas	Deponit CA-N	48.27	15.67	0.7	4.56	2.92	5.37	0.78	0.65	3.7067	1.675		84.30
Calculated	**MiR1m**	**58.04**	**20.29**	**1.14**	**6.33**	**3.54**	**4.75**	**0.67**	**0.67**	**3.11**	**1.46**		100
Measured	**Deponit CA-N**	**57.26**	**18.59**	**0.83**	**5.41**	**3.46**	**6.37**	**0.93**	**0.77**	**4.40**	**1.99**		100
	Difference	**0.78**	**1.70**	**0.31**	**0.92**	**0.08**	**–1.62**	**–0.25**	**–0.10**	**–1.29**	**–0.53**		0

Task Ku36R1
Date 2007-03-14
Chi-sqr 1.98
R factor 0.43
Path C:\SQ files\Indian\In36\As36.tsk

Composition Table for Oxides.

		SiO2	Al2O3	TiO2	Fe2O3	MgO	CaO	K2O	Na2O	CO2	SO3	H2O	Sb2O3
Phase													
Montmorillonite	85.6	52.01	15.7	0.36	7.45	3.89	1.07	0.05	1.01				
Illite	2	1.02	0.73					0.18					
Albite	0.2	0.12	0.03						0.02				
Anatase	0.3			0.25									
Anorthite	0.1	0.06	0.05				0.03						
Calcite	0.6						0.36			0.29			
Cristobalite	0	0											
Goethite	0.8				0.72							0.08	
Gypsum	0.3						0.1				0.15	0.07	
Hematite	0.4				0.42								
Lepidocrocite	0.6				0.51							0.06	
Maghemite	2.8				2.86								
Magnesite	0					0				0			
Magnetite	0.1				0.12								
Microcline	0	0.02	0.01					0.01					
Muscovite	1.4	0.62	0.52					0.16				0.06	
Orthoclase	0	0.02	0.01					0.01					
Pyrite	1.1				0.73						1.46		
Quartz	0	0											
Rutile	0.5			0.52									
Tridymite	0.5	0.47											
Vaterite	0.3						0.15			0.12			
Heulandite	2.2	1.34	0.33				0.18					0.34	

		SiO2	Al2O3	TiO2	Fe2O3	MgO	CaO	K2O	Na2O	CO2	SO3	H2O	Sum
Calc	Ku36R1	55.68	17.38	1.13	12.81	3.89	1.89	0.41	1.03	0.41	1.61	0.61	96.24
Meas	Ku36R1	53.09	15.97	0.78	11.07	3.8	2.25	0.16	1.51	0.6606	0.05		89.34
Calculated	**Ku36R1**	**57.86**	**18.06**	**1.17**	**13.31**	**4.04**	**1.96**	**0.43**	**1.07**	**0.43**	**1.67**		100
Measured	**Ku36R1**	**59.42**	**17.88**	**0.87**	**12.39**	**4.25**	**2.52**	**0.18**	**1.69**	**0.74**	**0.06**		100
	Difference	**–1.57**	**0.18**	**0.30**	**0.92**	**–0.21**	**–0.55**	**0.25**	**–0.62**	**–0.31**	**1.62**		0

Task Ku37R1
Date 2007-03-11
Chi-sqr 2.3
R factor 0.47
Path C:\SQ files\Indian\In37\As37.tsk

Composition Table for Oxides.

		SiO2	Al2O3	TiO2	Fe2O3	MgO	CaO	K2O	Na2O	CO2	SO3	H2O
Phase												
Montmorillonite	86.4	51.3	17.66	0.45	8.59	2.56	0.13	0.05	1.58			
Illite	0.6	0.32	0.23					0.06				
Albite	0.4	0.25	0.07						0.04			
Anatase	0.6			0.56								
Anorthite	0.2	0.06	0.05				0.03					
Calcite	1						0.58			0.46		
Cristobalite	0	0										
Goethite	1.3				1.17							0.13
Gypsum	0.7						0.21				0.31	0.14
Hematite	0.3				0.3							
Lepidocrocite	0.3				0.26							0.03
Maghemite	0.4				0.39							
Magnesite	0.5					0.25				0.27		
Magnetite	0.1				0.14							
Microcline	0	0.03	0.01					0.01				
Muscovite	2.4	1.08	0.92					0.28				0.11
Orthoclase	0	0.03	0.01					0.01				
Pyrite	0.5				0.35						0.69	
Quartz	1.6	1.55										
Rutile	0.6			0.58								
Tridymite	1	0.99										
Vaterite	0.5						0.3			0.23		

		SiO2	Al2O3	TiO2	Fe2O3	MgO	CaO	K2O	Na2O	CO2	SO3	H2O	Sum
Calc	Ku37R1	55.61	18.95	1.59	11.2	2.81	1.25	0.41	1.62	0.96	1.00	0.41	95.40
Meas	Ku37R1	53	18.51	0.87	10.2	2.65	1.02	0.14	2.9	1.2478	0.2		90.74
Calculated	**Ku37R1**	**58.29**	**19.86**	**1.67**	**11.74**	**2.95**	**1.31**	**0.43**	**1.70**	**1.01**	**1.05**		100
Measured	**Ku37R1**	**58.41**	**20.40**	**0.96**	**11.24**	**2.92**	**1.12**	**0.15**	**3.20**	**1.38**	**0.22**		100
	Difference	**–0.12**	**–0.54**	**0.71**	**0.50**	**0.02**	**0.19**	**0.28**	**–1.50**	**–0.37**	**0.83**		0

Task Ku38R1
Date 2007-03-11
Chi-sqr 2.27
R factor 0.45
Path C:\SQ files\Indian\In38\As38.tsk

Composition Table for Oxides.

		SiO2	Al2O3	TiO2	Fe2O3	MgO	CaO	K2O	Na2O	CO2	SO3	H2O
Phase												
Montmorillonite	79.1	45.17	16.8	1.07	8.47	2.08	0.23		1.53			
Illite	1.2											
Albite	0.4	0.27	0.08						0.05			
Anatase	1			0.96								
Anorthite	0.1	0.06	0.05				0.03					
Calcite	0.5						0.25			0.2		
Cristobalite	0	0.02										
Goethite	1.4				1.24							0.14
Gypsum	1.4						0.47				0.67	0.3
Hematite	0				0.03							
Lepidocrocite	0.6				0.58							0.06
Maghemite	0.7				0.69							
Magnesite	0.4					0.2				0.22		
Magnetite	0.9				0.88							
Microcline	0	0.03	0.01					0.01				
Muscovite	4.6	2.06	1.75					0.54				0.21
Orthoclase	0.5	0.3	0.09					0.08				
Pyrite	0.5				0.31						0.61	
Quartz	3.9	3.89										
Rutile	0.4			0.36								
Tridymite	1.9	1.94										
Vaterite	0						0			0		

		SiO2	Al2O3	TiO2	Fe2O3	MgO	CaO	K2O	Na2O	CO2	SO3	H2O	Sum
Calc	Ku38R1	53.74	18.78	2.39	12.2	2.28	0.98	0.63	1.58	0.42	1.28	0.71	94.28
Meas	Ku38R1	53.91	17.5	1.67	10.13	2.41	1.28	0.06	2.32	1.1744	0.125		90.58
Calculated	**Ku38R1**	**57.00**	**19.92**	**2.54**	**12.94**	**2.42**	**1.04**	**0.67**	**1.68**	**0.45**	**1.36**		100
Measured	**Ku38R1**	**59.52**	**19.32**	**1.84**	**11.18**	**2.66**	**1.41**	**0.07**	**2.56**	**1.30**	**0.14**		100
	Difference	**–2.52**	**0.60**	**0.69**	**1.76**	**–0.24**	**–0.37**	**0.60**	**–0.89**	**–0.85**	**1.22**		0

Task Ku39R1
Date 2007-03-11
Chi-sqr 2.12
R factor 0.51
Path C:\SQ files\Indian\In39\As39.tsk

Composition Table for Oxides.

		SiO2	Al2O3	TiO2	Fe2O3	MgO	CaO	K2O	Na2O	CO2	SO3	H2O
Phase												
Montmorillonite	78.9	47.35	15.77	0.41	6.55	3.26	0.7	0.05	1			
Illite	1.3	0.66	0.48					0.12				
Albite	1.6	1.12	0.32						0.19			
Anatase	1.2			1.17								
Anorthite	0.2	0.07	0.06				0.03					
Calcite	1						0.58			0.46		
Cristobalite	0.3	0.29										
Goethite	1				0.89							0.1
Gypsum	0.6						0.2				0.28	0.13
Hematite	0.8				0.79							
Lepidocrocite	0.6				0.53							0.06
Maghemite	1.4				1.47							
Magnesite	0.7					0.34				0.37		
Magnetite	0.9				0.91							
Microcline	1.6	1.01	0.29					0.26				
Muscovite	2.5	1.14	0.97					0.3				0.11
Orthoclase	0	0.03	0.01					0.01				
Pyrite	1.1				0.75						1.49	
Quartz	0	0										
Rutile	0.1			0.12								
Tridymite	3.2	3.2										
Vaterite	0.1						0.04			0.04		

		SiO2	Al2O3	TiO2	Fe2O3	MgO	CaO	K2O	Na2O	CO2	SO3	H2O	Sum
Calc	Ku39R1	54.87	17.9	1.7	11.89	3.6	1.55	0.74	1.19	0.87	1.77	0.4	96.08
Meas	Ku39R1	52.09	17.99	0.93	11.24	3.6	1.25	0.17	1.66	0.4037	0.025		89.36
Calculated	**Ku39R1**	**57.11**	**18.63**	**1.77**	**12.38**	**3.75**	**1.61**	**0.77**	**1.24**	**0.91**	**1.84**		100
Measured	**Ku39R1**	**58.29**	**20.13**	**1.04**	**12.58**	**4.03**	**1.40**	**0.19**	**1.86**	**0.45**	**0.03**		100
	Difference	**–1.18**	**–1.50**	**0.73**	**–0.20**	**–0.28**	**0.21**	**0.58**	**–0.62**	**0.45**	**1.81**		0

Task Ku40R1
Date 2007-03-11
Chi-sqr 2.02
R factor 0.33
Path C:\SQ files\Indian\In40\As40.tsk

Composition Table for Oxides.

		SiO2	Al2O3	TiO2	Fe2O3	MgO	CaO	K2O	Na2O	CO2	SO3	H2O
Phase												
Montmorillonite	87	48.51	20.15	1.36	9.04	1.87	0.51	0.05	1.47			
Illite	1	0.52	0.38					0.09				
Albite	0.9	0.63	0.18						0.11			
Anatase	0.9			0.91								
Anorthite	0.1	0.06	0.05				0.03					
Calcite	0						0			0		
Cristobalite	0.4	0.37										
Goethite	1.3				1.18							0.13
Gypsum	2.2						0.72				1.02	0.46
Hematite	0				0.03							
Lepidocrocite	0.5				0.48							0.05
Maghemite	0.4				0.39							
Magnesite	0.3					0.13				0.15		
Magnetite	0.1				0.11							
Microcline	0.4	0.26	0.07					0.07				
Muscovite	0.1	0.03	0.03					0.01				0
Orthoclase	0.4	0.27	0.08					0.07				
Pyrite	0.3				0.21						0.41	
Quartz	0.5	0.53										
Rutile	0.2			0.16								
Tridymite	2.5	2.53										
Vaterite	0.3						0.15			0.12		

		SiO2	Al2O3	TiO2	Fe2O3	MgO	CaO	K2O	Na2O	CO2	SO3	H2O	Sum
Calc	Ku40R1	53.71	20.94	2.43	11.44	2	1.41	0.29	1.58	0.27	1.43	0.64	95.50
Meas	Ku40R1	47.05	18.25	1.85	12.45	1.82	0.73	0.12	1.96	0.5505	0.225		85.01
Calculated	**Ku40R1**	**56.24**	**21.93**	**2.54**	**11.98**	**2.09**	**1.48**	**0.30**	**1.65**	**0.28**	**1.50**		100
Measured	**Ku40R1**	**55.35**	**21.47**	**2.18**	**14.65**	**2.14**	**0.86**	**0.14**	**2.31**	**0.65**	**0.26**		100
	Difference	**0.89**	**0.46**	**0.37**	**–2.67**	**–0.05**	**0.62**	**0.16**	**–0.65**	**–0.36**	**1.23**		0

Task	WyR1a
Date	2007-03-15
Chi-sqr	3.27
R factor	0.38
Path	C:\SQ files\Wyoming\MxR1all\MxR1a.tsk

Composition Table for Oxides.

		SiO2	Al2O3	TiO2	Fe2O3	MgO	CaO	K2O	Na2O	CO2	SO3	H2O
Phase												
Montmorillonite	85.8	55.03	18.64	0.09	3.4	2.38	0.2	0.05	1.83			
Illite	0.6	0.3	0.22					0.06				
Albite	1.5	1.06	0.3						0.18			
Anatase	0.4			0.43								
Anorthite	2.7	1.17	0.99				0.55					
Calcite	0.1						0.08			0.06		
Cristobalite	0.7	0.74										
Goethite	0				0.03							0
Gypsum	0.5						0.17				0.24	0.11
Hematite	0				0.02							
Lepidocrocite	0.7				0.64							0.07
Magnetite	0.1				0.06							
Microcline	0.4	0.29	0.08					0.08				
Muscovite	1.5	0.68	0.58					0.18				0.07
Orthoclase	0.4	0.23	0.07					0.06				
Pyrite	0.5				0.36						0.73	
Quartz	2.6	2.58										
Tridymite	1.3	1.3										

		SiO2	Al2O3	TiO2	Fe2O3	MgO	CaO	K2O	Na2O	CO2	SO3	H2O	Sum
Calc	WyR1a	63.38	20.88	0.52	4.51	2.38	1	0.43	2.01	0.06	0.97	0.25	96.14
Meas	MX-80 R1	57.33	18.51	0.15	3.6	2.31	1.28	0.51	2.04	1.14	0.73		87.59
Calculated	**WyR1a**	**65.92**	**21.72**	**0.54**	**4.69**	**2.48**	**1.04**	**0.45**	**2.09**	**0.06**	**1.01**		100
Measured	**MX-80 R1**	**65.45**	**21.13**	**0.17**	**4.11**	**2.64**	**1.46**	**0.58**	**2.33**	**1.30**	**0.83**		100
	Difference	**0.47**	**0.59**	**0.37**	**0.58**	**–0.16**	**–0.42**	**–0.13**	**–0.24**	**–1.24**	**0.18**		0

Task	WyR1b
Date	2007-03-15
Chi-sqr	2.86
R factor	0.36
Path	C:\SQ files\Wyoming\MxR1all\MxR1b.tsk

Composition Table for Oxides.

		SiO2	Al2O3	TiO2	Fe2O3	MgO	CaO	K2O	Na2O	CO2	SO3	H2O
Phase												
Montmorillonite	81.1	52.02	17.62	0.09	3.22	2.25	0.19	0.05	1.73			
Illite	0.7	0.36	0.26					0.07				
Albite	0.7	0.45	0.13						0.08			
Anatase	0.3			0.32								
Anorthite	0.9	0.38	0.32				0.18					
Calcite	0.5						0.28			0.22		
Cristobalite	0.8	0.78										
Goethite	0.6				0.54							0.06
Gypsum	1.1						0.34				0.49	0.22
Hematite	0.1				0.08							
Lepidocrocite	0.9				0.79							0.09
Magnetite	0.2				0.17							
Microcline	0.3	0.21	0.06					0.06				
Muscovite	3.2	1.46	1.24					0.38				0.15
Orthoclase	1.9	1.26	0.36					0.33				
Pyrite	0.6				0.38						0.76	
Quartz	3.6	3.56										
Tridymite	2.6	2.65										

		SiO2	Al2O3	TiO2	Fe2O3	MgO	CaO	K2O	Na2O	CO2	SO3	H2O	Sum
Calc	WyR1b	63.13	19.99	0.41	5.18	2.25	0.99	0.89	1.81	0.22	1.25	0.52	96.12
Meas	MX-80 R1	57.33	18.51	0.15	3.6	2.31	1.28	0.51	2.04	1.14	0.73		87.59
Calculated	**WyR1b**	**65.68**	**20.80**	**0.43**	**5.39**	**2.34**	**1.03**	**0.93**	**1.88**	**0.23**	**1.30**		100
Measured	**MX-80 R1**	**65.45**	**21.13**	**0.17**	**4.11**	**2.64**	**1.46**	**0.58**	**2.33**	**1.30**	**0.83**		100
	Difference	**0.23**	**–0.33**	**0.26**	**1.28**	**–0.30**	**–0.43**	**0.34**	**–0.45**	**–1.07**	**0.47**		0

Task WyR1c
Date 2007-03-15
Chi-sqr 3.83
R factor 0.43
Path C:\SQ files\Wyoming\MxR1all\MxR1c.tsk

Composition Table for Oxides.

		SiO2	Al2O3	TiO2	Fe2O3	MgO	CaO	K2O	Na2O	CO2	SO3	H2O
Phase												
Montmorillonite	82.3	52.81	17.89	0.09	3.27	2.28	0.19	0.05	1.75			
Illite	0.6	0.3	0.21					0.05				
Albite	1.4	0.99	0.28						0.17			
Anatase	0			0.04								
Anorthite	1.6	0.7	0.59				0.32					
Calcite	0.1						0.04			0.04		
Cristobalite	0.1	0.08										
Goethite	0.2				0.19							0.02
Gypsum	1.3						0.41				0.58	0.26
Hematite	0				0.02							
Lepidocrocite	0.8				0.75							0.08
Magnetite	0.1				0.06							
Microcline	2.4	1.54	0.44					0.4				
Muscovite	3.2	1.44	1.22					0.38				0.14
Orthoclase	0	0.01	0					0				
Pyrite	0.6				0.38						0.76	
Quartz	2.5	2.45										
Tridymite	2.9	2.87										

		SiO2	Al2O3	TiO2	Fe2O3	MgO	CaO	K2O	Na2O	CO2	SO3	H2O	Sum
Calc	WyR1c	63.19	20.63	0.13	4.67	2.28	0.96	0.88	1.92	0.04	1.34	0.5	96.04
Meas	MX-80 R1	57.33	18.51	0.15	3.6	2.31	1.28	0.51	2.04	1.14	0.73		87.59
Calculated	**WyR1c**	**65.80**	**21.48**	**0.14**	**4.86**	**2.37**	**1.00**	**0.92**	**2.00**	**0.04**	**1.40**		100
Measured	**MX-80 R1**	**65.45**	**21.13**	**0.17**	**4.11**	**2.64**	**1.46**	**0.58**	**2.33**	**1.30**	**0.83**		100
	Difference	**0.34**	**0.35**	**–0.04**	**0.75**	**–0.26**	**–0.46**	**0.33**	**–0.33**	**–1.26**	**0.57**		0

Task WyR1m
Date 2007-03-17
Chi-sqr 3.37
R factor 0.36
Path C:\SQ files\Wyoming\MxR1all\MxR1m.tsk

Composition Table for Oxides.

		SiO2	Al2O3	TiO2	Fe2O3	MgO	CaO	K2O	Na2O	CO2	SO3	H2O
Phase												
Montmorillonite	83.8	53.77	18.22	0.09	3.33	2.32	0.19	0.05	1.78			
Illite	0.7	0.34	0.24					0.06				
Albite	1.2	0.81	0.23						0.14			
Anatase	0			0								
Anorthite	1.3	0.55	0.47				0.26					
Calcite	0.2						0.13			0.1		
Cristobalite	0	0										
Goethite	0				0							0
Gypsum	0.7						0.22				0.31	0.14
Hematite	0				0.02							
Lepidocrocite	0.4				0.34							0.04
Magnetite	0.1				0.07							
Microcline	0	0.01	0					0				
Muscovite	4.7	2.14	1.82					0.56				0.21
Orthoclase	0.5	0.3	0.08					0.08				
Pyrite	0.5				0.31						0.62	
Quartz	2.4	2.39										
Tridymite	3	3.04										

		SiO2	Al2O3	TiO2	Fe2O3	MgO	CaO	K2O	Na2O	CO2	SO3	H2O	Sum
Calc	WyR1m	63.35	21.06	0.09	4.07	2.32	0.8	0.75	1.92	0.1	0.93	0.39	95.39
Meas	MX-80 R1	57.33	18.51	0.15	3.6	2.31	1.28	0.51	2.04	1.14	0.73		87.59
Calculated	**WyR1m**	**66.41**	**22.08**	**0.09**	**4.27**	**2.43**	**0.84**	**0.79**	**2.01**	**0.10**	**0.97**		100
Measured	**MX-80 R1**	**65.45**	**21.13**	**0.17**	**4.11**	**2.64**	**1.46**	**0.58**	**2.33**	**1.30**	**0.83**		100
	Difference	**0.96**	**0.95**	**–0.08**	**0.16**	**–0.21**	**–0.62**	**0.20**	**–0.32**	**–1.19**	**0.15**		0

Task WySt
Date 2007-03-15
Chi-sqr 2.36
R factor 0.29
Path C:\SQ files\Wyoming\MxHi\MxStri.tsk

Composition Table for Oxides.		SiO2	Al2O3	TiO2	Fe2O3	MgO	CaO	K2O	Na2O	CO2	SO3	H2O
Phase												
Montmorillonite	82.5	52.96	17.94	0.09	3.28	2.29	0.19	0.05	1.76			
Illite	0.7	0.36	0.26					0.06				
Albite	2.8	1.91	0.54						0.33			
Anatase	0.4			0.36								
Anorthite	1.8	0.79	0.67				0.37					
Calcite	1.3						0.75			0.59		
Cristobalite	0.2	0.25										
Goethite	0				0							0
Gypsum	1.4						0.46				0.66	0.3
Hematite	0.5				0.5							
Lepidocrocite	0.3				0.23							0.03
Magnetite	0.4				0.36							
Microcline	0	0.02	0					0				
Muscovite	2.4	1.1	0.94					0.29				0.11
Orthoclase	0	0.02	0					0				
Pyrite	0.8				0.56						1.12	
Quartz	2.6	2.59										
Tridymite	1.7	1.75										

		SiO2	Al2O3	TiO2	Fe2O3	MgO	CaO	K2O	Na2O	CO2	SO3	H2O	Sum
Calc	WySt	61.75	20.35	0.45	4.93	2.29	1.77	0.4	2.09	0.59	1.78	0.44	96.40
Meas	MX-80 Stripa	58.7	19.15	0.21	3.97	2.51	1.45	0.5	2.4	1.65	0.83		91.37
Calculated	**WySt**	**64.06**	**21.11**	**0.47**	**5.11**	**2.38**	**1.84**	**0.41**	**2.17**	**0.61**	**1.85**		100
Measured	**MX-80 Stripa**	**64.25**	**20.96**	**0.23**	**4.35**	**2.75**	**1.59**	**0.55**	**2.63**	**1.81**	**0.90**		100
	Difference	**–0.19**	**0.15**	**0.24**	**0.77**	**–0.37**	**0.25**	**–0.13**	**–0.46**	**–1.20**	**0.94**		0

Task WyL1
Date 2007-03-15
Chi-sqr 2.3
R factor 0.33
Path C:\SQ files\Wyoming\MxHi\MxLOT1.tsk

Composition Table for Oxides.		SiO2	Al2O3	TiO2	Fe2O3	MgO	CaO	K2O	Na2O	CO2	SO3	H2O
Phase												
Montmorillonite	79.5	51.05	17.3	0.09	3.17	2.2	0.3	0.05	1.53			
Illite	0.8	0.41	0.29					0.07				
Albite	0.4	0.26	0.07						0.05			
Anatase	0.1			0.13								
Anorthite	2	0.87	0.74				0.41					
Calcite	0						0			0		
Cristobalite	1.4	1.4										
Goethite	0				0							0
Gypsum	0.7						0.22				0.31	0.14
Hematite	0.9				0.86							
Lepidocrocite	0.5				0.44							0.05
Magnetite	0.1				0.09							
Microcline	0.3	0.21	0.06					0.05				
Muscovite	5.1	2.32	1.97					0.61				0.23
Orthoclase	0	0.02	0					0				
Pyrite	0.6				0.4						0.8	
Quartz	2.5	2.54										
Tridymite	5	5										

		SiO2	Al2O3	TiO2	Fe2O3	MgO	CaO	K2O	Na2O	CO2	SO3	H2O	Sum
Calc	WyL1	64.08	20.43	0.22	4.96	2.2	0.93	0.78	1.58	0	1.11	0.42	96.29
Meas	MX-80 LOT1	61.35	19.18	0.14	3.56	2.25	1.18	0.47	1.95	1.03	0.80		91.91
Calculated	**WyL1**	**66.55**	**21.22**	**0.23**	**5.15**	**2.28**	**0.97**	**0.81**	**1.64**	**0.00**	**1.15**		100
Measured	**MX-80 LOT1**	**66.75**	**20.87**	**0.15**	**3.87**	**2.45**	**1.28**	**0.51**	**2.12**	**1.12**	**0.87**		100
	Difference	**–0.20**	**0.35**	**0.08**	**1.28**	**–0.16**	**–0.32**	**0.30**	**–0.48**	**–1.12**	**0.28**		0

Task WyL2
Date 2007-03-15
Chi-sqr 2.66
R factor 0.33
Path C:\SQ files\Wyoming\MxHi\MxLOT2.tsk

Composition Table for Oxides.

		SiO2	Al2O3	TiO2	Fe2O3	MgO	CaO	K2O	Na2O	CO2	SO3	H2O
Phase												
Montmorillonite	79.8	51.25	17.36	0.09	3.18	2.21	0.3	0.05	1.53			
Illite	0.7	0.37	0.27					0.07				
Albite	1	0.71	0.2						0.12			
Anatase	0.2			0.15								
Anorthite	3	1.3	1.11				0.61					
Calcite	0						0			0		
Cristobalite	2.5	2.52										
Goethite	0.1				0.06							0.01
Gypsum	0.9						0.29				0.41	0.18
Hematite	0.1				0.1							
Lepidocrocite	0.9				0.78							0.09
Magnetite	0.1				0.08							
Microcline	0	0.02	0					0				
Muscovite	2.6	1.17	0.99					0.31				0.12
Orthoclase	0	0.02	0					0				
Pyrite	0.6				0.37						0.74	
Quartz	3.8	3.75										
Tridymite	3.8	3.77										

		SiO2	Al2O3	TiO2	Fe2O3	MgO	CaO	K2O	Na2O	CO2	SO3	H2O	Sum
Calc	WyL2	64.88	19.93	0.24	4.57	2.21	1.2	0.43	1.65	0	1.15	0.4	96.26
Meas	MX-80 LOT2	62.23	18.39	0.14	3.67	2.24	1.2	0.45	1.76	1.21	0.78		92.07
Calculated	**WyL2**	**67.40**	**20.70**	**0.25**	**4.75**	**2.30**	**1.25**	**0.45**	**1.71**	**0.00**	**1.19**		100
Measured	**MX-80 LOT2**	**67.59**	**19.97**	**0.15**	**3.99**	**2.43**	**1.30**	**0.49**	**1.91**	**1.32**	**0.84**		100
	Difference	**–0.19**	**0.73**	**0.10**	**0.76**	**–0.14**	**–0.06**	**–0.04**	**–0.20**	**–1.32**	**0.35**		0

Task WyR1
Date 2007-03-15
Chi-sqr 2.52
R factor 0.31
Path C:\SQ files\Wyoming\MxHi\MxR1.tsk

Composition Table for Oxides.

		SiO2	Al2O3	TiO2	Fe2O3	MgO	CaO	K2O	Na2O	CO2	SO3	H2O
Phase												
Montmorillonite	82.7	53.07	17.98	0.09	3.29	2.29	0.31	0.05	1.59			
Illite	0.8	0.38	0.27					0.07				
Albite	1.7	1.14	0.32						0.2			
Anatase	0.3			0.28								
Anorthite	1.5	0.64	0.54				0.3					
Calcite	0.1						0.06			0.04		
Cristobalite	0.6	0.62										
Goethite	0				0							0
Gypsum	0.7						0.22				0.31	0.14
Hematite	0.2				0.23							
Lepidocrocite	0.4				0.33							0.04
Magnetite	0.1				0.08							
Microcline	0	0.02	0					0				
Muscovite	3.5	1.6	1.36					0.42				0.16
Orthoclase	0	0.02	0					0				
Pyrite	0.6				0.41						0.82	
Quartz	3	3										
Tridymite	3.9	3.91										

		SiO2	Al2O3	TiO2	Fe2O3	MgO	CaO	K2O	Na2O	CO2	SO3	H2O	Sum
Calc	WyR1	64.4	20.47	0.37	4.34	2.29	0.89	0.54	1.79	0.04	1.13	0.34	96.26
Meas	MX-80 R1	57.33	18.51	0.15	3.6	2.31	1.28	0.51	2.04	1.14	0.73		87.59
Calculated	**WyR1**	**66.90**	**21.27**	**0.38**	**4.51**	**2.38**	**0.92**	**0.56**	**1.86**	**0.04**	**1.17**		100
Measured	**MX-80 R1**	**65.45**	**21.13**	**0.17**	**4.11**	**2.64**	**1.46**	**0.58**	**2.33**	**1.30**	**0.83**		100
	Difference	**1.45**	**0.13**	**0.21**	**0.40**	**–0.26**	**–0.54**	**–0.02**	**–0.47**	**–1.26**	**0.35**		0

Task WyR1m
Date 2007-03-15
Chi-sqr 2.65
R factor 0.28
Path C:\SQ files\Wyoming\MxHi\MxR1m.tsk

Composition Table for Oxides.		SiO2	Al2O3	TiO2	Fe2O3	MgO	CaO	K2O	Na2O	CO2	SO3	H2O
Phase												
Montmorillonite	83.9	53.85	18.24	0.09	3.34	2.32	0.32	0.05	1.61			
Illite	0.8	0.4	0.29					0.07				
Albite	0.6	0.41	0.12						0.07			
Anatase	0			0								
Anorthite	1.7	0.71	0.61				0.33					
Calcite	0						0			0		
Cristobalite	0.7	0.72										
Goethite	0				0							0
Gypsum	0.8						0.27				0.39	0.18
Hematite	0.4				0.36							
Lepidocrocite	0.4				0.36							0.04
Magnetite	0.1				0.09							
Microcline	0	0.02	0					0				
Muscovite	4.4	1.99	1.69					0.52				0.2
Orthoclase	0	0.02	0					0				
Pyrite	0.3				0.21						0.43	
Quartz	2.8	2.78										
Tridymite	3.1	3.14										

		SiO2	Al2O3	TiO2	Fe2O3	MgO	CaO	K2O	Na2O	CO2	SO3	H2O	Sum
Calc	WyR1m	64.04	20.95	0.09	4.36	2.32	0.92	0.64	1.68	0	0.82	0.42	95.82
Meas	MX-80 R1	57.33	18.51	0.15	3.6	2.31	1.28	0.51	2.04	1.14	0.73		87.59
Calculated	**WyR1m**	**66.83**	**21.86**	**0.09**	**4.55**	**2.42**	**0.96**	**0.67**	**1.75**	**0.00**	**0.86**		100
Measured	**MX-80 R1**	**65.45**	**21.13**	**0.17**	**4.11**	**2.64**	**1.46**	**0.58**	**2.33**	**1.30**	**0.83**		100
	Difference	**1.38**	**0.73**	**–0.08**	**0.44**	**–0.22**	**–0.50**	**0.09**	**–0.58**	**–1.30**	**0.03**		0

Task WyR2
Date 2007-03-15
Chi-sqr 2.66
R factor 0.32
Path C:\SQ files\Wyoming\MxHi\MxR2.tsk

Composition Table for Oxides.		SiO2	Al2O3	TiO2	Fe2O3	MgO	CaO	K2O	Na2O	CO2	SO3	H2O
Phase												
Montmorillonite	80	51.42	17.42	0.09	3.19	2.22	0.36	0.05	1.43			
Illite	0.7	0.38	0.27					0.07				
Albite	1.9	1.32	0.37						0.23			
Anatase	0.2			0.22								
Anorthite	2.8	1.21	1.03				0.57					
Calcite	0						0			0		
Cristobalite	0	0										
Goethite	0.6				0.56							0.06
Gypsum	1.1						0.36				0.51	0.23
Hematite	0				0.02							
Lepidocrocite	0.5				0.48							0.05
Magnetite	0.1				0.08							
Microcline	0	0.02	0					0				
Muscovite	2.5	1.15	0.98					0.3				0.11
Orthoclase	0.2	0.15	0.04					0.04				
Pyrite	0.9				0.58						1.17	
Quartz	3.2	3.17										
Tridymite	5.1	5.07										

		SiO2	Al2O3	TiO2	Fe2O3	MgO	CaO	K2O	Na2O	CO2	SO3	H2O	Sum
Calc	WyR2	63.89	20.11	0.31	4.91	2.22	1.29	0.46	1.66	0	1.68	0.45	96.53
Meas	MX-80 R2	61.17	19.24	0.14	3.63	2.32	1.31	0.52	1.94	1.10	0.65		92.02
Calculated	**WyR2**	**66.19**	**20.83**	**0.32**	**5.09**	**2.30**	**1.34**	**0.48**	**1.72**	**0.00**	**1.74**		100
Measured	**MX-80 R2**	**66.47**	**20.91**	**0.15**	**3.94**	**2.52**	**1.42**	**0.57**	**2.11**	**1.20**	**0.71**		100
	Difference	**–0.29**	**–0.08**	**0.17**	**1.14**	**–0.22**	**–0.09**	**–0.09**	**–0.39**	**–1.20**	**1.03**		0

Appendix 3

Input data										Calculation												Results	
		quartz part			Included part																		
			illite part			Fe(III) part																	
				Kaolinite part			C comp of Ca																
Acme No	A406190							S comp of Ca															
Group	Cz																						
Sample	DnNa						montm			DnNa	Formula w	Atoms %	Z	Eq, %	DnNa	atoms	Z	charge	atomic w	weight			DnNa
		0	0.26	0.39			0.35																
SiO2	44.87	0.00	0.24	0.34			0.42	1.000		18.81	60.08	0.313	4	1.25	Si	6.89	4	27.56	28.09	193.5		Si	6.89
Al2O3	26.21	0.00	0.30	0.49			0.22	1.000		5.736	101.96	0.113	3	0.34	Al	1.11	3	3.33	26.98	30.0		Al	1.11
TiO2	1.17				1.00		1.00			1.17	79.90	0.015	4	0.06	Σ tet	8.00		30.89		223.5		Sum tetrahedral	8.00
Fe2O3	9.49				0.74	1	1.00			7.023	159.69	0.088	3	0.26									
FeO						0	1.00			0	71.85	0.000	2	0.00	Al	1.37	3	4.10	26.98	36.9		Al	1.37
MgO	0.89				1	1	1.00			0.89	40.31	0.022	2	0.04	Ti	0.32	4	1.29	47.88	15.4		Ti	0.32
MgO						0				0	40.31	0.000	2	0.00	Fe3+	1.94	3	5.81	55.85	108.1		Fe(III)	1.94
CaO	0.02				1		1	1		0	56.08	0.000	2	0.00	Fe2+	0.00	2	0.00	55.85	0.0		Fe(II)	0.00
Na2O	1.33				1					1.33	61.98	0.043	1	0.04	Mg	0.49	2	0.97	24.31	11.8		Mg	0.49
K2O	1.3				0					0	94.20	0.000	1	0.00	Σ oct	4.11		12.17		172.2		Sum octahedral	4.11
Tot C	0.15				1					0.15					Ca	0.00	2.0	0.00	40.08	0.0		Ca	0.00
Tot S	0.01				1					0.01					Mg	0.00	2	0.00	24.31	0.0		Mg	0.00
															K	0.00	1	0.00	39.10	0.0		K	0.00
LOI	14														Na	0.94	1	0.94	22.99	21.7		Na	0.94
CEC	0.4														Σ int	0.94		0.94		21.7		Sum interlayer	0.94
									Si/Al	3.279													
	0.00								Si/tot	0.538					O	24	–2	–48.00	16.00	384.0		O	24.00
															H	4	1	4.00	1.01	4.0		H	4.00
															Unit cell weight					805.4		Unit cell weight	805.4
										Eq. sum				2.00	Charge balance calc			0.00				Tetr charge	–1.11
										oxygen + hydrogen				44.00								Octa charge	0.17
										scaling f				22.01								Total charge	–0.94
																						Tetra charge, %	118
																						CEC mont calc	1.17
																						CEC clay calc	0.41
																						CEC clay meas	0.40
																						Illite calc, %	26
	DnNa	Si	6.89	Al	1.11	Al	1.37	Ti	0.32	Fe	(III)	1.94	Fe	(II)	0.00	Mg	0.49	Ca	0.00	Mg	0.00	K	0.00	Na	0.94

	Input data									Calculation												Results	
		quartz part		Included part																			
		illite part		Fe(III) part																			
		Kaolinite part		C comp of Ca																			
Acme No	A401275						S comp of Ca																
Group	Cz																						
Sample	RoNa					montm				RoNa	Formula w	Atoms %	Z	Eq, %		RoNa	atoms	Z	charge	atomic w	weight		RoNa
		0	0.05	0.03		0.92																	
SiO2	51.93	0.00	0.04	0.02		0.94	1.000			48.72	60.08	0.811	4	3.24		Si	7.36	4	29.44	28.09	206.7		Si 7.36
Al2O3	15.54	0.00	0.08	0.06		0.86	1.000			13.35	101.96	0.262	3	0.79		Al	0.64	3	1.92	26.98	17.3		Al 0.64
TiO2	4.77				1.00	1.00				4.77	79.90	0.060	4	0.24		Σ tet	8.00		31.36		224.0		Sum tetrahedral 8.00
Fe2O3	12.5				0.80	1 1.00				10	159.69	0.125	3	0.38									
FeO						0 1.00				0	71.85	0.000	2	0.00		Al	1.74	3	5.21	26.98	46.9		Al 1.74
MgO	2.46				1	1 1.00				2.46	40.31	0.061	2	0.12		Ti	0.54	4	2.17	47.88	25.9		Ti 0.54
MgO						0				0	40.31	0.000	2	0.00		Fe3+	1.14	3	3.41	55.85	63.5		Fe(III) 1.14
CaO	0.63				1	1 1				0	56.08	0.000	2	0.00		Fe2+	0.00	2	0.00	55.85	0.0		Fe(II) 0.00
Na2O	2.52				1					2.52	61.98	0.081	1	0.08		Mg	0.55	2	1.11	24.31	13.5		Mg 0.55
K2O	0.41				0					0	94.20	0.000	1	0.00		Σ oct	3.97		11.90		149.8		Sum octahedral 3.97
Tot C	0.15				1					0.15						Ca	0.00	2.0	0.00	40.08	0.0		Ca 0.00
Tot S	0.01				1					0.01						Mg	0.00	2	0.00	24.31	0.0		Mg 0.00
																K	0.00	1	0.00	39.10	0.0		K 0.00
LOI	8.4															Na	0.74	1	0.74	22.99	17.0		Na 0.74
CEC	0.76															Σ int	0.74		0.74		17.0		Sum interlayer 0.74
									Si/Al	3.648													
	0.00															O	24	–2	–48.00	16.00	384.0		O 24.00
																H	4	1	4.00	1.01	4.0		H 4.00
																Unit cell weight					778.8		Unit cell weight 778.8
										Eq. sum				4.85		Charge balance calc 0.00							Tetr charge –0.64
										oxygen + hydrogen				44.00									Octa charge –0.10
										scaling f				9.08									Total charge –0.74
																							Tetra charge, % 87
																							CEC mont calc 0.95
																							CEC clay calc 0.87
																							CEC clay meas 0.76
																							Illite calc, % 5
	RoNa	Si	7.36	Al	0.64	Al	1.74	Ti	0.54	Fe	(III)	1.14	Fe	(II)	0.00	Mg	0.55	Ca	0.00	Mg	0.00	K	0.00	Na 0.74

Input data										Calculation												Results	
		quartz part			Included part																		
		illite part			Fe(III) part																		
		Kaolinite part			C comp of Ca																		
Acme No	A401275				S comp of Ca																		
Group	Cz																						
Sample	SkNa				montm					SkNa	Formula w	Atoms %	Z	Eq, %	SkNa	atoms	Z	charge	atomic w	weight			SkNa
		0	0.26	0.11		0.63																	
SiO2	51.62	0.00	0.22	0.09		0.69	1.000			35.64	60.08	0.593	4	2.37	Si	7.39	4	29.54	28.09	207.4		Si	7.39
Al2O3	18.66	0.00	0.36	0.17		0.48	1.000			8.893	101.96	0.174	3	0.52	Al	0.61	3	1.84	26.98	16.6		Al	0.61
TiO2	0.87				1	1.00				0.87	79.90	0.011	4	0.04	Σ tet	8.00		31.39		224.0		Sum tetrahedral	8.00
Fe2O3	13.07				0.89	1 1.00				11.63	159.69	0.146	3	0.44									
FeO						0 1.00				0	71.85	0.000	2	0.00	Al	1.56	3	4.67	26.98	42.0		Al	1.56
MgO	2.14				1	1 1.00				2.14	40.31	0.053	2	0.11	Ti	0.14	4	0.54	47.88	6.5		Ti	0.14
MgO						0				0	40.31	0.000	2	0.00	Fe3+	1.81	3	5.44	55.85	101.3		Fe(III)	1.81
CaO	0.02				1	1 1				0	56.08	0.000	2	0.00	Fe2+	0.00	2	0.00	55.85	0.0		Fe(II)	0.00
Na2O	1.58				1					1.58	61.98	0.051	1	0.05	Mg	0.66	2	1.32	24.31	16.1		Mg	0.66
K2O	1.97				0					0	94.20	0.000	1	0.00	Σ oct	4.17		11.98		165.9		Sum octahedral	4.17
Tot C	0.12				1					0.12					Ca	0.00	2.0	0.00	40.08	0.0		Ca	0.00
Tot S	0.02				1					0.02					Mg	0.00	2	0.00	24.31	0.0		Mg	0.00
															K	0.00	1	0.00	39.10	0.0		K	0.00
LOI	9.6														Na	0.63	1	0.63	22.99	14.6		Na	0.63
CEC	0.47														Σ int	0.63		0.63		14.6		Sum interlayer	0.63
									Si/Al	4.008													
	0.00														O	24	–2	–48.00	16.00	384.0		O	24.00
															H	4	1	4.00	1.01	4.0		H	4.00
															Unit cell weight					792.5		Unit cell weight	792.5
										Eq. sum				3.53	Charge balance calc			0.00				Tetr charge	–0.61
										oxygen + hydrogen				44.00								Octa charge	–0.02
										scaling f				12.45								Total charge	–0.63
																						Tetra charge, %	97
																						CEC mont calc	0.80
																						CEC clay calc	0.50
																						CEC clay meas	0.47
																						Illite calc, %	26

	SkNa	Si	7.39	Al	0.61	Al	1.56	Ti	0.14	Fe	(III)	1.81	Fe	(II)	0.00	Mg	0.66	Ca	0.00	Mg	0.00	K	0.00	Na	0.63

	Input data									Calculation													Results	
		quartz part			Included part																			
			illite part			Fe(III) part																		
				Kaolinite part		C comp of Ca																		
Acme No	A401275						S comp of Ca																	
Group	Cz																							
Sample	StNa					montm				StNa	Formula w	Atoms %	Z	Eq, %		StNa	atoms	Z	charge	atomic w	weight		StNa	
		0	0.06	0.08		0.86																		
SiO2	50.46	0.00	0.05	0.06		0.89	1.000			44.99	60.08	0.749	4	2.99		Si	7.18	4	28.71	28.09	201.6		Si	7.18
Al2O3	18.28	0.00	0.10	0.14		0.76	1.000			13.93	101.96	0.273	3	0.82		Al	0.82	3	2.47	26.98	22.2		Al	0.82
TiO2	3.46				1	1.00				3.46	79.90	0.043	4	0.17		Σ tet	8.00		31.18		223.8		Sum tetrahedral	8.00
Fe2O3	12.03				0.95	1	1.00			11.43	159.69	0.143	3	0.43										
FeO						0	1.00			0	71.85	0.000	2	0.00		Al	1.80	3	5.39	26.98	48.5		Al	1.80
MgO	1.85				1	1	1.00			1.85	40.31	0.046	2	0.09		Ti	0.42	4	1.66	47.88	19.9		Ti	0.42
MgO						0				0	40.31	0.000	2	0.00		Fe3+	1.37	3	4.12	55.85	76.6		Fe(III)	1.37
CaO	0.41				1		1	1		0	56.08	0.000	2	0.00		Fe2+	0.00	2	0.00	55.85	0.0		Fe(II)	0.00
Na2O	2.51				1					2.51	61.98	0.081	1	0.08		Mg	0.44	2	0.88	24.31	10.7		Mg	0.44
K2O	0.45				0					0	94.20	0.000	1	0.00		Σ oct	4.02		12.05		155.7		Sum octahedral	4.02
Tot C	0.13				1					0.13						Ca	0.00	2.0	0.00	40.08	0.0		Ca	0.00
Tot S	0.01				1					0.01						Mg	0.00	2	0.00	24.31	0.0		Mg	0.00
																K	0.00	1	0.00	39.10	0.0		K	0.00
LOI	9.3															Na	0.78	1	0.78	22.99	17.8		Na	0.78
CEC	0.76															Σ int	0.78		0.78		17.8		Sum interlayer	0.78
									Si/Al	3.229														
	0.00															O	24	–2	–48.00	16.00	384.0		O	24.00
																H	4	1	4.00	1.01	4.0		H	4.00
																Unit cell weight					785.3		Unit cell weight	785.3
										Eq. sum				4.59		Charge balance calc			0.00				Tetr charge	–0.82
										oxygen + hydrogen				44.00									Octa charge	0.05
										scaling f				9.59									Total charge	–0.78
																							Tetra charge, %	106
																							CEC mont calc	0.99
																							CEC clay calc	0.85
																							CEC clay meas	0.76
																							Illite calc, %	6

StNa	Si	7.18	Al	0.82	Al	1.80	Ti	0.42	Fe	(III)	1.37	Fe	(II)	0.00	Mg	0.44	Ca	0.00	Mg	0.00	K	0.00	Na	0.78

Input data										Calculation												Results	
		quartz part			Included part																		
		illite part			Fe(III) part																		
		Kaolinite part			C comp of Ca																		
Acme No	A401275						S comp of Ca																
Group	De																						
Sample	HoNa					montm				HoNa	Formula w	Atoms %	Z	Eq, %		HoNa	atoms	Z	charge	atomic w	weight		HoNa
		0	0.26	0.00		0.74																	
SiO2	56.6	0.00	0.22	0.00		0.78	1.000			44.43	60.08	0.739	4	2.96		Si	7.84	4	31.37	28.09	220.2		Si 7.84
Al2O3	15.68	0.00	0.39	0.00		0.61	1.000			9.566	101.96	0.188	3	0.56		Al	0.16	3	0.48	26.98	4.3		Al 0.16
TiO2	0.69				1.00	1.00				0.69	79.90	0.009	4	0.03		Σ tet	8.00		31.84		224.5		Sum tetrahedral 8.00
Fe2O3	10.32				0.97	1 1.00				10.01	159.69	0.125	3	0.38									
FeO						0 1.00				0	71.85	0.000	2	0.00		Al	1.83	3	5.49	26.98	49.4		Al 1.83
MgO	3.13				0.97	1 1.00				3.036	40.31	0.075	2	0.15		Ti	0.09	4	0.37	47.88	4.4		Ti 0.09
MgO						0				0	40.31	0.000	2	0.00		Fe3+	1.33	3	3.99	55.85	74.3		Fe(III) 1.33
CaO	0.17				1	1 1				0	56.08	0.000	2	0.00		Fe2+	0.00	2	0.00	55.85	0.0		Fe(II) 0.00
Na2O	2.08				1					2.08	61.98	0.067	1	0.07		Mg	0.80	2	1.60	24.31	19.4		Mg 0.80
K2O	2.24				0					0	94.20	0.000	1	0.00		Σ oct	4.05		11.45		147.5		Sum octahedral 4.05
Tot C	0.2				1					0.2						Ca	0.00	2.0	0.00	40.08	0.0		Ca 0.00
Tot S	0.01				1					0.01						Mg	0.00	2	0.00	24.31	0.0		Mg 0.00
																K	0.00	1	0.00	39.10	0.0		K 0.00
LOI	8.2															Na	0.71	1	0.71	22.99	16.4		Na 0.71
CEC	0.57															Σ int	0.71		0.71		16.4		Sum interlayer 0.71
									Si/Al	4.644													
	0.00															O	24	–2	–48.00	16.00	384.0		O 24.00
																H	4	1	4.00	1.01	4.0		H 4.00
																Unit cell weight					776.4		Unit cell weight 776.4
										Eq. sum				4.15		Charge balance calc			0.00				Tetr charge –0.16
										oxygen + hydrogen				44.00									Octa charge –0.55
										scaling f				10.61									Total charge –0.71
																							Tetra charge, % 22
																							CEC mont calc 0.92
																							CEC clay calc 0.68
																							CEC clay meas 0.57
																							Illite calc, % 26
	HoNa	Si	7.84	Al	0.16	Al	1.83	Ti	0.09	Fe	(III)	1.33	Fe	(II)	0.00	Mg	0.80	Ca	0.00	Mg	0.00	K	0.00	Na 0.71

Input data										Calculation												Results	
		quartz part			Included part																		
			illite part			Fe(III) part																	
				Kaolinite part			C comp of Ca																
Acme No	A401275							S comp of Ca															
Group	De																						
Sample	RöNa						montm			RöNa	Formula w	Atoms %	Z	Eq, %		RöNa	atoms	Z	charge	atomic w	weight		RöNa
		0	0.35	0.07			0.58																
SiO2	49.05	0.00	0.30	0.06			0.64	1.000		31.48	60.08	0.524	4	2.10		Si	7.28	4	29.12	28.09	204.5	Si	7.28
Al2O3	21.1	0.00	0.47	0.10			0.43	1.000		9.025	101.96	0.177	3	0.53		Al	0.72	3	2.16	26.98	19.4	Al	0.72
TiO2	0.92				1.00		1.00			0.92	79.90	0.012	4	0.05		Σ tet	8.00		31.28		223.9	Sum tetrahedral	8.00
Fe2O3	11.87				0.71	1	1.00			8.428	159.69	0.106	3	0.32									
FeO						0	1.00			0	71.85	0.000	2	0.00		Al	1.74	3	5.22	26.98	46.9	Al	1.74
MgO	2.59				1	1	1.00			2.59	40.31	0.064	2	0.13		Ti	0.16	4	0.64	47.88	7.7	Ti	0.16
MgO						0				0	40.31	0.000	2	0.00		Fe3+	1.47	3	4.40	55.85	81.9	Fe(III)	1.47
CaO	0.16				1		1	1		0	56.08	0.000	2	0.00		Fe2+	0.00	2	0.00	55.85	0.0	Fe(II)	0.00
Na2O	1.51				1					1.51	61.98	0.049	1	0.05		Mg	0.89	2	1.79	24.31	21.7	Mg	0.89
K2O	2.72				0					0	94.20	0.000	1	0.00		Σ oct	4.26		12.04		158.2	Sum octahedral	4.26
Tot C	0.13				1					0.13						Ca	0.00	2.0	0.00	40.08	0.0	Ca	0.00
Tot S	0				1					0						Mg	0.00	2	0.00	24.31	0.0	Mg	0.00
																K	0.00	1	0.00	39.10	0.0	K	0.00
LOI	9.6															Na	0.68	1	0.68	22.99	15.6	Na	0.68
CEC	0.4															Σ int	0.68		0.68		15.6	Sum interlayer	0.68
									Si/Al	3.488													
	0.00															O	24	–2	–48.00	16.00	384.0	O	24.00
																H	4	1	4.00	1.01	4.0	H	4.00
																Unit cell weight					785.7	Unit cell weight	785.7
										Eq. sum				3.17		Charge balance calc			0.00			Tetr charge	–0.72
										oxygen + hydrogen				44.00								Octa charge	0.04
										scaling f				13.89								Total charge	–0.68
																						Tetra charge, %	106
																						CEC mont calc	0.86
																						CEC clay calc	0.50
																						CEC clay meas	0.40
																						Illite calc, %	35

RöNa	Si	7.28	Al	0.72	Al	1.74	Ti	0.16	Fe	(III)	1.47	Fe	(II)	0.00	Mg	0.89	Ca	0.00	Mg	0.00	K	0.00	Na	0.68

Input data										Calculation												Results	
		quartz part		Included part																			
		illite part			Fe(III) part																		
		Kaolinite part			C comp of Ca																		
Acme No	A401275					S comp of Ca																	
Group	De																						
Sample	ÖlNa				montm			ÖlNa	Formula w	Atoms %	Z	Eq, %		ÖlNa	atoms	Z	charge	atomic w	weight			ÖlNa	
		0	0.11	0.01	0.88																		
SiO2	53.52	0.00	0.09	0.01	0.90	1.000		48.4	60.08	0.806	4	3.22		Si	7.55	4	30.21	28.09	212.2			Si	7.55
Al2O3	13.29	0.00	0.18	0.02	0.80	1.000		10.63	101.96	0.209	3	0.63		Al	0.45	3	1.34	26.98	12.0			Al	0.45
TiO2	2.81			1.00	1.00			2.81	79.90	0.035	4	0.14		Σ tet	8.00		31.55		224.2			Sum tetrahedral	8.00
Fe2O3	12.37			0.9	1	1.00		11.13	159.69	0.139	3	0.42											
FeO					0	1.00		0	71.85	0.000	2	0.00		Al	1.51	3	4.53	26.98	40.7			Al	1.51
MgO	4.07			1	1	1.00		4.07	40.31	0.101	2	0.20		Ti	0.33	4	1.32	47.88	15.8			Ti	0.33
MgO					0			0	40.31	0.000	2	0.00		Fe3+	1.31	3	3.92	55.85	73.0			Fe(III)	1.31
CaO	0.54			1	1	1		0	56.08	0.000	2	0.00		Fe2+	0.00	2	0.00	55.85	0.0			Fe(II)	0.00
Na2O	2.59			1				2.59	61.98	0.084	1	0.08		Mg	0.95	2	1.89	24.31	23.0			Mg	0.95
K2O	0.93			0				0	94.20	0.000	1	0.00		Σ oct	4.09		11.66		152.5			Sum octahedral	4.09
Tot C	0.61			1				0.61						Ca	0.00	2.0	0.00	40.08	0.0			Ca	0.00
Tot S	0.04			1				0.04						Mg	0.00	2	0.00	24.31	0.0			Mg	0.00
														K	0.00	1	0.00	39.10	0.0			K	0.00
LOI	9.3													Na	0.78	1	0.78	22.99	18.0			Na	0.78
CEC	0.67													Σ int	0.78		0.78		18.0			Sum interlayer	0.78
							Si/Al	4.553															
	0.00													O	24	–2	–48.00	16.00	384.0			O	24.00
														H	4	1	4.00	1.01	4.0			H	4.00
														Unit cell weight					782.8			Unit cell weight	782.8
								Eq. sum				4.69		Charge balance calc			0.00					Tetr charge	–0.45
								oxygen + hydrogen				44.00										Octa charge	–0.34
								scaling f				9.38										Total charge	–0.78
																						Tetra charge, %	57
																						CEC mont calc	1.00
																						CEC clay calc	0.88
																						CEC clay meas	0.67
																						Illite calc, %	11

ÖlNa Si 7.55 Al 0.45 Al 1.51 Ti 0.33 Fe (III) 1.31 Fe (II) 0.00 Mg 0.95 Ca 0.00 Mg 0.00 K 0.00 Na 0.78

Input data										Calculation												Results	
		quartz part		Included part																			
		illite part			Fe(III) part																		
			Kaolinite part		C comp of Ca																		
Acme No	A401275					S comp of Ca																	
Group	Ge																						
Sample	FrNa				montm				FrNa	Formula w	Atoms %	Z	Eq, %	FrNa	atoms	Z	charge	atomic w	weight			FrNa	
		0	0.40	0.12	0.48																		
SiO2	52.58	0.00	0.36	0.10	0.55	1.000			28.72	60.08	0.478	4	1.91	Si	7.49	4	29.97	28.09	210.5			Si	7.49
Al2O3	22.13	0.00	0.50	0.17	0.33	1.000			7.344	101.96	0.144	3	0.43	Al	0.51	3	1.52	26.98	13.7			Al	0.51
TiO2	0.97			1.00	1.00				0.97	79.90	0.012	4	0.05	Σ tet	8.00		31.49		224.1			Sum tetrahedral	8.00
Fe2O3	6.91			0.93	1	1.00			6.426	159.69	0.080	3	0.24										
FeO					0	1.00			0	71.85	0.000	2	0.00	Al	1.75	3	5.26	26.98	47.3			Al	1.75
MgO	2.32			1	1	1.00			2.32	40.31	0.058	2	0.12	Ti	0.19	4	0.76	47.88	9.1			Ti	0.19
MgO					0				0	40.31	0.000	2	0.00	Fe3+	1.26	3	3.79	55.85	70.5			Fe(III)	1.26
CaO	0.1			1		1	1		0	56.08	0.000	2	0.00	Fe2+	0.00	2	0.00	55.85	0.0			Fe(II)	0.00
Na2O	1.78			1					1.78	61.98	0.057	1	0.06	Mg	0.90	2	1.80	24.31	21.9			Mg	0.90
K2O	3.05			0					0	94.20	0.000	1	0.00	Σ oct	4.11		11.61		148.8			Sum octahedral	4.11
Tot C	0.8			1					0.8					Ca	0.00	2.0	0.00	40.08	0.0			Ca	0.00
Tot S	0.17			1					0.17					Mg	0.00	2	0.00	24.31	0.0			Mg	0.00
														K	0.00	1	0.00	39.10	0.0			K	0.00
LOI	9.5													Na	0.90	1	0.90	22.99	20.7			Na	0.90
CEC	0.34													Σ int	0.90		0.90		20.7			Sum interlayer	0.90
								Si/Al	3.911														
	0.00													O	24	–2	–48.00	16.00	384.0			O	24.00
														H	4	1	4.00	1.01	4.0			H	4.00
														Unit cell weight					781.6			Unit cell weight	781.6
									Eq. sum				2.81	Charge balance calc			0.00					Tetr charge	–0.51
									oxygen + hydrogen				44.00									Octa charge	–0.39
									scaling f				15.68									Total charge	–0.90
																						Tetra charge, %	56
																						CEC mont calc	1.15
																						CEC clay calc	0.55
																						CEC clay meas	0.34
																						Illite calc, %	40
	FrNa	Si	7.49	Al	0.51	Al	1.75	Ti	0.19	Fe	(III)	1.26	Fe	(II)	0.00	Mg	0.90	Ca	0.00	Mg	0.00	K	0.00	Na	0.90

Input data												Calculation												Results	
		quartz part		Included part																					
		illite part		Fe(III) part																					
		Kaolinite part		C comp of Ca																					
Acme No	A304319					S comp of Ca																			
Group	Mi																								
Sample	MiCa1					montm						MiCa1	Formula w	Atoms %	Z	Eq, %		MiCa1	atoms	Z	charge	atomic w	weight		MiCa1
		0	0.06	0.00		0.94																			
SiO2	50.16	0.00	0.05	0.00		0.95	1.000					47.78	60.08	0.795	4	3.18		Si	7.84	4	31.35	28.09	220.1		Si	7.84
Al2O3	17.44	0.00	0.10	0.00		0.90	1.000					15.63	101.96	0.307	3	0.92		Al	0.16	3	0.49	26.98	4.4		Al	0.16
TiO2	0.68		0.06		1.00	0.94						0.68	79.90	0.009	4	0.03		Σ tet	8.00		31.84		224.5		Sum tetrahedral	8.00
Fe2O3	3.85		0.06		0.96	1	0.94					3.474	159.69	0.044	3	0.13										
FeO			0.06			0	0.94					0	71.85	0.000	2	0.00		Al	2.86	3	8.57	26.98	77.1		Al	2.86
MgO	2.55		0.06		1	1	0.94					2.397	40.31	0.059	2	0.12		Ti	0.08	4	0.34	47.88	4.0		Ti	0.08
MgO						0						0	40.31	0.000	2	0.00		Fe3+	0.43	3	1.29	55.85	23.9		Fe(III)	0.43
CaO	2.55				1		1	1				2.247	56.08	0.040	2	0.08		Fe2+	0.00	2	0.00	55.85	0.0		Fe(II)	0.00
Na2O	0.02				1							0.02	61.98	0.001	1	0.00		Mg	0.59	2	1.17	24.31	14.2		Mg	0.59
K2O	0.45				0							0	94.20	0.000	1	0.00		Σ oct	3.96		11.37		119.3		Sum octahedral	3.96
Tot C	0.05				1							0.05						Ca	0.39	2.0	0.79	40.08	15.8		Ca	0.39
Tot S	0.04				1							0.04						Mg	0.00	2	0.00	24.31	0.0		Mg	0.00
																		K	0.00	1	0.00	39.10	0.0		K	0.00
LOI	21.6																	Na	0.01	1	0.01	22.99	0.1		Na	0.01
CEC	0.8																	Σ int	0.40		0.01		0.1		Sum interlayer	0.40
Illite	5									Si/Al		3.058														
	0.00																	O	24	–2	–48.00	16.00	384.0		O	24.00
																		H	4	1	4.00	1.01	4.0		H	4.00
																		Unit cell weight					732.0		Unit cell weight	732.0
												Eq. sum				4.46		Charge balance calc			–0.79				Tetr charge	–0.16
												oxygen + hydrogen				44.00									Octa charge	–0.63
												scaling f				9.86									Total charge	–0.80
																									Tetra charge, %	20
																									CEC mont calc	1.09
																									CEC clay calc	1.02
																									CEC clay meas	0.80
																									Illite calc, %	6
	MiCa1	Si	7.84	Al	0.16	Al	2.86	Ti	0.08	Fe	(III)	0.43	Fe	(II)	0.00	Mg	0.59	Ca	0.39	Mg	0.00	K	0.00		Na	0.01

	Input data									Calculation												Results	
		quartz part		Included part																			
		illite part		Fe(III) part																			
		Kaolinite part		C comp of Ca																			
Acme No	A304319			S comp of Ca																			
Group	Mi																						
Sample	MiCa2					montm				MiCa2	Formula w	Atoms %	Z	Eq, %		MiCa2	atoms	Z	charge	atomic w	weight		MiCa2
		0	0.06	0.00		0.94																	
SiO2	51.01	0.00	0.05	0.00		0.95	1.000			48.59	60.08	0.809	4	3.23		Si	7.83	4	31.31	28.09	219.8		Si	7.83
Al2O3	17.86	0.00	0.10	0.00		0.90	1.000			16	101.96	0.314	3	0.94		Al	0.17	3	0.52	26.98	4.7		Al	0.17
TiO2	0.69		0.06		1.00	0.94				0.69	79.90	0.009	4	0.03		Σ tet	8.00		31.83		224.5		Sum tetrahedral	8.00
Fe2O3	3.92		0.06		0.96	1	0.94			3.537	159.69	0.044	3	0.13									
FeO			0.06			0	0.94			0	71.85	0.000	2	0.00		Al	2.87	3	8.60	26.98	77.3		Al	2.87
MgO	2.59		0.06		1	1	0.94			2.435	40.31	0.060	2	0.12		Ti	0.08	4	0.33	47.88	4.0		Ti	0.08
MgO						0				0	40.31	0.000	2	0.00		Fe3+	0.43	3	1.29	55.85	23.9		Fe(III)	0.43
CaO	2.61				1		1	1		2.26	56.08	0.040	2	0.08		Fe2+	0.00	2	0.00	55.85	0.0		Fe(II)	0.00
Na2O	0.02				1					0.02	61.98	0.001	1	0.00		Mg	0.58	2	1.17	24.31	14.2		Mg	0.58
K2O	0.46				0					0	94.20	0.000	1	0.00		Σ oct	3.96		11.39		119.5		Sum octahedral	3.96
Tot C	0.06				1					0.06						Ca	0.39	2.0	0.78	40.08	15.6		Ca	0.39
Tot S	0.04				1					0.04						Mg	0.00	2	0.00	24.31	0.0		Mg	0.00
																K	0.00	1	0.00	39.10	0.0		K	0.00
LOI	20.4															Na	0.01	1	0.01	22.99	0.1		Na	0.01
CEC	0.8															Σ int	0.40		0.01		0.1		Sum interlayer	0.40
Illite	5								Si/Al	3.037													
	0.00															O	24	–2	–48.00	16.00	384.0		O	24.00
																H	4	1	4.00	1.01	4.0		H	4.00
																Unit cell weight					732.1		Unit cell weight	732.1
										Eq. sum				4.55		Charge balance calc			–0.78				Tetr charge	–0.17
										oxygen + hydrogen				44.00									Octa charge	–0.61
										scaling f				9.68									Total charge	–0.79
																							Tetra charge, %	22
																							CEC mont calc	1.07
																							CEC clay calc	1.01
																							CEC clay meas	0.80
																							Illite calc, %	6

MiCa2 $Si_{7.83}$ $Al_{0.17}$ $Al_{2.87}$ $Ti_{0.08}$ $Fe(III)_{0.43}$ $Fe(II)_{0.00}$ $Mg_{0.58}$ $Ca_{0.39}$ $Mg_{0.00}$ $K_{0.00}$ Na 0.01

Input data										Calculation												Results	
		quartz part			Included part																		
		illite part			Fe(III) part																		
		Kaolinite part			C comp of Ca																		
Acme No	A304319						S comp of Ca																
Group	Mi																						
Sample	MiNa1					montm				MiNa1	Formula w	Atoms %	Z	Eq, %		MiNa1	atoms	Z	charge	atomic w	weight		MiNa1
		0	0.06	0.00		0.94																	
SiO2	53.03	0.00	0.05	0.00		0.95	1.000			50.51	60.08	0.841	4	3.36		Si	7.85	4	31.40	28.09	220.5		Si	7.85
Al2O3	18.45	0.00	0.10	0.00		0.90	1.000			16.53	101.96	0.324	3	0.97		Al	0.15	3	0.45	26.98	4.0		Al	0.15
TiO2	0.72		0.06		1.00	0.94				0.72	79.90	0.009	4	0.04		Σ tet	8.00		31.85		224.5		Sum tetrahedral	8.00
Fe2O3	4.01		0.06		0.96	1	0.94			3.619	159.69	0.045	3	0.14									
FeO			0.06			0	0.94			0	71.85	0.000	2	0.00		Al	2.88	3	8.63	26.98	77.7		Al	2.88
MgO	2.73		0.06		1	1	0.94			2.566	40.31	0.064	2	0.13		Ti	0.08	4	0.34	47.88	4.0		Ti	0.08
MgO						0				0	40.31	0.000	2	0.00		Fe3+	0.42	3	1.27	55.85	23.6		Fe(III)	0.42
CaO	1.93				1		1	1		1.113	56.08	0.020	2	0.04		Fe2+	0.00	2	0.00	55.85	0.0		Fe(II)	0.00
Na2O	1.16				1					1.16	61.98	0.037	1	0.04		Mg	0.59	2	1.19	24.31	14.4		Mg	0.59
K2O	0.48				0					0	94.20	0.000	1	0.00		Σ oct	3.98		11.43		119.8		Sum octahedral	3.98
Tot C	0.16				1					0.16						Ca	0.19	2.0	0.37	40.08	7.4		Ca	0.19
Tot S	0.04				1					0.04						Mg	0.00	2	0.00	24.31	0.0		Mg	0.00
																K	0.00	1	0.00	39.10	0.0		K	0.00
LOI	17.4															Na	0.35	1	0.35	22.99	8.0		Na	0.35
CEC	0.87															Σ int	0.53		0.35		8.0		Sum interlayer	0.53
Illite	6								Si/Al	3.056													
	0.00															O	24	–2	–48.00	16.00	384.0		O	24.00
																H	4	1	4.00	1.01	4.0		H	4.00
																Unit cell weight					740.3		Unit cell weight	740.3
										Eq. sum				4.71		Charge balance calc			–0.37				Tetr charge	–0.15
										oxygen + hydrogen				44.00									Octa charge	–0.57
										scaling f				9.34									Total charge	–0.72
																							Tetra charge, %	21
																							CEC mont calc	0.97
																							CEC clay calc	0.91
																							CEC clay meas	0.87
																							Illite calc, %	6

	MiNa1	Si	7.85	Al	0.15	Al	2.88	Ti	0.08	Fe	(III)	0.42	Fe	(II)	0.00	Mg	0.59	Ca	0.19	Mg	0.00	K	0.00	Na	0.35

Input data									Calculation												Results	
		quartz part		Included part																		
		illite part		Fe(III) part																		
		Kaolinite part		C comp of Ca																		
Acme No	A507676			S comp of Ca																		
Group	Mi																					
Sample	MiNa2			montm					MiNa2	Formula w	Atoms %	Z	Eq, %	MiNa2	atoms	Z	charge	atomic w	weight		MiNa2	
		0	0.06	0.00		0.94																
SiO2	59.58	0.00	0.05	0.00		0.95	1.000		56.75	60.08	0.945	4	3.78	Si	7.73	4	30.94	28.09	217.2		Si	7.73
Al2O3	21.88	0.00	0.10	0.00		0.90	1.000		19.6	101.96	0.385	3	1.15	Al	0.27	3	0.80	26.98	7.2		Al	0.27
TiO2	0.84		0.06	1.00		0.94			0.84	79.90	0.011	4	0.04	Σ tet	8.00		31.73		224.4		Sum tetrahedral	8.00
Fe2O3	4.64		0.06	0.96	1	0.94			4.187	159.69	0.052	3	0.16									
FeO			0.06		0	0.94			0	71.85	0.000	2	0.00	Al	2.88	3	8.65	26.98	77.8		Al	2.88
MgO	3.06		0.06	1	1	0.94			2.876	40.31	0.071	2	0.14	Ti	0.09	4	0.34	47.88	4.1		Ti	0.09
MgO					0				0	40.31	0.000	2	0.00	Fe3+	0.43	3	1.29	55.85	24.0		Fe(III)	0.43
CaO	0.14			1		1	1		0	56.08	0.000	2	0.00	Fe2+	0.00	2	0.00	55.85	0.0		Fe(II)	0.00
Na2O	3.09			1					3.09	61.98	0.100	1	0.10	Mg	0.58	2	1.17	24.31	14.2		Mg	0.58
K2O	0.52			0					0	94.20	0.000	1	0.00	Σ oct	3.98		11.45		120.1		Sum octahedral	3.98
Tot C	0.4			1					0.4					Ca	0.00	2.0	0.00	40.08	0.0		Ca	0.00
Tot S	0.04			1					0.04					Mg	0.00	2	0.00	24.31	0.0		Mg	0.00
														K	0.00	1	0.00	39.10	0.0		K	0.00
LOI	6.3													Na	0.82	1	0.82	22.99	18.8		Na	0.82
CEC	0.82													Σ int	0.82		0.82		18.8		Sum interlayer	0.82
Illite	6							Si/Al	2.895													
	0.00													O	24	–2	–48.00	16.00	384.0		O	24.00
														H	4	1	4.00	1.01	4.0		H	4.00
														Unit cell weight					751.3		Unit cell weight	751.3
									Eq. sum				5.37	Charge balance calc			0.00				Tetr charge	–0.27
									oxygen + hydrogen				44.00								Octa charge	–0.55
									scaling f				8.19								Total charge	–0.82
																					Tetra charge, %	33
																					CEC mont calc	1.09
																					CEC clay calc	1.02
																					CEC clay meas	0.82
																					Illite calc, %	6

MiNa2 Si $_{7.73}$ Al $_{0.27}$ Al $_{2.88}$ Ti $_{0.09}$ Fe (III) $_{0.43}$ Fe (II) $_{0.00}$ Mg $_{0.58}$ Ca $_{0.00}$ Mg $_{0.00}$ K $_{0.00}$ Na 0.82

Input data										Calculation													Results	
		quartz part		Included part																				
		illite part		Fe(III) part																				
		Kaolinite part		C comp of Ca																				
Acme No	A301179			S comp of Ca																				
Group	In																							
Sample	Ku36Na			montm						Ku36Na	Formula w	Atoms %	Z	Eq, %		Ku36Na	atoms	Z	charge	atomic w	weight		Ku36Na	
		0	0.01	0.00		0.99																		
SiO2	56.69	0.00	0.01	0.00		0.99	1.000			56.25	60.08	0.936	4	3.74		Si	7.71	4	30.85	28.09	216.6		Si	7.71
Al2O3	17.21	0.00	0.02	0.00		0.98	1.000			16.9	101.96	0.331	3	0.99		Al	0.29	3	0.86	26.98	7.8		Al	0.29
TiO2	0.35		0.01		1.00	0.99				0.35	79.90	0.004	4	0.02		Σ tet	8.00		31.71		224.4		Sum tetrahedral	8.00
Fe2O3	8.75		0.01		0.93	1	0.99			8.056	159.69	0.101	3	0.30										
FeO			0.01			0	0.99			0	71.85	0.000	2	0.00		Al	2.44	3	7.33	26.98	65.9		Al	2.44
MgO	3.59		0.01		1	1	0.99			3.554	40.31	0.088	2	0.18		Ti	0.04	4	0.14	47.88	1.7		Ti	0.04
MgO						0				0	40.31	0.000	2	0.00		Fe3+	0.83	3	2.49	55.85	46.4		Fe(III)	0.83
CaO	0.31				1		1	1		0.153	56.08	0.003	2	0.01		Fe2+	0.00	2	0.00	55.85	0.0		Fe(II)	0.00
Na2O	3.1				1					3.1	61.98	0.100	1	0.10		Mg	0.73	2	1.45	24.31	17.7		Mg	0.73
K2O	0.12				0					0	94.20	0.000	1	0.00		Σ oct	4.04		11.42		131.7		Sum octahedral	4.04
Tot C	0.03				1					0.03						Ca	0.02	2.0	0.04	40.08	0.9		Ca	0.02
Tot S	0.01				1					0.01						Mg	0.00	2	0.00	24.31	0.0		Mg	0.00
																K	0.00	1	0.00	39.10	0.0		K	0.00
LOI	9.3															Na	0.82	1	0.82	22.99	18.9		Na	0.82
CEC	1.00															Σ int	0.85		0.82		18.9		Sum interlayer	0.85
									Si/Al	3.328														
	0.00															O	24	–2	–48.00	16.00	384.0		O	24.00
																H	4	1	4.00	1.01	4.0		H	4.00
																Unit cell weight					763.0		Unit cell weight	763.0
										Eq. sum				5.34		Charge balance calc			–0.04				Tetr charge	–0.29
										oxygen + hydrogen				44.00									Octa charge	–0.58
										scaling f				8.24									Total charge	–0.87
																							Tetra charge, %	33
																							CEC mont calc	1.14
																							CEC clay calc	1.13
																							CEC clay meas	1.00
																							Illite calc, %	1
	Ku36Na	Si	7.71	Al	0.29	Al	2.44	Ti	0.04	Fe	(III)	0.83	Fe	(II)	0.00	Mg	0.73	Ca	0.02	Mg	0.00	K	0.00	Na	0.82

	Input data								Calculation											Results	
		quartz part		Included part																	
			illite part		Fe(III) part																
				Kaolinite part		C comp of Ca															
Acme No	A301179						S comp of Ca														
Group	In																				
Sample	Ku37Na					montm			Ku37Na	Formula w	Atoms %	Z	Eq, %	Ku37Na	atoms	Z	charge	atomic w	weight		Ku37Na
		0	0.01	0.00		0.99															
SiO2	53.61	0.00	0.01	0.00		0.99	1.000		53.19	60.08	0.885	4	3.54	Si	7.54	4	30.16	28.09	211.8	Si	7.54
Al2O3	18.65	0.00	0.02	0.00		0.98	1.000		18.31	101.96	0.359	3	1.08	Al	0.46	3	1.38	26.98	12.4	Al	0.46
TiO2	0.45		0.01		1.00	0.99			0.45	79.90	0.006	4	0.02	Σ tet	8.00		31.54		224.2	Sum tetrahedral	8.00
Fe2O3	10.59		0.01		0.85	1	0.99		8.911	159.69	0.112	3	0.33								
FeO			0.01			0	0.99		0	71.85	0.000	2	0.00	Al	2.60	3	7.80	26.98	70.2	Al	2.60
MgO	2.3		0.01		1	1	0.99		2.277	40.31	0.056	2	0.11	Ti	0.05	4	0.19	47.88	2.3	Ti	0.05
MgO						0			0	40.31	0.000	2	0.00	Fe3+	0.95	3	2.85	55.85	53.1	Fe(III)	0.95
CaO	0.18				1		1	1	0	56.08	0.000	2	0.00	Fe2+	0.00	2	0.00	55.85	0.0	Fe(II)	0.00
Na2O	2.37				1				2.37	61.98	0.076	1	0.08	Mg	0.48	2	0.96	24.31	11.7	Mg	0.48
K2O	0.09				0				0	94.20	0.000	1	0.00	Σ oct	4.08		11.81		137.3	Sum octahedral	4.08
Tot C	0.06				1				0.06					Ca	0.00	2.0	0.00	40.08	0.0	Ca	0.00
Tot S	0.01				1				0.01					Mg	0.00	2	0.00	24.31	0.0	Mg	0.00
														K	0.00	1	0.00	39.10	0.0	K	0.00
LOI	11.7													Na	0.65	1	0.65	22.99	15.0	Na	0.65
CEC	0.88													Σ int	0.65		0.65		15.0	Sum interlayer	0.65
								Si/Al	2.904												
	0.00													O	24	–2	–48.00	16.00	384.0	O	24.00
														H	4	1	4.00	1.01	4.0	H	4.00
														Unit cell weight					764.4	Unit cell weight	764.4
									Eq. sum				5.17	Charge balance calc			0.00			Tetr charge	–0.46
									oxygen + hydrogen				44.00							Octa charge	–0.19
									scaling f				8.52							Total charge	–0.65
																				Tetra charge, %	71
																				CEC mont calc	0.85
																				CEC clay calc	0.84
																				CEC clay meas	0.88
																				Illite calc, %	1
	Ku37Na	Si	7.54	Al	0.46	Al	2.60	Ti	0.05	Fe	(III)	0.95	Fe	(II)	0.00	Mg	0.48	Ca	0.00	Mg	0.00	K	0.00	Na	0.65

	Input data								Calculation											Results	
		quartz part		Included part																	
		illite part		Fe(III) part																	
		Kaolinite part		C comp of Ca																	
				S comp of Ca																	
Acme No	A301179																				
Group	In																				
Sample	Ku38Na					montm			Ku38Na	Formula w	Atoms %	Z	Eq, %	Ku38Na	atoms	Z	charge	atomic w	weight		Ku38Na
		0	0.00	0.00		1.00															
SiO2	51.93	0.00	0.00	0.00		1.00	1.000		51.93	60.08	0.864	4	3.46	Si	7.30	4	29.20	28.09	205.0	Si	7.30
Al2O3	19.32	0.00	0.00	0.00		1.00	1.000		19.32	101.96	0.379	3	1.14	Al	0.70	3	2.10	26.98	18.9	Al	0.70
TiO2	1.27		0.00		1.00	1.00			1.27	79.90	0.016	4	0.06	Σ tet	8.00		31.30		223.9	Sum tetrahedral	8.00
Fe2O3	10.19		0.00		0.96	1 1.00			9.782	159.69	0.123	3	0.37								
FeO			0.00			0 1.00			0	71.85	0.000	2	0.00	Al	2.50	3	7.50	26.98	67.5	Al	2.50
MgO	2.1		0.00		1	1 1.00			2.1	40.31	0.052	2	0.10	Ti	0.13	4	0.54	47.88	6.4	Ti	0.13
MgO						0			0	40.31	0.000	2	0.00	Fe3+	1.03	3	3.10	55.85	57.8	Fe(III)	1.03
CaO	0.36				1	1	1		0.063	56.08	0.001	2	0.00	Fe2+	0.00	2	0.00	55.85	0.0	Fe(II)	0.00
Na2O	2.41				1				2.41	61.98	0.078	1	0.08	Mg	0.44	2	0.88	24.31	10.7	Mg	0.44
K2O	0.03				0				0	94.20	0.000	1	0.00	Σ oct	4.11		12.02		142.4	Sum octahedral	4.11
Tot C	0.06				1				0.06					Ca	0.01	2.0	0.02	40.08	0.4	Ca	0.01
Tot S	0.01				1				0.01					Mg	0.00	2	0.00	24.31	0.0	Mg	0.00
														K	0.00	1	0.00	39.10	0.0	K	0.00
LOI	12.1													Na	0.66	1	0.66	22.99	15.1	Na	0.66
CEC	0.90													Σ int	0.67		0.66		15.1	Sum interlayer	0.67
								Si/Al	2.688												
	0.00													O	24	–2	–48.00	16.00	384.0	O	24.00
														H	4	1	4.00	1.01	4.0	H	4.00
														Unit cell weight					769.4	Unit cell weight	769.4
									Eq. sum				5.21	Charge balance calc			–0.02			Tetr charge	–0.70
									oxygen + hydrogen				44.00							Octa charge	0.02
									scaling f				8.45							Total charge	–0.68
																				Tetra charge, %	104
																				CEC mont calc	0.88
																				CEC clay calc	0.88
																				CEC clay meas	0.90
																				Illite calc, %	0
	Ku38Na	Si	7.30	Al	0.70	Al	2.50	Ti	0.13	Fe	(III)	1.03	Fe	(II)	0.00	Mg	0.44	Ca	0.01	Mg	0.00	K	0.00	Na	0.66

	Input data									Calculation														Results	
		quartz part			Included part																				
			illite part			Fe(III) part																			
				Kaolinite part			C comp of Ca																		
Acme No	A301179							S comp of Ca																	
Group	In																								
Sample	Ku39Na						montm			Ku39Na	Formula w	Atoms %	Z	Eq, %	Ku39Na	atoms	Z	charge	atomic w	weight			Ku39Na	
		0	0.02	0.00			0.98																		
SiO2	55.99	0.00	0.02	0.00			0.98	1.000		55.11	60.08	0.917	4	3.67	Si	7.62	4	30.48	28.09	214.0			Si	7.62	
Al2O3	18.68	0.00	0.04	0.00			0.96	1.000		18.01	101.96	0.353	3	1.06	Al	0.38	3	1.14	26.98	10.2			Al	0.38	
TiO2	0.47		0.02		1.00		0.98			0.47	79.90	0.006	4	0.02	Σ tet	8.00		31.62		224.3			Sum tetrahedral	8.00	
Fe2O3	8.51		0.02		0.91	1	0.98			7.589	159.69	0.095	3	0.29											
FeO			0.02			0	0.98			0	71.85	0.000	2	0.00	Al	2.56	3	7.67	26.98	69.0			Al	2.56	
MgO	3.34		0.02		1	1	0.98			3.273	40.31	0.081	2	0.16	Ti	0.05	4	0.20	47.88	2.3			Ti	0.05	
MgO						0				0	40.31	0.000	2	0.00	Fe3+	0.79	3	2.37	55.85	44.1			Fe(III)	0.79	
CaO	0.17				1		1	1		0.013	56.08	0.000	2	0.00	Fe2+	0.00	2	0.00	55.85	0.0			Fe(II)	0.00	
Na2O	2.95				1					2.95	61.98	0.095	1	0.10	Mg	0.67	2	1.35	24.31	16.4			Mg	0.67	
K2O	0.17				0					0	94.20	0.000	1	0.00	Σ oct	4.07		11.58		131.8			Sum octahedral	4.07	
Tot C	0.03				1					0.03					Ca	0.00	2.0	0.00	40.08	0.1			Ca	0.00	
Tot S	0.01				1					0.01					Mg	0.00	2	0.00	24.31	0.0			Mg	0.00	
															K	0.00	1	0.00	39.10	0.0			K	0.00	
LOI	9.7														Na	0.79	1	0.79	22.99	18.2			Na	0.79	
CEC	0.99														Σ int	0.79		0.79		18.2			Sum interlayer	0.79	
									Si/Al	3.06															
	0.00														O	24	–2	–48.00	16.00	384.0			O	24.00	
															H	4	1	4.00	1.01	4.0			H	4.00	
															Unit cell weight					762.3			Unit cell weight	762.3	
										Eq. sum				5.30	Charge balance calc			0.00					Tetr charge	–0.38	
										oxygen + hydrogen				44.00									Octa charge	–0.42	
										scaling f				8.31									Total charge	–0.79	
																							Tetra charge, %	48	
																							CEC mont calc	1.04	
																							CEC clay calc	1.02	
																							CEC clay meas	0.99	
																							Illite calc, %	2	
	Ku39Na	Si	7.62	Al	0.38	Al	2.56	Ti	0.05	Fe	(III)	0.79	Fe	(II)	0.00	Mg	0.67	Ca	0.00	Mg	0.00	K	0.00	Na	0.79

Input data									Calculation												Results	
		quartz part			Included part																	
		illite part			Fe(III) part																	
		Kaolinite part			C comp of Ca																	
Acme No	A301179						S comp of Ca															
Group	In																					
Sample	Ku40Na					montm			Ku40Na	Formula w	Atoms %	Z	Eq, %	Ku40Na	atoms	Z	charge	atomic w	weight		Ku40Na
		0	0.01	0.00		0.99																
SiO2	50.44	0.00	0.01	0.00		0.99		1.000	50.05	60.08	0.833	4	3.33	Si	7.13	4	28.52	28.09	200.3		Si	7.13
Al2O3	21.16	0.00	0.02	0.00		0.98		1.000	20.78	101.96	0.408	3	1.22	Al	0.87	3	2.61	26.98	23.4		Al	0.87
TiO2	1.38		0.01		1.00	0.99			1.38	79.90	0.017	4	0.07	Σ tet	8.00		31.13		223.7		Sum tetrahedral	8.00
Fe2O3	11.8		0.01		0.8	1 0.99			9.346	159.69	0.117	3	0.35									
FeO			0.01			0 0.99			0	71.85	0.000	2	0.00	Al	2.62	3	7.86	26.98	70.7		Al	2.62
MgO	1.56		0.01		1	1 0.99			1.544	40.31	0.038	2	0.08	Ti	0.15	4	0.59	47.88	7.1		Ti	0.15
MgO						0			0	40.31	0.000	2	0.00	Fe3+	1.00	3	3.01	55.85	56.0		Fe(III)	1.00
CaO	0.04				1	1	1		0	56.08	0.000	2	0.00	Fe2+	0.00	2	0.00	55.85	0.0		Fe(II)	0.00
Na2O	2.73				1				2.73	61.98	0.088	1	0.09	Mg	0.33	2	0.66	24.31	8.0		Mg	0.33
K2O	0.08				0				0	94.20	0.000	1	0.00	Σ oct	4.10		12.11		141.7		Sum octahedral	4.10
Tot C	0.17				1				0.17					Ca	0.00	2.0	0.00	40.08	0.0		Ca	0.00
Tot S	0.01				1				0.01					Mg	0.00	2	0.00	24.31	0.0		Mg	0.00
														K	0.00	1	0.00	39.10	0.0		K	0.00
LOI	10.7													Na	0.75	1	0.75	22.99	17.3		Na	0.75
CEC	0.88													Σ int	0.75		0.75		17.3		Sum interlayer	0.75
								Si/Al	2.409													
	0.00					from bulk								O	24	–2	–48.00	16.00	384.0		O	24.00
														H	4	1	4.00	1.01	4.0		H	4.00
														Unit cell weight					770.8		Unit cell weight	770.8
									Eq. sum				5.14	Charge balance calc			0.00				Tetr charge	–0.87
									oxygen + hydrogen				44.00								Octa charge	0.11
									scaling f				8.56								Total charge	–0.75
																					Tetra charge, %	115
																					CEC mont calc	0.98
																					CEC clay calc	0.97
																					CEC clay meas	0.88
																					Illite calc, %	1
	Ku40Na	Si	7.13	Al	0.87	Al	2.62	Ti	0.15	Fe	(III)	1.00	Fe	(II)	0.00	Mg	0.33	Ca	0.00	Mg	0.00	K	0.00	Na	0.75

Input data										Calculation												Results	
		quartz part		Included part																			
		illite part		Fe(III) part																			
		Kaolinite part		C comp of Ca																			
Acme No	A301179			S comp of Ca																			
Group	US																						
Sample	WyCa			montm						WyCa	Formula w	Atoms %	Z	Eq, %		WyCa	atoms	Z	charge	atomic w	weight		WyCa
		0	0.01	0.00		0.99																	
SiO2	57.35	0.00	0.01	0.00		0.99		1.000		56.9	60.08	0.947	4	3.79		Si	7.92	4	31.70	28.09	222.6		Si	7.92
Al2O3	19.88	0.00	0.02	0.00		0.98		1.000		19.52	101.96	0.383	3	1.15		Al	0.08	3	0.23	26.98	2.0		Al	0.08
TiO2	0.14		0.01		1.00	0.99				0.14	79.90	0.002	4	0.01		Σ tet	8.00		31.92		224.6		Sum tetrahedral	8.00
Fe2O3	3.63		0.01		0.98	1	0.99			3.522	159.69	0.044	3	0.13									
FeO			0.01			0	0.99			0	71.85	0.000	2	0.00		Al	3.13	3	9.39	26.98	84.4		Al	3.13
MgO	2.33		0.01		1	1	0.99			2.307	40.31	0.057	2	0.11		Ti	0.01	4	0.06	47.88	0.7		Ti	0.01
MgO						0				0	40.31	0.000	2	0.00		Fe3+	0.37	3	1.11	55.85	20.6		Fe(III)	0.37
CaO	2.58				1		1	1		1.828	56.08	0.033	2	0.07		Fe2+	0.00	2	0.00	55.85	0.0		Fe(II)	0.00
Na2O	0.07				1					0.07	61.98	0.002	1	0.00		Mg	0.48	2	0.96	24.31	11.6		Mg	0.48
K2O	0.1				0					0	94.20	0.000	1	0.00		Σ oct	3.99		11.51		117.4		Sum octahedral	3.99
Tot C	0.15				1					0.15						Ca	0.27	2.0	0.55	40.08	10.9		Ca	0.27
Tot S	0.03				1					0.03						Mg	0.00	2	0.00	24.31	0.0		Mg	0.00
																K	0.00	1	0.00	39.10	0.0		K	0.00
LOI	13.7															Na	0.02	1	0.02	22.99	0.4		Na	0.02
CEC	0.77															Σ int	0.29		0.02		0.4		Sum interlayer	0.29
Illite	6								Si/Al	2.915														
	0.00															O	24	–2	–48.00	16.00	384.0		O	24.00
																H	4	1	4.00	1.01	4.0		H	4.00
																Unit cell weight					730.4		Unit cell weight	730.4
										Eq. sum				5.26		Charge balance calc			–0.55				Tetr charge	–0.08
										oxygen + hydrogen				44.00									Octa charge	–0.49
										scaling f				8.37									Total charge	–0.56
																							Tetra charge, %	13
																							CEC mont calc	0.77
																							CEC clay calc	0.76
																							CEC clay meas	0.77
																							Illite calc, %	1

	WyCa	Si	7.92	Al	0.08	Al	3.13	Ti	0.01	Fe	(III)	0.37	Fe	(II)	0.00	Mg	0.48	Ca	0.27	Mg	0.00	K	0.00	Na	0.02

Input data									Calculation											Results	
		quartz part			Included part																
		illite part			Fe(III) part																
		Kaolinite part			C comp of Ca																
Acme No	A304319				S comp of Ca																
Group	US																				
Sample	WyCa2					montm			WyCa2	Formula w	Atoms %	Z	Eq, %	WyCa2	atoms	Z	charge	atomic w	weight		WyCa2
		0	0.01	0.00		0.99															
SiO2	53.78	0.00	0.01	0.00		0.99	1.000		53.36	60.08	0.888	4	3.55	Si	7.98	4	31.92	28.09	224.1	Si	7.98
Al2O3	18.22	0.00	0.02	0.00		0.98	1.000		17.89	101.96	0.351	3	1.05	Al	0.02	3	0.06	26.98	0.6	Al	0.02
TiO2	0.13		0.01		1.00	0.99			0.13	79.90	0.002	4	0.01	Σ tet	8.00		31.98		224.7	Sum tetrahedral	8.00
Fe2O3	3.39		0.01		0.98	1 0.99			3.289	159.69	0.041	3	0.12								
FeO			0.01			0 0.99			0	71.85	0.000	2	0.00	Al	3.13	3	9.40	26.98	84.5	Al	3.13
MgO	2.12		0.01		1	1 0.99			2.099	40.31	0.052	2	0.10	Ti	0.01	4	0.06	47.88	0.7	Ti	0.01
MgO						0			0	40.31	0.000	2	0.00	Fe3+	0.37	3	1.11	55.85	20.7	Fe(III)	0.37
CaO	2.35				1	1 1			1.568	56.08	0.028	2	0.06	Fe2+	0.00	2	0.00	55.85	0.0	Fe(II)	0.00
Na2O	0.05				1				0.05	61.98	0.002	1	0.00	Mg	0.47	2	0.94	24.31	11.4	Mg	0.47
K2O	0.07				0				0	94.20	0.000	1	0.00	Σ oct	3.99		11.50		117.3	Sum octahedral	3.99
Tot C	0.16				1				0.16					Ca	0.25	2.0	0.50	40.08	10.1	Ca	0.25
Tot S	0.02				1				0.02					Mg	0.00	2	0.00	24.31	0.0	Mg	0.00
														K	0.00	1	0.00	39.10	0.0	K	0.00
LOI	19.8													Na	0.01	1	0.01	22.99	0.3	Na	0.01
CEC	0.77													Σ int	0.27		0.01		0.3	Sum interlayer	0.27
Illite	6							Si/Al	2.982												
	0.00													O	24	–2	–48.00	16.00	384.0	O	24.00
														H	4	1	4.00	1.01	4.0	H	4.00
														Unit cell weight					730.3	Unit cell weight	730.3
									Eq. sum				4.90	Charge balance calc			–0.50			Tetr charge	–0.02
									oxygen + hydrogen				44.00							Octa charge	–0.50
									scaling f				8.99							Total charge	–0.52
																				Tetra charge, %	4
																				CEC mont calc	0.71
																				CEC clay calc	0.70
																				CEC clay meas	0.77
																				Illite calc, %	1

WyCa2 Si 7.98 Al 0.02 Al 3.13 Ti 0.01 Fe (III) 0.37 Fe (II) 0.00 Mg 0.47 Ca 0.25 Mg 0.00 K 0.00 Na 0.01

	Input data									Calculation												Results	
		quartz part		Included part																			
		illite part		Fe(III) part																			
		Kaolinite part		C comp of Ca																			
Acme No	A301179						S comp of Ca																
Group	US																						
Sample	WyMg1					montm				WyMg1	Formula w	Atoms %	Z	Eq, %		WyMg1	atoms	Z	charge	atomic w	weight		WyMg1
		0	0.01	0.00		0.99																	
SiO2	56.8	0.00	0.01	0.00		0.99		1.000		56.36	60.08	0.938	4	3.75		Si	7.91	4	31.63	28.09	222.1	Si	7.91
Al2O3	19.61	0.00	0.02	0.00		0.98		1.000		19.26	101.96	0.378	3	1.13		Al	0.09	3	0.28	26.98	2.5	Al	0.09
TiO2	0.14		0.01		1.00	0.99				0.14	79.90	0.002	4	0.01		Σ tet	8.00		31.91		224.6	Sum tetrahedral	8.00
Fe2O3	3.64		0.01		0.98	1	0.99			3.532	159.69	0.044	3	0.13									
FeO			0.01			0	0.99			0	71.85	0.000	2	0.00		Al	3.09	3	9.28	26.98	83.4	Al	3.09
MgO	3.9		0.01		1	0.64	0.99			2.471	40.31	0.061	2	0.12		Ti	0.01	4	0.06	47.88	0.7	Ti	0.01
MgO						0.36				1.39	40.31	0.034	2	0.07		Fe3+	0.37	3	1.12	55.85	20.8	Fe(III)	0.37
CaO	0.03				1		1	1		0	56.08	0.000	2	0.00		Fe2+	0.00	2	0.00	55.85	0.0	Fe(II)	0.00
Na2O	0.08				1					0.08	61.98	0.003	1	0.00		Mg	0.52	2	1.03	24.31	12.6	Mg	0.52
K2O	0.11				0					0	94.20	0.000	1	0.00		Σ oct	4.00		11.49		117.5	Sum octahedral	4.00
Tot C	0.14				1					0.14						Ca	0.00	2.0	0.00	40.08	0.0	Ca	0.00
Tot S	0.01				1					0.01						Mg	0.29	2	0.58	24.31	7.1	Mg	0.29
																K	0.00	1	0.00	39.10	0.0	K	0.00
LOI	15.3															Na	0.02	1	0.02	22.99	0.5	Na	0.02
CEC	0.79															Σ int	0.31		0.60		7.6	Sum interlayer	0.31
Illite	6								Si/Al	2.927													
	0.00															O	24	–2	–48.00	16.00	384.0	O	24.00
																H	4	1	4.00	1.01	4.0	H	4.00
																Unit cell weight					737.7	Unit cell weight	737.7
										Eq. sum				5.22		Charge balance calc			0.00			Tetr charge	–0.09
										oxygen + hydrogen				44.00								Octa charge	–0.51
										scaling f				8.43								Total charge	–0.60
																						Tetra charge, %	15
																						CEC mont calc	0.82
																						CEC clay calc	0.81
																						CEC clay meas	0.79
																						Illite calc, %	1

WyMg1 $Si_{7.91}$ $Al_{0.09}$ $Al_{3.09}$ $Ti_{0.01}$ $Fe(III)_{0.37}$ $Fe(II)_{0.00}$ $Mg_{0.52}$ $Ca_{0.00}$ $Mg_{0.29}$ $K_{0.00}$ Na 0.02

Input data										Calculation												Results	
		quartz part			Included part																		
			illite part			Fe(III) part																	
				Kaolinite part			C comp of Ca																
Acme No	A304319							S comp of Ca															
Group	US																						
Sample	WyMg2						montm			WyMg2	Formula w	Atoms %	Z	Eq, %	WyMg2	atoms	Z	charge	atomic w	weight			WyMg2
		0	0.01	0.00			0.99																
SiO2	53.37	0.00	0.01	0.00			0.99	1.000		52.95	60.08	0.881	4	3.53	Si	7.96	4	31.83	28.09	223.5		Si	7.96
Al2O3	17.91	0.00	0.02	0.00			0.98	1.000		17.59	101.96	0.345	3	1.03	Al	0.04	3	0.12	26.98	1.1		Al	0.04
TiO2	0.12		0.01		1.00		0.99			0.12	79.90	0.002	4	0.01	Σ tet	8.00		31.96		224.6		Sum tetrahedral	8.00
Fe2O3	3.28		0.01		0.98	1	0.99			3.182	159.69	0.040	3	0.12									
FeO			0.01			0	0.99			0	71.85	0.000	2	0.00	Al	3.07	3	9.22	26.98	82.9		Al	3.07
MgO	3.77		0.01		1	0.66	0.99			2.463	40.31	0.061	2	0.12	Ti	0.01	4	0.05	47.88	0.6		Ti	0.01
MgO						0.34				1.269	40.31	0.031	2	0.06	Fe3+	0.36	3	1.08	55.85	20.1		Fe(III)	0.36
CaO	0.03				1		1	1		0	56.08	0.000	2	0.00	Fe2+	0.00	2	0.00	55.85	0.0		Fe(II)	0.00
Na2O	0.05				1					0.05	61.98	0.002	1	0.00	Mg	0.55	2	1.10	24.31	13.4		Mg	0.55
K2O	0.08				0					0	94.20	0.000	1	0.00	Σ oct	4.00		11.46		117.1		Sum octahedral	4.00
Tot C	0.13				1					0.13					Ca	0.00	2.0	0.00	40.08	0.0		Ca	0.00
Tot S	0.02				1					0.02					Mg	0.28	2	0.57	24.31	6.9		Mg	0.28
															K	0.00	1	0.00	39.10	0.0		K	0.00
LOI	21.2														Na	0.01	1	0.01	22.99	0.3		Na	0.01
CEC	0.79														Σ int	0.30		0.58		7.2		Sum interlayer	0.30
Illite	6								Si/Al	3.011													
	0.00														O	24	–2	–48.00	16.00	384.0		O	24.00
															H	4	1	4.00	1.01	4.0		H	4.00
															Unit cell weight					737.0		Unit cell weight	737.0
										Eq. sum				4.87	Charge balance calc			0.00				Tetr charge	–0.04
										oxygen + hydrogen				44.00								Octa charge	–0.54
										scaling f				9.03								Total charge	–0.58
																						Tetra charge, %	7
																						CEC mont calc	0.79
																						CEC clay calc	0.78
																						CEC clay meas	0.79
																						Illite calc, %	1
	WyMg2	Si	7.96	Al	0.04	Al	3.07	Ti	0.01	Fe	(III)	0.36	Fe	(II)	0.00	Mg	0.55	Ca	0.00	Mg	0.28	K	0.00	Na	0.01

Input data											Calculation											Results	
		quartz part		Included part																			
		illite part		Fe(III) part																			
		Kaolinite part		C comp of Ca																			
Acme No	A301179			S comp of Ca																			
Group	US																						
Sample	WyK			montm							WyK	Formula w	Atoms %	Z	Eq, %	WyK	atoms	Z	charge	atomic w	weight		WyK
		0	0.01	0.00		0.99																	
SiO2	60.3	0.00	0.01	0.00		0.99	1.000				59.83	60.08	0.996	4	3.98	Si	7.93	4	31.70	28.09	222.6	Si	7.93
Al2O3	20.7	0.00	0.02	0.00		0.98	1.000				20.33	101.96	0.399	3	1.20	Al	0.07	3	0.22	26.98	2.0	Al	0.07
TiO2	0.14		0.01		1.00	0.99					0.14	79.90	0.002	4	0.01	Σ tet	8.00		31.93		224.6	Sum tetrahedral	8.00
Fe2O3	3.85		0.01		0.98	1	0.99				3.735	159.69	0.047	3	0.14								
FeO			0.01			0	0.99				0	71.85	0.000	2	0.00	Al	3.10	3	9.30	26.98	83.6	Al	3.10
MgO	2.46		0.01		1	1	0.99				2.435	40.31	0.060	2	0.12	Ti	0.01	4	0.06	47.88	0.7	Ti	0.01
MgO						0					0	40.31	0.000	2	0.00	Fe3+	0.37	3	1.12	55.85	20.8	Fe(III)	0.37
CaO	0.08				1		1	1			0	56.08	0.000	2	0.00	Fe2+	0.00	2	0.00	55.85	0.0	Fe(II)	0.00
Na2O	0.09				1						0.09	61.98	0.003	1	0.00	Mg	0.48	2	0.96	24.31	11.7	Mg	0.48
K2O	4.52				0.81						3.661	94.20	0.078	1	0.08	Σ oct	3.97		11.43		116.8	Sum octahedral	3.97
Tot C	0.14				1						0.14					Ca	0.00	2.0	0.00	40.08	0.0	Ca	0.00
Tot S	0.01				1						0.01					Mg	0.00	2	0.00	24.31	0.0	Mg	0.00
																K	0.62	1	0.62	39.10	24.2	K	0.62
LOI	7.8															Na	0.02	1	0.02	22.99	0.5	Na	0.02
CEC	0.84															Σ int	0.64		0.64		24.7	Sum interlayer	0.64
Illite	13									Si/Al	2.943												
	0.41															O	24	–2	–48.00	16.00	384.0	O	24.00
																H	4	1	4.00	1.01	4.0	H	4.00
																Unit cell weight					754.1	Unit cell weight	754.1
											Eq. sum				5.53	Charge balance calc			0.00			Tetr charge	–0.07
											oxygen + hydrogen				44.00							Octa charge	–0.57
											scaling f				7.96							Total charge	–0.64
																						Tetra charge, %	12
																						CEC mont calc	0.85
																						CEC clay calc	0.84
																						CEC clay meas	0.84
																						Illite calc, %	1

	WyK	Si	7.93	Al	0.07	Al	3.10	Ti	0.01	Fe	(III)	0.37	Fe	(II)	0.00	Mg	0.48	Ca	0.00	Mg	0.00	K	0.62	Na	0.02

Input data											Calculation											Results	
		quartz part			Included part																		
		illite part			Fe(III) part																		
		Kaolinite part			C comp of Ca																		
Acme No	A304319					S comp of Ca																	
Group	US																						
Sample	WyK2					montm					WyK2	Formula w	Atoms %	Z	Eq, %		WyK2	atoms	Z	charge	atomic w	weight		WyK2
		0	0.01	0.00		0.99																	
SiO2	58.62	0.00	0.01	0.00		0.99	1.000				58.16	60.08	0.968	4	3.87		Si	7.96	4	31.83	28.09	223.5	Si	7.96
Al2O3	19.77	0.00	0.02	0.00		0.98	1.000				19.41	101.96	0.381	3	1.14		Al	0.04	3	0.13	26.98	1.2	Al	0.04
TiO2	0.14		0.01		1.00	0.99					0.14	79.90	0.002	4	0.01		Σ tet	8.00		31.96		224.6	Sum tetrahedral	8.00
Fe2O3	3.66		0.01		0.98	1	0.99				3.551	159.69	0.044	3	0.13									
FeO			0.01			0	0.99				0	71.85	0.000	2	0.00		Al	3.09	3	9.26	26.98	83.3	Al	3.09
MgO	2.45		0.01		1	1	0.99				2.426	40.31	0.060	2	0.12		Ti	0.01	4	0.06	47.88	0.7	Ti	0.01
MgO						0					0	40.31	0.000	2	0.00		Fe3+	0.37	3	1.10	55.85	20.4	Fe(III)	0.37
CaO	0.08				1		1	1			0	56.08	0.000	2	0.00		Fe2+	0.00	2	0.00	55.85	0.0	Fe(II)	0.00
Na2O	0.11				1						0.11	61.98	0.004	1	0.00		Mg	0.49	2	0.99	24.31	12.0	Mg	0.49
K2O	4.01				0.87						3.489	94.20	0.074	1	0.07		Σ oct	3.96		11.40		116.4	Sum octahedral	3.96
Tot C	0.12				1						0.12						Ca	0.00	2.0	0.00	40.08	0.0	Ca	0.00
Tot S	0.02				1						0.02						Mg	0.00	2	0.00	24.31	0.0	Mg	0.00
																	K	0.61	1	0.61	39.10	23.8	K	0.61
LOI	10.8																Na	0.03	1	0.03	22.99	0.7	Na	0.03
CEC	0.84																Σ int	0.64		0.64		24.5	Sum interlayer	0.64
Illite	13									Si/Al	2.996													
	0.41																O	24	–2	–48.00	16.00	384.0	O	24.00
																	H	4	1	4.00	1.01	4.0	H	4.00
																	Unit cell weight					753.5	Unit cell weight	753.5
											Eq. sum				5.35		Charge balance calc			0.00			Tetr charge	–0.04
											oxygen + hydrogen				44.00								Octa charge	–0.60
											scaling f				8.22								Total charge	–0.64
																							Tetra charge, %	7
																							CEC mont calc	0.85
																							CEC clay calc	0.84
																							CEC clay meas	0.84
																							Illite calc, %	1

	WyK2	Si	7.96	Al	0.04	Al	3.09	Ti	0.01	Fe	(III)	0.37	Fe	(II)	0.00	Mg	0.49	Ca	0.00	Mg	0.00	K	0.61	Na	0.03

Input data										Calculation												Results	
		quartz part		Included part																			
		illite part			Fe(III) part																		
		Kaolinite part			C comp of Ca																		
Acme No	A301179					S comp of Ca																	
Group	US																						
Sample	WyNa					montm				WyNa	Formula w	Atoms %	Z	Eq, %	WyNa	atoms	Z	charge	atomic w	weight			WyNa
		0	0.01	0.00		0.99																	
SiO2	60.95	0.00	0.01	0.00		0.99	1.000			60.47	60.08	1.006	4	4.03	Si	7.89	4	31.57	28.09	221.6		Si	7.89
Al2O3	21.25	0.00	0.02	0.00		0.98	1.000			20.87	101.96	0.409	3	1.23	Al	0.11	3	0.32	26.98	2.9		Al	0.11
TiO2	0.14		0.01		1.00	0.99				0.14	79.90	0.002	4	0.01	Σ tet	8.00		31.89		224.6		Sum tetrahedral	8.00
Fe2O3	3.94		0.01		0.98	1	0.99			3.823	159.69	0.048	3	0.14									
FeO			0.01			0	0.99			0	71.85	0.000	2	0.00	Al	3.10	3	9.30	26.98	83.7		Al	3.10
MgO	2.54		0.01		1	1	0.99			2.515	40.31	0.062	2	0.12	Ti	0.01	4	0.05	47.88	0.7		Ti	0.01
MgO						0				0	40.31	0.000	2	0.00	Fe3+	0.38	3	1.13	55.85	21.0		Fe(III)	0.38
CaO	0.09				1		1	1		0	56.08	0.000	2	0.00	Fe2+	0.00	2	0.00	55.85	0.0		Fe(II)	0.00
Na2O	2.55				1					2.55	61.98	0.082	1	0.08	Mg	0.49	2	0.98	24.31	11.9		Mg	0.49
K2O	0.1				0					0	94.20	0.000	1	0.00	Σ oct	3.98		11.46		117.2		Sum octahedral	3.98
Tot C	0.15				1					0.15					Ca	0.00	2.0	0.00	40.08	0.0		Ca	0.00
Tot S	0.03				1					0.03					Mg	0.00	2	0.00	24.31	0.0		Mg	0.00
															K	0.00	1	0.00	39.10	0.0		K	0.00
LOI	8.5														Na	0.65	1	0.65	22.99	14.8		Na	0.65
CEC	0.86														Σ int	0.65		0.65		14.8		Sum interlayer	0.65
Illite	3								Si/Al	2.898													
	0.00														O	24	–2	–48.00	16.00	384.0		O	24.00
															H	4	1	4.00	1.01	4.0		H	4.00
															Unit cell weight					744.6		Unit cell weight	744.6
										Eq. sum				5.61	Charge balance calc 0.00							Tetr charge	–0.11
										oxygen + hydrogen				44.00								Octa charge	–0.54
										scaling f				7.84								Total charge	–0.65
																						Tetra charge, %	17
																						CEC mont calc	0.87
																						CEC clay calc	0.86
																						CEC clay meas	0.86
																						Illite calc, %	1

	WyNa	Si	7.89	Al	0.11	Al	3.10	Ti	0.01	Fe	(III)	0.38	Fe	(II)	0.00	Mg	0.49	Ca	0.00	Mg	0.00	K	0.00	Na	0.65

Input data										Calculation												Results	
		quartz part			Included part																		
		illite part			Fe(III) part																		
		Kaolinite part			C comp of Ca																		
Acme No	A304319						S comp of Ca																
Group	US																						
Sample	WyNa2					montm				WyNa2	Formula w	Atoms %	Z	Eq, %		WyNa2	atoms	Z	charge	atomic w	weight		WyNa2
		0	0.01	0.00		0.99																	
SiO2	58.87	0.00	0.01	0.00		0.99	1.000			58.41	60.08	0.972	4	3.89		Si	7.95	4	31.78	28.09	223.2	Si	7.95
Al2O3	20.08	0.00	0.02	0.00		0.98	1.000			19.72	101.96	0.387	3	1.16		Al	0.05	3	0.16	26.98	1.5	Al	0.05
TiO2	0.14		0.01		1.00	0.99				0.14	79.90	0.002	4	0.01		Σ tet	8.00		31.95		224.6	Sum tetrahedral	8.00
Fe2O3	3.61		0.01		0.98	1	0.99			3.502	159.69	0.044	3	0.13									
FeO			0.01			0	0.99			0	71.85	0.000	2	0.00		Al	3.11	3	9.32	26.98	83.8	Al	3.11
MgO	2.36		0.01		1	1	0.99			2.336	40.31	0.058	2	0.12		Ti	0.01	4	0.06	47.88	0.7	Ti	0.01
MgO						0				0	40.31	0.000	2	0.00		Fe3+	0.36	3	1.08	55.85	20.0	Fe(III)	0.36
CaO	0.1				1		1	1		0	56.08	0.000	2	0.00		Fe2+	0.00	2	0.00	55.85	0.0	Fe(II)	0.00
Na2O	2.47				1					2.47	61.98	0.080	1	0.08		Mg	0.47	2	0.95	24.31	11.5	Mg	0.47
K2O	0.08				0					0	94.20	0.000	1	0.00		Σ oct	3.95		11.40		116.1	Sum octahedral	3.95
Tot C	0.14				1					0.14						Ca	0.00	2.0	0.00	40.08	0.0	Ca	0.00
Tot S	0.02				1					0.02						Mg	0.00	2	0.00	24.31	0.0	Mg	0.00
																K	0.00	1	0.00	39.10	0.0	K	0.00
LOI	11.8															Na	0.65	1	0.65	22.99	15.0	Na	0.65
CEC	0.86															Σ int	0.65		0.65		15.0	Sum interlayer	0.65
Illite	3								Si/Al	2.962													
	0.00															O	24	–2	–48.00	16.00	384.0	O	24.00
																H	4	1	4.00	1.01	4.0	H	4.00
																Unit cell weight					743.7	Unit cell weight	743.7
										Eq. sum				5.38		Charge balance calc			0.00			Tetr charge	–0.05
										oxygen + hydrogen				44.00								Octa charge	–0.60
										scaling f				8.17								Total charge	–0.65
																						Tetra charge, %	8
																						CEC mont calc	0.88
																						CEC clay calc	0.87
																						CEC clay meas	0.86
																						Illite calc, %	1
	WyNa2	Si	7.95	Al	0.05	Al	3.11	Ti	0.01	Fe	(III)	0.36	Fe	(II)	0.00	Mg	0.47	Ca	0.00	Mg	0.00	K	0.00	Na	0.65

ISSN 1404-0344
CM Digitaltryck AB, Bromma, 2007